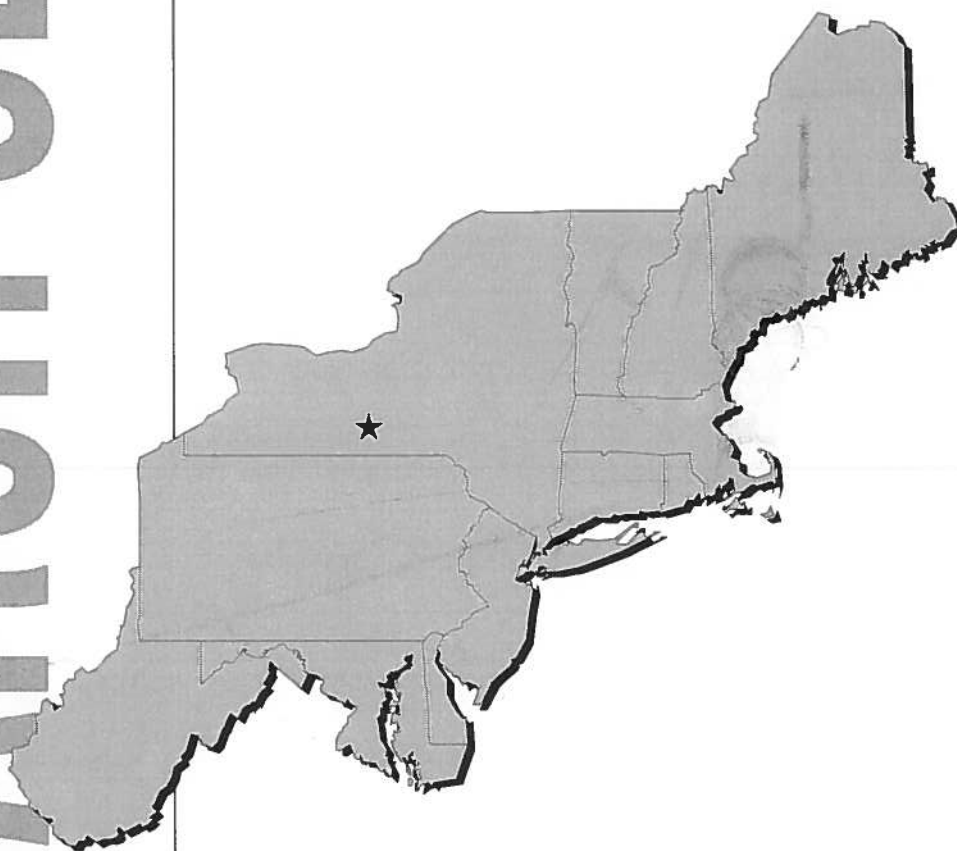


NORTHEAST REGIONAL CLIMATE CENTER

A Simple Method for Predicting Snowpack Water Equivalent in the Northeastern United States

Daniel Samelson



Cornell University
Ithaca, New York
Publication No. RR 92-1
January 1992

The mission of the Northeast Regional Climate Center (NRCC) is to facilitate and enhance the collection, dissemination and use of climate data as well as to monitor and assess climatic conditions and impacts in the twelve-state, northeastern region of the United States. Implementing this mission involves three programmatic objectives: 1) the development and management of regional climate data bases, 2) the dissemination of information and educational services regarding climate and its impacts, and 3) the performance and support of applied climate research.

Established in 1983, the Northeast Regional Climate Center (NRCC) is one of six regional climate centers now operating throughout the nation. These regional centers serve as sources of climate data and information to public and private institutions and individuals as well as expertise on local and regional climate problems. The Center's staff cooperate with State Climatologists and research scientists in disseminating climate data and information, analyzing environmental and economic impacts of climate variability, and developing new applications of weather and climate data for agriculture, business, industry, and government operations.

The NRCC Research Report series is intended to make available to interested users the full results of climate research that has been supported by the NRCC. This report series supplements the normal reporting of research results in professional journals and provides an outlet for more complete and comprehensive accounts of work performed than is generally possible in journals.

For further information please write or call:

Northeast Regional Climate Center
1123 Bradfield Hall
Cornell University
Ithaca, New York 14853-1901
(607) 255-1751



The Northeast Regional Climate Center is supported by a Grant from the National Oceanic and Atmospheric Administration.

A Simple Method for Predicting Snowpack Water Equivalent in the Northeastern United States

Daniel Samelson

Northeast Regional Climate Center
Research Series
Publication No. RR 92-1
January 1992

Abstract

Increasing the spatial density of Northeastern United States locations for which daily snowpack water equivalent (SWE) information is available would be useful for flood forecasts and agricultural, urban, and recreational water supply prediction. To that end statistical regression models were developed using as predictors meteorological variables available at National Co-Operative Observer Program (Co-Op) sites. The 15 National Weather Service Offices (NWSOs) in New York and New England were the source of 28- to 35-year daily summary data sets which included SWE. These sets were used to develop the models. Monthly NWSO models, all predicting the square root of SWE, were created for the climatological winter months of December, January, and February, as well as for November, March, and April. Predictors included the square root of snow depth, the number of consecutive days with the maximum temperature below freezing, the snowfall during the 24 hours preceding the day of prediction, and the water equivalent of precipitation which fell in that period. Values of R^2 ranged from 43.3% to 87.5% for the winter months, with 67% of all predictions still falling within $\pm 15\%$ of observed when calculated for a 10 inch (25 cm) SWE.

The stations were then grouped, first monthly by geographic regions, and then into one "Total" group encompassing all 15 NWSOs for each month. Winter groups combining the data for the three winter months, and also a "Total" winter group, combining all 15 NWSOs and 3 months, were created. Models developed for these groups provided a separate intercept term for each station (and month in the case of the "Total" winter group), but included one parameter estimate per predictor for all sites. All of these

models also included a correction factor for rain on snow events. In the case of the winter "Total" model, 45 monthly station models were reduced to a single equation. This model still exhibited an R^2 of 72.0%.

Independent verification studies were performed to determine the degree to which the NWSO-derived models could predict SWE for Co-Op stations. Periodic Co-Op snow survey data was used to determine both the efficacy of the models as well as the NWSO model best suited for use at a Co-Op station. Results showed that SWE at each Co-Op station was well predicted by the models from at least one NWSO, with results at least as good as those from developmental sites. Model-described variation ranged from 60.0% to 81.0% for most January data, and from 54.0% to 90.0% for most February data.

A method was developed to assist potential users in determining the appropriate model for a given location. Predictions for stations in western New York which receive Lake Effect snow may be made using Buffalo or Rochester models with comparable results. Syracuse models should be used at Central New York sites with Lake Effect snow, while Binghamton models should be used at those sites not affected by these snows. In the mountains and valleys of the Adirondacks and Catskills, two criteria may be used. Caribou, ME, models should be used for prediction if a station has single digit ($^{\circ}\text{F}$) long-term monthly average minimum temperatures, or, if these temperatures are double digit, the site is above 1200 feet in elevation. If these criteria are not met, Albany models yield best results.

Further calibration studies are needed to determine if these models are equally useful in the remainder of the Northeastern United States and whether they have applications in adjacent Canadian provinces.

Acknowledgements

I would like to thank my committee, Dan Wilks and Charles McCulloch, who exhibited utmost patience with my efforts to come to grips with my topic, and were always available for advice when the quagmire of climatological statistical analysis became overpowering. I hope the result was worth the wait.

I am indebted to Keith Eggleston, New York State Climatologist with the Northeast Regional Climate Center. His preparation of databases and expertise with innumerable pieces of software eliminated many roadblocks in the course of this research.

The Agronomy department, later known as the Department of Soil, Crop, and Atmospheric Sciences at Cornell University, was unfailing in its financial support through Teaching Assistantships, Graduate Research Assistantships, and temporary employment as the local Co-Operative Observer. Although I know the department received much for their money, I still would like to think the support was because of something worthwhile they saw in this student. Whatever the reason, it was deeply appreciated.

When Tom Schmidlin offered that introductory course he never imagined that 25% of the class would be using this forum to thank him. If anyone should ask me how I entered this field I can honestly say it was his fault. He didn't have to be such an incredibly positive influence.

My thanks go to all members of what is now the Atmospheric Sciences group at Cornell; undergraduates, graduates, alumni, and staff, because you have recently become too numerous to mention individually, except,

perhaps for Pam Vitale, who has kept day-to-day operations running smoothly and still hasn't melted the keyboard on this terminal with her typing speed.

Tom Niziol, Ken Remington, Al Lazo, and all the others at NWSFO Buffalo were always encouraging and enthusiastic about my research and the Weather Service. My thanks is in the form of models which I hope will be a useful addition to their in-house array of forecasting methods.

Thanks go to my parents, my brother, and his family for support when it was needed. I couldn't have finished without you.

Finally, thanks to Olga and Essa, who urged me to take that summer course so many years back, and then assured my graduate career would never be dull.

Table of Contents

List of Tables	x
List of Figures	xii
1. Introduction	1
2. The Definition and Theory of Snowmelt	8
<u>2.1. The Energy Balance Approach</u>	10
2.1.1. <i>Radiative Transfer</i>	12
2.1.1.1. Shortwave Radiation	12
2.1.1.2 . Longwave Radiation	14
2.1.2. <i>Turbulent Transfer</i>	16
2.1.2.1. Sensible Heat Transfer	17
2.1.2.2. Latent Heat Transfer (excluding rain on snow)	20
2.1.3. <i>Soil Heat Transfer</i>	23
2.1.4. <i>Excess Heat in the Snowpack</i>	24
<u>2.2. The Water Balance Approach</u>	26
<u>2.3. Rain on Snow</u>	27
3. Survey of Operational Snowmelt Prediction Models	29
4. Model Development	41
<u>4.1. Data Preparation</u>	41
<u>4.2. Exploratory Model Building</u>	47
<u>4.3. Results of Model Development</u>	50
<u>4.4. Comparison of New Models with Degree-Day Models</u>	71
<u>4.5. Discussion of Monthly Station Models</u>	78
<u>4.6. Development of Grouped Models</u>	83

Table of Contents (continued)

5. Model Verification on Independent Data	103
<u>5.1. Data Preparation</u>	103
<u>5.2. Verification Results and Discussion</u>	107
6. Summary	124
7. Appendix A - Stepwise Selection	125
8. Appendix B - Standardized Residual Analysis	127
9. Appendix C - Method of Box and Cox	135
10. Appendix D - Slope and Intercept Models with Dummy Variables	138
11. Appendix E - Developmental vs. Independent Data Sets- some considerations	145
12. Literature Cited	149

List of Tables

Table 1. Variables required for energy balance approach.	page 26
Table 2. Selected Degree-day models.	31
Table 3. Proxy variables for energy and water balance approaches.	35
Table 4. R^2 of models incorporating proxies.	36
Table 5. NWSO identifiers and snow data length of record.	42
Table 6. Potential predictors of SWE.	45
Table 7. December station prediction models.	52
Table 8. January station prediction models.	53
Table 9. February station prediction models.	54
Table 10. December parameter estimate t-ratios.	56
Table 11. January parameter estimate t-ratios.	57
Table 12. February parameter estimate t-ratios.	58
Table 13. November station prediction models.	60
Table 14. March station prediction models.	61
Table 15. April station prediction models.	62
Table 16. November parameter estimate t-ratios.	63
Table 17. March parameter estimate t-ratios.	64
Table 18. April parameter estimate t-ratios.	65
Table 19. 67% prediction intervals transformed back to SWE.	67
Table 20. December comparison: Cummdd and Maxinrow models.	72
Table 21. January comparison: Cummdd and Maxinrow models.	73
Table 22. February comparison: Cummdd and Maxinrow models.	74
Table 23. November comparison: Cummdd and Maxinrow models.	75
Table 24. March comparison: Cummdd and Maxinrow models.	76

Table 25. April comparison: Cumddd and Maxinrow models.	77
Table 26. January change in daily SWE predicted by Cumddd.	78
Table 27. Correlations of Maxinrow with mean snowpack density.	80
Table 28a. December coastal grouped model.	86
Table 28b. December mountain grouped model.	87
Table 28c. December western New York grouped model.	88
Table 28d. December "total" grouped model.	89
Table 29a. January coastal grouped model.	90
Table 29b. January mountain grouped model.	91
Table 29c. January western New York grouped model.	92
Table 29d. January "total" grouped model.	93
Table 30a. February coastal grouped model.	94
Table 30b. February mountain grouped model.	95
Table 30c. February western New York grouped model.	96
Table 30d. February "total" grouped model.	97
Table 31a. Winter coastal grouped model.	98
Table 31b. Winter mountain grouped model.	99
Table 31c. Winter western New York grouped model.	100
Table 31d. Winter "total" grouped model.	101
Table 32. Co-Operative stations used in verification studies.	106
Table 33. Co-Op stations with preferred NWSO prediction models.	109
Table 34. Verification: NWSO models with January Co-Op data.	113
Table 35. Verification: NWSO models with February Co-Op data.	117
Table C1. $L(\lambda)$ values for power transformation determination.	137
Table D1. Breakdown of terms in grouped model testing.	140
Table D2. Sequential term removal in grouped model development.	142

List of Figures

Figure 1. National Weather Service offices in the Northeast	page 3
Figure 2. Co-Op stations in the Northeastern U. S.	5
Figure 3. Timing of variable observation at NWSOs	43
Figure 4. SWE vs. snow depth for Binghamton in January	69
Figure 5. Example 67% prediction limits for $RMSE = 0.25$	70
Figure 6. Mean snowpack density vs. Maxinrow	82
Figure 7. Northeastern United States grouped regions	85
Figure 8. Timing of variable observations at Co-Op stations	104
Figure 9. Verification Co-Op stations with NWSOs in New York	105
Figure 10. January minimum Co-Op temperatures, preferred NWSO	110
Figure 11. February minimum Co-Op temperatures, preferred NWSO	111
Figure 12. Co-Op station elevations and preferred NWSO models	112
Figure B1. Perfect standardized residual plot (idealized)	129
Figure B2. Standardized residual plot exhibiting increasing variance	131
Figure B3. Standardized residual plot exhibiting curvature	133
Figure B4. Standardized residual plot for transformed model	134
Figure E1. Standardized residual plot exhibiting underprediction	146

1. Introduction

Snowmelt affects everyone in the Northeastern United States, through its role in influencing agricultural water supplies, river flooding, reservoir levels (see Work, 1953 for Western U. S. examples which also apply to the Northeast), and in its most recently recognized position as purveyor of concentrated quantities of acid material in the acid shock phenomenon (Prévost, 1991). In contrast to large parts of the mountainous areas of Western North America, where snowcover remains for the entire winter season (if not semi-permanently), the snowpack in the Northeastern United States fluctuates. This fluctuation is not only with respect to the amount of snow on the ground, but also the duration of the snowpack, and how frequently a snowpack even exists. When examining snowcover records extending back to the 1950s, coastal locations such as New York City have experienced at least 2 inches (5cm) of snowpack depth only on about 15% of all days in January. This is in contrast to more northerly sites such as Caribou, Maine, where a minimum 2 inch snowpack depth has occurred on approximately 70% of all January days. Since a substantial percentage of annual precipitation falls as snow in the Northeast, and is thus held in storage for varying lengths of time, the importance of understanding snowmelt is clear. To be able to predict daily snowmelt, or at least how much water is in storage on a daily basis, would be useful in predicting water supplies for agricultural, urban, and recreational uses. Forecasting extreme snowmelt inputs into rivers would provide advance warning to appropriate agencies for the protection of lives and property against flooding.

Presently sites in the Northeast which actually measure snowmelt are limited to a small number of research facilities, such as the United States Army Corps of Engineers Cold Regions Research and Engineering Laboratory in Hanover, New Hampshire. These are data-intensive locations which monitor many meteorological variables and also use lysimeters to measure daily meltwater. These stations are of limited use, however, in providing snowmelt information for the entire region, simply because of their small number.

Buttle and Xu (1988), studying a location just north of Lake Ontario, reported a method which suggests an alternative to daily snowmelt measurements. Snowpack water equivalent (SWE) is the depth of water per unit area obtained when the snow over the same area is completely melted. If SWE at a location is observed from one day to the next, negative changes after accounting for precipitation may be attributed to snowmelt. This simplification ignores sublimation and evaporation from the snowpack, assuming these events to be negligible on a daily basis.

New York and New England have 15 National Weather Service Offices (NWSOs) which measure SWE daily (see Figure 1), an immediate improvement with respect to both station density and geographic coverage over the research sites. However, a drawback of using stations providing point measurements is the non-representativeness of a given station within its surrounding area. For example, the NSWO at Albany, NY is less than 300 feet (95m) above mean sea level (msl). SWE values measured there probably have little in common with SWE quantities in the mountains of the Adirondacks, 1300 to 4500 feet (400 to 1400m) above the Albany station. A site located in the Adirondacks would be more representative, but no

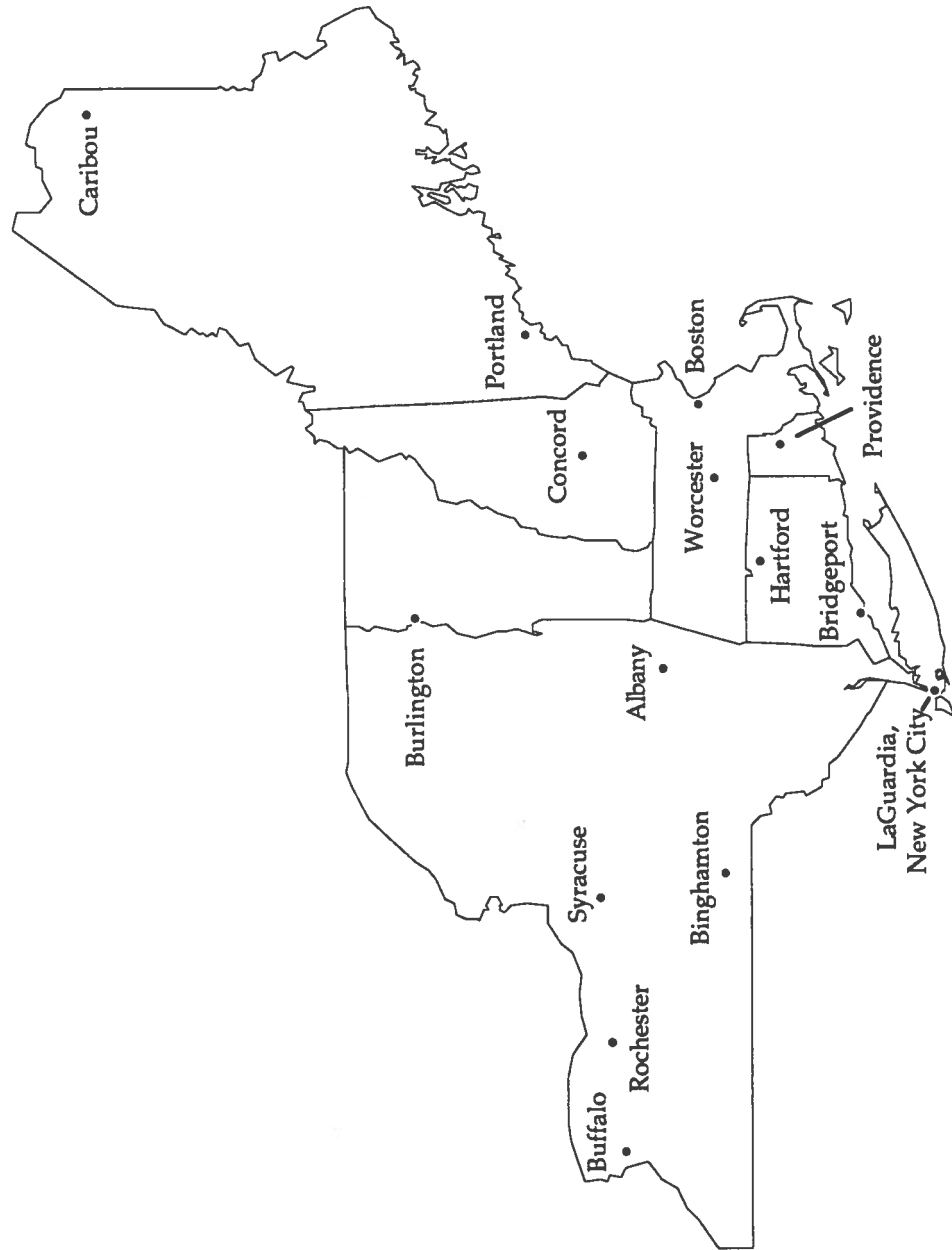


Figure 1. National Weather Service Offices (NWSOs) in New York and New England.

NWSO exists in that area. Further increasing the number of stations used for reporting would be a step toward alleviating the problem of non-representative coverage. Rather than spend large sums in developing new stations, use can be made of an additional network which is already in place.

The National Co-Operative Observer Program (Co-Op) consists of over 11,000 sites nationwide (National Cooperative Observer Newsletter, 1983), of which approximately 250 are in New York and another 250 are in New England (see Figure 2). Although the operators of this network do not measure SWE, they do measure, on a daily basis, several climatological variables which have the potential to provide physically-based estimates of SWE. The variables reported at Co-Op stations are 24-hour maximum and minimum temperatures, daily snow depth, and 24-hour snowfall and precipitation. This last quantity is the liquid equivalent of actual precipitation, be it solid, liquid, or a mixture of the two. These stations also participate in periodic snow surveys during which SWE is also directly measured.

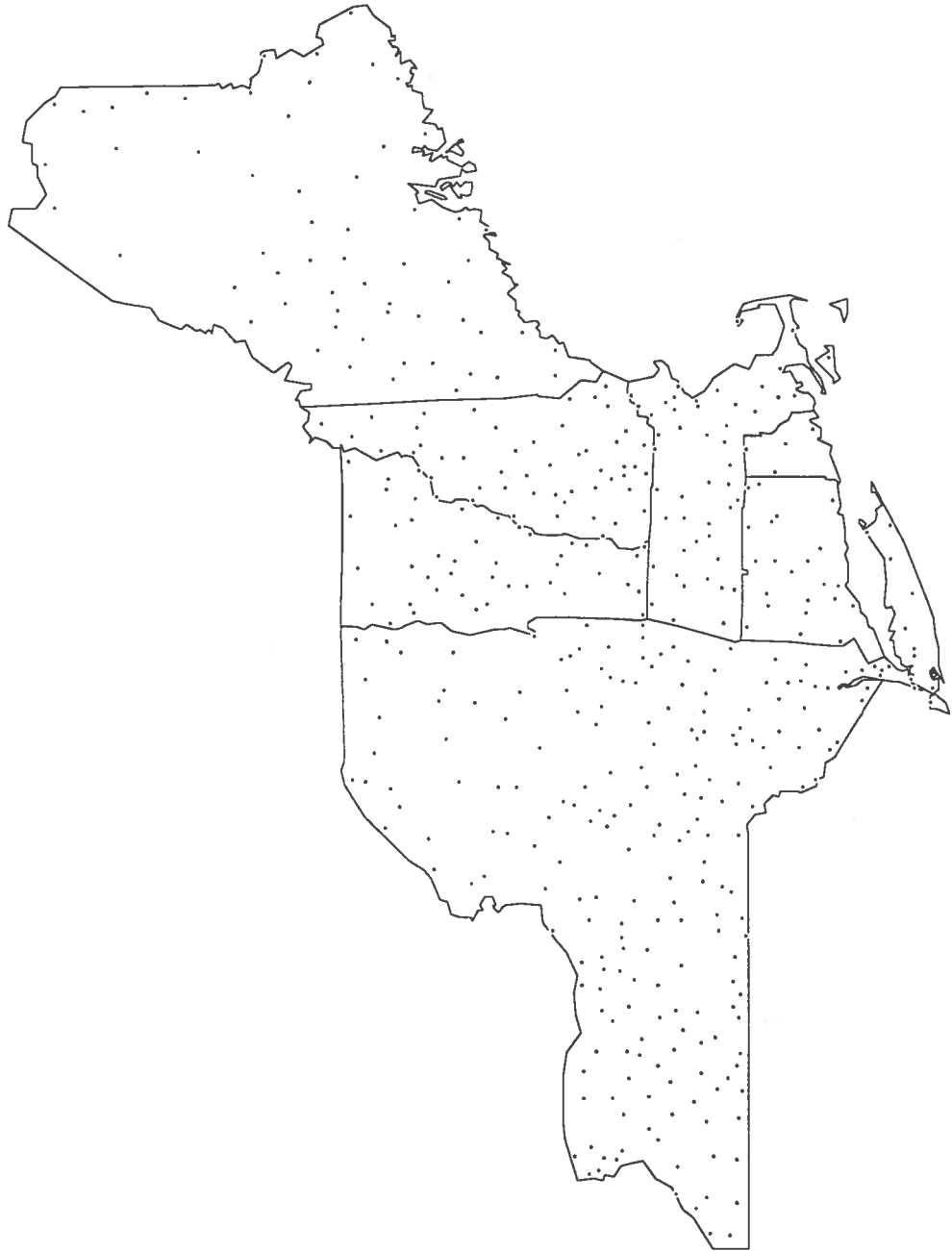


Figure 2. National Co-Operative Observer Stations in the Northeastern United States.

The goal of this thesis is to produce a system for predicting SWE using variables available at Co-Op stations. Actual SWE measurements from NWSO stations will be used to develop models. The models will then be verified using the independent snow survey data for the Co-Op stations. Completed models may then be utilized by those interests concerned with SWE or snowmelt. These include

- 1) National Weather Service Hydrologists monitoring snowmelt flood situations, who could estimate snowmelt from day to day using SWE predictions.
- 2) Agricultural Meteorologists forecasting the component of growing season water supplies due to SWE in watersheds.
- 3) Urban officials planning summer water usage policies based on winter SWE amounts affecting storage reservoirs.
- 4) Building Engineers requiring snow load information for structures, by determining snowpack mass from historical records of snow depth and predicted SWE. This would be useful not only for design studies, but also for the determination of real-time safety hazards.

In order to understand the relationship of observed meteorological variables to SWE, section 2 of this thesis will examine the theory behind the physical basis of snowmelt. This may also yield insight with regard to extracting additional information from the available data. Following the description of theory, section 3 on operational models describes related efforts by other workers, highlighting different approaches, and presenting techniques of developing proxies for the physical components of snowmelt. A list of potential predictor variables will be created and presented there. Section 4 on model development will describe the procedures used in development and testing of statistical regression models. Final station- and

month-specific models will be shown. A method for combining models, thereby creating new models suitable for more general use, will be described. At the end of this section these increasingly more general products will be presented and discussed. In the model verification section, performance of all of the models will be examined using independent Co-Op snow survey data. Finally, the results of the entire project will be summarized, followed by several appendices with more detailed explanations of some of the statistical procedures used in this study.

2. The Definition and Theory of Snowmelt

The snowpack and its surroundings are interwoven in a system of energy and mass exchange processes. The actual melting of snow is but one permutation of the complex array of energy and mass transfers between the snowpack, the sun, atmosphere and clouds, underlying soil, surrounding topography and vegetation, and precipitation.

Snowmelt is defined as that water produced by the melting of snow which actually leaves the bottom of the snowpack. This occurs only after sufficient heat has been supplied to first raise the internal snowpack temperature to the freezing point, and then to melt enough snow to satisfy the free-water holding capacity of the pack. Free-water holding capacity is that maximum amount of water which can be held within the pore space of the snowpack by capillary action. This corresponds to a threshold snowpack density of 40-45%, obtained by dividing SWE by the corresponding snow depth, before water begins to drain from the snowpack base (Bertle, 1966).

The energy supplied to the snowpack comes from several sources. Various forms of radiative transfer tend to dominate, but on a day-to-day basis other sources can play important roles. The difference between air temperature and the snowpack surface temperature drives an energy flux of sensible heat (i.e.; heat flowing from a relatively warm region to a relatively cold region). The moisture content of the overlying air, in conjunction with snowpack surface conditions, induces either evaporation or condensation of liquid water, or sublimation or deposition of solid water. These phase changes are mass transfers accompanied by energy transfers, in the form of latent heat (i.e.; energy stored as water changes phase from solid

to liquid to gas, and which is released as the reverse processes occur), between the snowpack and the atmosphere. Although mass transfer at first glance may seem only to be addition or removal of some phase of water from the snowpack, it must be remembered that even new precipitation is involved with energy transfer, the direction of which merely depends on the relative temperature of the precipitation and the snowpack surface. An extreme example is the heat supplied when rain falls onto the surface of the snow.

The underlying soil represents another source or sink of energy for the snowpack. Since the potential for evaporation of soil moisture into snowpack air spaces is reduced by winter temperatures, especially if the soil itself is frozen, heat exchange between the soil and snowpack is primarily sensible.

A snowpack is not one homogeneous material, but consists of layers of differing densities, some of which may even be ice. Heat flux into and through the snowpack, therefore, does not occur uniformly, but with virtually infinite variation, in the horizontal as well as the vertical dimension. Melting of crystals at the surface does not guarantee similar melting throughout the pack, nor does it necessarily result in uniform liquid water percolation down through the snow. The net effect is an extremely complex system which must be simplified if it is to be usefully described by an operational SWE prediction model.

For most purposes in this investigation the snowpack will be viewed as a one-layer homogeneous system. This simplification will hold for most of the concepts presented, although some mention of the ability of solar radiation to partially penetrate the snowpack will be made. Non-

homogeneity will also be briefly treated when discussing the heat used to raise the snowpack to the freezing point of water.

There are three interrelated theoretical methods of depicting snowmelt. First, the energy balance approach describes the heat exchange between the snowpack and its surroundings. A positive imbalance indicates a net heat transfer to the snowpack. This excess is used to raise the snowpack temperature and melt snow. Second, the water balance approach is a mass conservation method which accounts for additions to and losses of SWE. A net loss can be attributed to snowmelt after all other sources and sinks have been considered. Third is a hybrid approach used when liquid precipitation falls on snow. Rain both alters the water balance of the snowpack and serves as an additional source of heat.

2.1 The Energy Balance Approach

A balance exists between the snowpack and its surroundings with respect to energy, or heat transfer. The snowpack gains energy, or heat, in the form of radiation from the sun, and infrared radiation from the atmosphere, clouds, vegetation, and adjacent topographic features. Warm air over the snowpack not only supplies heat, but also provides moisture for liquid condensation or solid deposition onto the pack. These phase changes supply heat to the snow. Another source of heat is underlying soil with a temperature greater than that of the snowpack base. The snowpack loses heat through infrared radiation, sensible heat transfer to colder overlying air, liquid water evaporation or solid water sublimation into a dry air mass, and loss to soil colder than the snowpack base.

When the contribution of all of the sources and sinks are summed, what remains is net energy transfer either toward or away from the snowpack. Net heat gains by the snowpack are partially utilized in raising the snowpack temperature to the freezing point. The remainder are then used to melt snow. Net heat losses by the snowpack result in cooling of the snow temperature, which more than offsets any heat released into the pack by the freezing of internal free water. This entire framework represents the energy balance of the snowpack.

Nineteenth century Russian, as cited in Kuz'min (1972), and early 20th century German researchers, cited in Wilson (1941), first approached the snowmelt problem quantitatively, but it was Wilson (1941) who published the first English-language presentation of the thermodynamics of snowmelt. The components of this theory have been incorporated into snowpack energy balance equations by many investigators (e.g.; U. S. Army Corps of Engineers {USACOE}, 1956), presented here following Kuz'min (1972) and Fleming (1975):

$$W_R + W_k + W_e + W_s + W_h + W_b = 0 \quad (1)$$

where all units are in Watts/m², the rate of energy exchange per unit surface area, and

- W_R = radiative heat transfer between the snowpack and the sun, atmosphere, and opaque or solid objects
- W_k = sensible heat transfer between the snowpack and the atmosphere
- W_e = latent heat transfer between the snowpack and the atmosphere
- W_s = soil heat exchange with the snowpack
- W_h = heat transfer which changes snow temperature
- W_b = heat expenditure to melt snow, or the heat gain caused by freezing liquid water in the snowpack

Positive values for the first four terms represent transfers toward the snowpack. If W_b is brought over to the right hand side of the equation, the sum of the left hand side, if positive, indicates heat available for melting, while a negative sum indicates freezing of liquid water.

It is useful to examine each of the components in greater detail.

2.1.1 Radiative Transfer

The radiation term consists of both shortwave or solar radiation (the wavelength range 0.15 - 3.0 μm , consisting of ultraviolet, visible, and "near" infrared), and longwave or terrestrial radiation (in the "far" infrared wavelength range 3.0 - 100 μm). The 3.0 μm cutoff is the wavelength where Planck's electromagnetic emission curves for the sun and earth intersect. Short- and longwave radiation are further divided into incoming and outgoing components with respect to the upper surface of the snowpack. Net radiation is described by the following relationship:

$$W_R = S\downarrow + S\uparrow + L\downarrow + L\uparrow \quad (2)$$

where the arrows denote incoming (down, toward the snowpack) and outgoing (up, away from the snowpack) components of solar or shortwave (S) and longwave (L) radiation.

2.1.1.1 Shortwave Radiation

Incoming shortwave is composed of both direct and indirect, or diffuse,

radiation. The amount of direct beam energy is dependent upon angle of incidence and cloud cover, and, if observed over 24 hours, daylength. The indirect portion is a result of scattering by atmospheric gasses, particulates, clouds, and multiple reflections between clouds and the snowcover. Since snow is somewhat transparent to shortwave radiation, the amount of solar radiation affecting the energy budget of the snowpack is divided between that contacting the surface only, and that entering and penetrating to a depth. Assuming a homogeneous snowpack and ignoring internal reflections, the penetrating component behaves according to Beer's Law (Oke, 1978). The amount reaching a level beneath the surface decreases exponentially according to:

$$S_z = S_{\text{surface}} e^{-az} \quad (3)$$

where radiation terms are in W/m^2 and

S_{surface} = incoming solar radiation incident upon the snowpack surface

S_z = incoming solar radiation reaching depth z (cm) in the snowpack

e = base of natural logarithms

a = extinction coefficient (0.07 to 1.5 cm^{-1} , depending on snow conditions {Baker, et al., 1991})

Baker, et al. (1991), summarizing earlier work on extinction coefficients affecting solar radiation passing through snow, calculated penetration depths ranging from 5 to 99 cm. These levels are where the radiation has been reduced to 0.1% of the radiation striking the snowpack surface. It follows that beneath shallow snowcovers the solar radiation which actually passes through to the underlying surface should not be included in the radiation affecting the pack, but will affect the soil transfer term.

Outgoing shortwave radiation is that portion of the incoming shortwave reflected by the snow surface, along with internal snowpack reflections, and is characterized by the albedo of the snowpack. The albedo varies with the age and depth of a snowpack with values ranging between 0.2 and 0.8. Clean, fresh snow is much more reflective than older snow containing dirt. Albedo is also affected by the underlying surface when snow depths are less than about 5 cm over bare soil, 7.5 cm over sod, and 15 cm over alfalfa (Baker, et al.,1991). These investigators reported lower albedos in snowpacks more shallow than these depths.

Net shortwave radiation may be described as follows (Kuz'min,1972):

$$S = S\uparrow + S\downarrow = (S_D + S_{dif}) * (1 - r) - S_h \quad (4)$$

where radiation is in W/m^2 and

S = net shortwave radiation

S_D = direct beam radiation

S_{dif} = diffuse radiation

r = albedo (dimensionless)

S_h = shortwave radiation which reaches the sub-snow surface

2.1.1.2 Longwave Radiation

Longwave radiation from a solid is determined by its surface temperature and emissivity, or how efficiently the surface emits radiation. For air, increased moisture and particulate contents are associated with higher emissivities (Oke, 1978). Incoming longwave radiation (L) from the atmosphere is a function primarily of the characteristics of the planetary boundary layer (PBL), the lowest 1 km of the atmosphere. Since the PBL,

like the snowpack itself, is not homogeneous, each layer with its own temperature, moisture, and particulate content has a unique long-wave emissivity. Although the longwave radiation striking the snowpack surface is a composite function of the various temperatures and emissivities of the layers within the PBL, for simplicity the mean temperature and emissivity of the bulk PBL may be used as the controlling factors (Oke, 1978). Beneath vegetation, the temperature and emissivity of the closed canopy replace those of the PBL in determining incoming longwave radiation.

The rate of longwave energy emission per unit surface area is described by the Stefan-Boltzman Law:

$$L = \epsilon \sigma T^4 \quad (5)$$

where

L = longwave energy flux (W/m^2)

ϵ = longwave emissivity of the radiation source (dimensionless)

σ = Stefan-Boltzman constant ($5.67 \times 10^{-8} \text{ J}/\text{m}^2 \text{ K}^{-4} \text{ s}^{-1}$)

T = appropriate source temperature in degrees Kelvin

Outgoing longwave radiation is a function of snowpack surface temperature and an emissivity of nearly one. Clear nights are characterized by unsaturated layers (with respect to water vapor) throughout the atmosphere, with relatively low emissivities. Since these layers also tend to cool with height, and are typically colder than the snowpack surface, net longwave radiation is negative, or outgoing on clear nights. Conversely, since cloudy layers have higher emissivities than dry layers, net longwave radiation approaches zero and may actually be positive on overcast nights,

because clouds will absorb terrestrial radiation and reradiate back to the snowpack. Net positive longwave radiation is only the case if cloud base temperatures are warmer than snowpack temperatures (Oke,1978).

During the day, while incoming longwave changes little from that occurring at night, the outgoing longwave may be higher simply because of higher surface temperatures (Oke,1978). This assumes that the temperature of the snow surface fluctuates diurnally.

2.1.2 Turbulent Transfer

Sensible heat exchange (W_k in equation 1) between the snowpack surface and the atmosphere occurs when warm or cold air relative to the snowpack surface lies over or moves past the snowpack. Latent heat exchange (W_E in equation 1) accompanies vertical mass transfer of water by phase change at the snowpack surface. The direction of mass transfer depends on the moisture content, or dewpoint, of the air over the snow, as well as the dewpoint temperature (the temperature to which air at constant pressure must be cooled in order to saturate the air with respect to liquid water) of the snow surface. It is reasonable to assume that the air adjacent to the snowpack surface is probably saturated.

Sensible and latent heat exchange between the surface of the snowpack and overlying atmospheric layers are similar in both their physical basis and mathematical formulations. In both cases there are two regions of transfer:

- 1) The laminar boundary layer, where heat and mass exchange is by molecular diffusion in effectively still air.
- 2) The atmospheric boundary layer, where energy and mass exchange occur by turbulent transfer.

Although conceptually different, these regions are virtually impossible to decouple because of the indistinct transition between layers.

2.1.2.1 Sensible heat transfer

When warm air, relative to the snowpack surface, is above the snowpack, sensible heat transfer is positive (toward the pack), while cold overlying air results in a negative sensible heat flux (away from the pack). As described earlier, heat will flow from warmer regions to colder regions. Within the laminar boundary layer heat transfer is a molecular diffusion process driven by the temperature gradient across the layer. This can be represented mathematically as:

$$W_K = \rho c_p k_{hd} \partial\theta / \partial z \quad (6)$$

where

ρ = air density within the laminar layer (kg/m^3)

c_p = specific heat of air at constant pressure ($1010 \text{ J kg}^{-1} \text{ }^\circ\text{C}^{-1}$)

k_{hd} = molecular diffusion coefficient for sensible heat
($\approx 0.19 \times 10^{-4} \text{ m}^2/\text{s}^{-1}$ at 0°C)

$\partial\theta / \partial z$ = vertical potential temperature gradient in the laminar layer ($^\circ\text{C/m}$)

The laminar layer temperature gradient is maintained by the mixing action of wind and turbulence in the atmospheric boundary layer, which supplies

large quantities of warm or cold air to the top of the laminar layer. These serve respectively as energy sources and sinks. Since molecular diffusion is a very slow, thermal gradient-dependent process, the large gradient which may be assured by the presence of sources or sinks can compensate for the inhibiting effect of slow molecular diffusion.

Turbulent transfer is summarized after Male & Granger (1981) and Olyphant & Isard (1988) in two ways. The first is a generalized approach which simply views turbulent transfer as diffusion on a much larger scale than molecular, and includes the effect of vertical motions within the eddy diffusivity, or turbulent transfer coefficient. This factor describes how effectively the turbulence is able to transmit energy. Essentially, vigorous turbulence moving energy down a temperature gradient is more effective than are calm conditions. The formulation is therefore identical to molecular diffusion through the laminar layer (equation 6), with the exception of the coefficient:

$$W_K = \rho c_p k_{ht} \partial \theta / \partial z \quad (7)$$

where

k_{ht} = eddy diffusivity or turbulent transfer coefficient
of sensible heat ($m^2 s^{-1}$)

The other method, eddy correlation, involves sampling of the vertical wind and temperature fluctuations, and thereby directly observing turbulence. It is described as follows:

$$W_K = -\rho c_p \overline{\theta' w'} \quad (8)$$

where

θ' = the difference between the instantaneous potential temperature at a level within the atmospheric layer and the mean potential temperature of that level over time ($^{\circ}\text{C}$)

w' = the difference between the mean vertical wind speed and the instantaneous vertical component, with positive values for upward vertical wind (m/s)

The overbarred quantity is the mean product of the two fluctuations, and indicates the covariance of temperature and vertical velocity.

For example, if net positive anomalies in layer temperature tend to occur ($\theta' > 0$) when vertical wind anomalies are negative, or downward ($w' < 0$), the mean value of the product of these two terms will be negative. The requirement for mass to be conserved dictates that simultaneously cold air ($\theta' < 0$) must also be transporting away from the surface ($w' > 0$), also resulting in a negative product of the two terms. In other words, the tendency is for warm air to be transported on a net basis to the snowpack surface. The sign of W_k is therefore positive, indicating a sensible heat flux toward the snowpack (Oke, 1978). More generally, a positive flux ($W_k > 0$) indicates stable stratification in the atmosphere, possibly characterized by an actual temperature increase with height, but at least a temperature profile non-conducive to convection. A negative flux ($W_k < 0$) indicates an unstable lapse rate, where potential temperature decreases with height, and convection will tend to move heat away from the snowpack. Because of the tendency for the snowpack to cool and stabilize the air immediately above the surface, negative flux probably only occurs when an extremely cold air

mass settles over the area.

Sensible heat exchange not involving atmosphere-snowpack interactions occurs when rain falls on snow. This will be discussed in section 2.3.

2.1.2.2 Latent heat transfer (excluding rain on snow)

The vertical water vapor distribution within the atmosphere, in conjunction with the temperature and character of the snowpack surface, determines what phase change of water will occur at the top of the snowpack. If the surface is dry, water vapor may deposit as a solid (deposition) with a release of heat, or snow crystals may change from solid to gas (sublimation) and remove energy from the snowpack in the process. If a thin layer of liquid water exists on the upper snowpack surface, either condensation of water vapor may occur onto that layer with a release of energy, or water may evaporate from the layer, removing heat. If the moisture gradient points away from the surface (i.e.; lower concentrations at the snowpack), condensation or deposition will occur. Conversely, dry air over the snow surface will support evaporation or sublimation.

Latent heat transport through the laminar boundary layer is a molecular diffusion process driven by the water vapor gradient. This is summarized as follows using evaporation or condensation as the phase change causing the energy transfer (after Oke,1978):

$$W_e = \rho L_v k_{ed} \partial q / \partial z \quad (9)$$

where

ρ = air density (kg/m^3)

L_v = latent heat of vaporization ($2.5 \times 10^6 \text{ J kg}^{-1}$ at 0°C)

K_{ed} = molecular diffusivity for water vapor ($\approx 0.21 \times 10^{-4} \text{ m}^2/\text{s}$ at 0°C)

$\partial q / \partial z$ = vertical specific humidity gradient in the laminar layer ($\{\text{kg water}/\text{kg air}\} \text{ m}^{-1}$)

Wind and turbulence supply moist or dry air to the top of the laminar boundary layer, providing the moisture source or sink. In a manner analogous to thermal diffusion of sensible heat, slow molecular diffusion of water vapor combined with the presence of moisture sources or sinks can cause the development of large specific humidity gradients across the laminar layer. These, in turn, then overcome the inhibiting effect of slow molecular diffusion.

Turbulent transfer of latent heat is summarized by Granger & Male (1981) and Olyphant & Isard (1988) using two approaches essentially identical to those which describe turbulent transfer of sensible heat. Equation (10) treats turbulent latent heat flux as large-scale diffusion, with the role of the vertical motions incorporated into the eddy diffusivity of latent heat. This term is the only difference between this equation and the laminar boundary layer latent heat diffusion formula (see equation 9).

$$W_e = \rho L_v k_{et} \partial q / \partial z \quad (10)$$

where

k_{et} = eddy diffusivity, or turbulent transfer coefficient of latent heat
(m^2/s)

The other method, eddy correlation, involves sampling of the vertical wind and specific humidity fluctuations to directly measure turbulence, and is described in equation (11):

$$W_e = -\rho L_v \overline{q'w'} \quad (11)$$

where

q' = the difference between the instantaneous specific humidity of a level within the atmospheric boundary layer and the mean specific humidity of that level over time

w' = the difference between the mean vertical wind speed and the instantaneous vertical component at the level

The overbarred quantity is the mean product of the two fluctuations over time, and indicates the covariance between specific humidity and vertical velocity.

As an example, if net positive anomalies in boundary layer specific humidity ($q' > 0$) occur and the net vertical motion anomalies are negative ($w' < 0$), or downward, the mean value of the product of these terms is negative. Conservation of mass restrictions require negative specific

moisture anomalies ($q' < 0$) to be simultaneously transporting away from the surface ($w' > 0$). In other words, the tendency is for moist air to be transported on a net basis to the snowpack surface. The sign of W_e is therefore positive, indicating a latent heat flux toward the snowpack.

More generally, the amount of heat transported depends on which phase change takes place at the snow surface. If there is a thin layer of liquid water surrounding snow flakes or crystals, condensation or evaporation will occur. This characterizes a snowpack with a surface temperature near freezing. If the snowpack is colder, sublimation or deposition will occur and the latent heat of fusion ($L_f = 2.8 \times 10^6 \text{ J/kg}$) would replace the latent heat of vaporization in the heat transfer relationships. Deposition and sublimation will cause larger energy transfers than condensation and evaporation.

Latent heat exchange which does not involve snowpack-atmosphere interactions occurs when rain falls on snow. This will be treated separately in section 2.3.

2.1.3 *Soil heat transfer*

When the soil temperature gradient points away from the soil surface there is a positive heat transfer to the snowpack. Conversely, a gradient toward the surface will remove heat from the snowpack. Kuz'min (1972) formulated this process of molecular conduction in the soil layer beneath the snowpack:

$$W_s = -\lambda \partial T / \partial z \quad (12)$$

where

λ = thermal conductivity of the soil ($\text{W m}^{-1} \text{ }^\circ\text{K}^{-1}$)

z = depth, with increasingly negative values away from the surface

$\partial T / \partial z$ = vertical temperature gradient of the soil layer beneath the snowpack ($^\circ\text{K/m}$)

The vertical temperature gradient of the soil may be influenced by solar radiation penetrating the snow cover and warming the soil surface, which can strongly affect the temperature gradient near the surface.

2.1.4 Excess Heat in the Snowpack

When the above terms in the energy balance equation are summed and the result is positive, excess heat has been transferred to the snowpack. If the snowpack temperature is less than 0°C , some, or all of this heat is used to bring the snowpack towards the freezing point. Any positive imbalance which then still exists is used to melt snow. This is certainly the case in shallow snowpacks and is a sufficient explanation for this investigation. Deeper snowpacks may have colder layers which are not warmed until water from melted crystals in higher layers percolates down.

The energy flux density, in $\text{MJoules/m}^2/\text{day}$, needed to melt an amount of snow depends on B , the thermal quality of the snow (USACOE,1956):

$$B = \frac{\text{heat required to produce a unit liquid volume from snow}}{\text{heat required to produce a unit liquid volume from ice at } 0^\circ \text{C}} \quad (13)$$

Since snow contains air spaces and may already contain free liquid water, less heat is required to produce a given volume of liquid water than is required by solid ice. Therefore, B is a function of snow density and liquid content compared with the density of ice, and will be less than 1 except when the snowpack is very cold and needs substantial warming before it reaches the freezing point. The excess heat supplied to the snowpack is then used to melt snow at the following rate (USACOE,1956):

$$M = B * (H_p / 3.35) \quad (14)$$

where each kilogram per square meter of water corresponds to a liquid depth of 1 millimeter and

M = meltwater in mm

B = thermal quality of snow, a dimensionless ratio

H_p = excess heat supplied to snowpack (MJoules/m²)

3.35 = the latent heat of fusion, or the number of MJoules/kg required to produce one mm of water from ice (USACOE,1956)

Snowmelt as defined by melted snow leaving the base of the snowpack will not occur until this melting has provided sufficient liquid to satisfy the free-water holding capacity of the snowpack. Only after this content has been reached will additional heat result in water leaving the base of the pack as snowmelt.

Table 1 shows the variables which need to be measured for a complete treatment of the snowpack energy balance.

Table 1. Variables required for the energy balance approach to snowmelt. Letters correspond to the terms which use the variable: R = radiation, H = sensible, E= latent, S = soil, I = warming snowpack.

Variable	Term
Incoming solar radiation	R
Albedo	R
Temperatures	
Snow surface	R, H, E
Vegetative canopy	R
Cloud base	R
Air- at surface	H
- through the planetary boundary layer	H, R
Soil- top	S
- subsurface	S
Snowpack - mean	I
Air density	H, E
Water vapor- surface	E
- through the planetary boundary layer	E, R

2.2 The Water Balance Approach

The second method of determining snowmelt is simply a mass conservation approach. The change in daily SWE equals the sum of inputs into the system (SWE of new snowfall, rainfall, condensation, and deposition) less the sum of outputs (melt, sublimation from the pack, evaporation of water in the pack) and is described by the following equation for any selected time period (after Kuz'min,1972):

$$\text{SWE}_f - \text{SWE}_i = (\text{Snfl} + \text{R} + \text{Con} + \text{Dep}) - (\text{M} + \text{Sub} + \text{Evap}) \quad (15)$$

where all values are in mm,cm, or inches of liquid water, and

SWE = initial and final snowpack water equivalents

Snfl = SWE of fresh snowfall

R = rainfall

Con = condensation onto a surface layer of water on the snowpack

Dep = deposition onto a cold, dry snowpack

M = snowmelt, the meltwater leaving the base of the snowpack

Sub = sublimation from the snowpack

Evap = evaporation of free water from the snowpack

The water balance components are regularly measured quantities except for those involving phase changes. Empirical results from the snowmelt literature, presented in section 3, lend support to the assumption that evaporation, condensation, sublimation, and deposition may be assumed to be negligible on a daily basis.

2.3 Rain on Snow

The amount of heat in rainwater depends on its temperature. Heat available for altering the snowpack is described as follows (USACOE,1956):

$$H_p = (T_r - T_s) * P_r * c_{pw} \quad (16)$$

where

H_p = heat from rainfall in Joules/m²

T_r = temperature of the rain in °C

T_s = temperature of the snow surface in °C

P_r = rainfall in m

c_{pw} = specific heat of water (4.19 × 10⁶ Joules/°C)/m³

When rain falls on snow several processes take place which change SWE. The effects range from primarily just an increase in SWE if the rain freezes on contact with the snowpack, to a large energy input in the form of sensible heat if the rain is much warmer than the snow. In the latter case rain will initially melt the surface layer and then flow down into the snowpack. As it cools the liquid loses sensible heat to the snowpack, and the process of melting involves latent heat exchange. This may be reversed if the water refreezes, releasing the latent heat of fusion into the surrounding snow. Additional rain allows liquid to continue moving through the snowpack. This begins to raise the snowpack temperature to 0°C, causing first a change in the shape of snow crystals, and then melt. Snow crystal changes result in a compaction of the snowpack, and melted crystals further reduce the depth of the snowpack (Bertle,1966). As the depth of the pack decreases, the freshly melted water and any free water formerly in the surface layer of the snowpack are released into lower layers of the pack. Unless the remaining snowpack is already at the free-water capacity, this released water will not leave the pack. The density of a snowpack which has received rainfall will, therefore, be greater than a pack of the same depth which never received liquid precipitation.

3. Survey of Operational Snowmelt Prediction Models

The following review must be prefaced by noting that snowmelt researchers have developed either general use models (e.g.; USACOE (1956), Anderson (1973)), or models specifically calibrated for an area or even a point site. Few details of predictor selection or statistics are supplied in publications. Apparently, what was important to the authors was simply the fact that their model worked.

Morris (1985) classified snowmelt prediction models into three categories. First, the lumped or conceptual models treat the snowpack as a homogeneous mass and combine theoretical concepts into various indices. Degree-day models are examples from this group. Second are what Morris called regression models. These also treat the snowpack as a slab, but include terms specifically describing the physics of snowmelt. The USACOE (1956) generalized equations are examples of this type, after regression has been performed to estimate the appropriate coefficients for each term. Finally, distributed models also include details of the processes within the snowpack. Anderson's (1976) model is an example.

Early attempts at predicting snowmelt relied heavily on the degree-day approach. Put simply, melt would only be predicted to occur if the mean or maximum temperature exceeded the freezing point of water. The melt rate was proportional to how far the appropriate temperature was above freezing, with a correction factor sometimes included in the form of an intercept. Empirical analysis was performed to obtain the melt factor coefficient, which would be multiplied by the number of degrees above freezing for a particular day (i.e.; degree-days) and then added to the constant

to yield daily snowmelt. Degree-days would equal zero if the observed temperature used in calculation fell below freezing. The resulting formula made intuitive sense, since daily melt would be greater for warmer temperatures. The limitations were also clear, for

- every site could possibly have a different melt factor,
- daily melt would reduce either to zero or to a non-zero constant if the temperature never rose above freezing, a problem if the appropriate temperature, measured at a height of 1.5 meters, was colder than the air closer to the snowpack surface,
- even using freezing as a base temperature was not necessarily statistically best for every location.

The use of average daily temperature would also conceal diurnal variations, especially in those regions experiencing large daily temperature ranges. Table 2 shows a sampling of degree-day models and the locations for which they were developed. Note that despite the lack of physical sophistication, degree-day models are still being developed because of their simplicity and minimal data requirements. The inconsistency of presentation is also evident in that most of these models do not supply a constant for days too cold for degree-days to be calculated.

Table 2. Selected degree-day models describing daily melt (M) in inches and temperature in $^{\circ}\text{F}$, except where noted. $(X)^{+}$ is equal to x if x is non-negative, and zero otherwise. Subscripted "max" and "min" refer to maximum and minimum daily temperatures, and "mean" refers to the average of max and min for a 24-hour period.

<u>Model</u>	<u>Location</u>	<u>Investigator (year)</u>
$M = 0.06 (T_{\text{mean}} - 24)^{+}$ or $M = 0.04 (T_{\text{max}} - 27)^{+}$	open sites of the Western U.S.	Wiesner (1970) after USACOE (1956)
$M = 0.05 (T_{\text{mean}} - 32)^{+}$ or $M = 0.04 (T_{\text{max}} - 42)^{+}$	forested sites of Western U.S.	
$M = 0.0115 \text{ "degree-day" (no base given)}$	Colorado mountains	Garstka, et al (1958)
Carr (1988) summarized the following models:		
$M = 0.0397 (T_{\text{mean}} - 27.6)^{+}$	New Brunswick	Psykiyewec, et al. (1968)
$M = (0.074 + 0.007 \text{ Rainfall}) * (T_{\text{mean}} - 32)^{+} + 0.05$ (also for rain on snow)	Western U.S.	USACOE (1956)
$M = 3.0 (T_{\text{mean}} + (T_{\text{min}} / 4.4)) * ((T_{\text{max}} - T_{\text{min}}) / 8) + T_{\text{min}}$	Western Canada mountain basin	Quick & Pipes (1975)
$M = 0.02 (T_{\text{max}} - 32)^{+}$	Southern Ontario	Bruce & Clark (1966)
$M = 0.08 (T_{\text{mean}} - 32)^{+}$	Southern Ontario	Carr (1988)
$M = 11.3 + 1.3 T_{\text{max}} (^{\circ}\text{C}) + 17.5 \text{ Cos}(\text{Julian day})$ (where January 1 is Julian day 1, and December 31 is either Julian day 365 or 366)	Ontario	Buttle (1990)
$M (\text{cm}) = 2.61 (T_{\text{mean}} - 0^{\circ}\text{C})^{+}$	Quebec	Prévost, et al. (1991)

Recognizing that snowcover remained intact for varying periods, Pysklywec et al. (1968) incorporated weighted degree-day information from previous days in order to include the changing character of the snowpack:

$$SM_n = b[0.6(T_n - C)^+ + 0.3(T_{n-1} - C)^+ + 0.1(T_{n-2} - C)^+] \quad (17)$$

where $(X)^+$ is equal to x if X is non-negative and 0 otherwise, and

SM_n = daily snowmelt on day n (inches/day)

C = base temperature ($^{\circ}F$)

b = constant

T_n = mean air temperature on day n ($^{\circ}F$)

T_{n-1} = mean air temperature on day $n-1$ ($^{\circ}F$)

T_{n-2} = mean air temperature on day $n-2$ ($^{\circ}F$)

Their results were said to have shown little difference from the simple degree-day form they developed, shown in table 2.

In 1941 Wilson published a treatise on the thermodynamics of snowmelt, which served as the apparent beginning of a physically based approach. Utilizing the thermodynamic snowmelt theory the Army Corps of Engineers produced generalized models in 1956 with statistical regression-derived coefficients. Western U.S. study sites were established at which most of the variables required by Wilson's theoretical description were measured. These included multi-level observations of atmospheric temperatures, moisture content, and winds, soil temperatures at different depths, and solar radiation. Initially each term in equation 1 was statistically modeled separately, yielding snowmelt by component. For example, melt due to incoming shortwave radiation on a flat, horizontal surface would be

a function of the incoming solar radiation, reduced by the albedo and angle of incidence of the solar beam. In practice, incoming solar radiation was a measured quantity, already accounting for angle of incidence. Melt due to this energy source was then only dependent on the albedo of the snow surface, since melt was considered to be confined to the upper surface of the snowpack.

In a similar manner the other terms were transformed from theory to operationally useful forms, or actually omitted because of comparative physical or statistical non-significance. An example of an open site regression model suitable for forest-free areas, created by combining the USACOE (1956) operational terms of the snowmelt energy balance model was presented by Pysklywec, et al. (1968):

$$m = 0.00508 (1-\alpha) R_s + 0.029 N (T_c - 32) + [0.0212 (T - 32)^+ - 0.84] (1-N) + 0.00629 (Z_a Z_b)^{-1/6} [(T - 32) p/p_0 + 8.59 (e_a - 6.11)] V \quad (18)$$

where $(X)^+$ is equal to x if X is non-negative and 0 otherwise, 32 refers to the snowpack surface temperature in °F, and

m = daily melt in inches

α = albedo (dimensionless)

R_s = solar radiation (Langley/day)

N = estimated cloud cover fraction

T_c = cloud base temperature (°F)

T = mean air temperature in the PBL at height Z_a (°F)

Z_a = height of wind measurement in the PBL (in feet)

Z_b = actual height of the surface wind measurement (in feet)

p = station pressure (mb)

p_0 = pressure corrected to sea level (mb)

e_a = vapor pressure (mb)

V = wind velocity at surface height Z_b (miles per hour)

The model accounts for net solar radiation in term 1, net longwave radiation under cloudy skies in term 2 and under clear to partly cloudy conditions in both terms 2 and 3, and sensible and latent heat transfer in term 4. The last term also includes a correction for air density, which makes the model useful at different elevations.

Recognizing the likelihood of stations not having a full complement of data, the USACOE developed proxy variables to use when specific energy balance components were not available. Proxies are variables which are physically and statistically related to component variables too difficult or expensive to measure. When combined with their regression coefficients, proxies represent an indirect method of approximating physically important components in the snowmelt model for which actual observations are impractical. For example, incoming solar radiation may be described by the duration of sunshine in minutes, or even by the maximum daily air temperature. These and others are listed in Table 3.

Table 3 : Proxy variables developed by the USACOE (1956).

<u>Proxy</u>	<u>Component</u>
Shortwave absorbed by snow	net shortwave shortwave + longwave = allwave radiation
Longwave radiation loss in open	net longwave
Daily maximum temperature (Tmax)	sensible and longwave heat transfer
Tmax X 12 hour wind run	sensible and longwave heat transfer
Dewpoint X 12 hour wind run	latent heat transfer
Vapor pressure	latent heat transfer

When statistical regression models for predicting snowmelt are developed, the coefficient of multiple correlation (R^2) describes the fraction of model-described variation of daily snowmelt. The R^2 values for models using these proxies are shown in Table 4 for open sites most similar to the NWSOs used in this project. The predominant importance of allwave radiation is clear.

Table 4 : Resulting R^2 of models incorporating proxies from Table 3 (USACOE,1956).

<u>Model with proxies for:</u>	<u>R^2</u>	<u>Time period</u>
allwave, sensible, latent	0.97	hourly
sensible and latent	0.46	hourly
allwave	0.94	daily
shortwave	0.65	daily
sensible, latent by Tmax alone	0.23	daily
Tmean (mean temperature) alone	0.08	daily

Since the USACOE's efforts, much work has focused on specific components of the energy balance. Pysklywec, et al. (1968), working in New Brunswick, Canada with limited data, developed their own proxies for some of the terms in the USACOE model. This model represents a blend of lumped, conceptual models and regression models, as described by Morris (1985). Their simplified model which includes these proxies is as follows:

$$m = 0.615 + 0.0373 \text{ SOL} + 0.0067R_L + 0.00201V(T-36)^+ + 0.0437V(RH) + 0.007Pr(T-32)^+ \quad (19)$$

where $R_L = 1440(0.757\sigma T^4 - 0.459)(1 - KN)$

where $(X)^+$ is equal to x if X is non-negative and 0 otherwise, melt(m) is in inches and

SOL = duration of sunshine (hours/day)

R_L = estimate of net longwave radiation (langleys/day) (USACOE,1956)

V = daily average wind velocity (miles/hour)

T = mean air temperature ($^{\circ}\text{F}$, but $^{\circ}\text{K}$ in the net longwave equation)

RH = relative humidity (fraction)

Pr = rainfall (inches/day)

K = cloud quality factor based on type of cloud (fraction)

N = amount of cloud cover in tenths

σ = Stefan-Boltzmann's constant (8.26×10^{-11} langleys/min/ K^4)

SOL, $V(T-36)$, and $V(RH)$ were proxies for incoming short wave, sensible heat transfer, and latent heat transfer respectively.

The point, or individual site, energy and mass balance model of Anderson (1976) is a distributed model according to the Morris (1985) scheme. It adds further information by not only including the thermodynamics of snowmelt, but also some of the physical processes occurring within the pack. This adds more complexity than the other models, which are primarily concerned with changes at the snowpack surface. Anderson's model, besides using moisture, temperature, wind, and precipitation, includes information about changes in snowpack density, as well as a term for rain on snow events. In a balsam fir forest in Quebec, Canada, this model described 86% of the variation in daily snowmelt (Prévost, et al., 1991). Despite the added complexity of the energy and mass balance model, these investigators achieved marginally better results for the

same data ($R^2 = 0.88$) with the much simpler temperature index model SNOW-17 by Anderson (1973). This used the following formula for rain on snow events, and a degree-day method (see equation 21) for other days.

$$m = [(6.1 \times 10^{-10}) (T_a + 273.16)^4] - 3.4 + [(2.1 \times 10^{-3}) P_x T_a] + \{1.4 f(u_a) [(e_a - 6.11) + (9.5 \times 10^{-5}) P_a T_a]\} \quad (20)$$

where hourly snowmelt in mm is predicted by

T_a = air temperature ($^{\circ}\text{C}$)

P_x = rainfall (mm)

$f(u_a)$ = "empirical wind function" (m/s)

e_a = vapor pressure of the air (mb)

P_a = seasonal average air pressure (mb)

Here the first term treats incoming longwave radiation, 3.4 mm/hr is the reduction in melt caused by outgoing longwave radiation, the third term is heat input to the snowpack from rain falling on snow, and the final bracketed term represents turbulent transfer of latent and sensible heat. With no liquid precipitation the model is replaced by the following:

$$M = M_f (T_a - 0^{\circ}\text{C})^+ \quad (21)$$

where $(X)^+$ is equal to x if X is non-negative and 0 otherwise, and

M = snowmelt (mm)

M_f = sinusoidal melt factor to allow for seasonal increase in solar radiation (mm/ $^{\circ}\text{C}$)

Several other researchers have reported results for operational prediction models with varying degrees of detail. They are summarized here.

In Arizona research, Ffolliott et al. (1989) mention that solar radiation can be estimated from cloud cover characteristics, and that it is used along with maximum and minimum temperatures and precipitation in a snowmelt model designed for what they referred to as shallow snowpacks.

Zuzel and Cox (1975) recognized the variety of possible variables available to researchers and performed principal component analysis and regression analysis to determine the best predictors. For an 11 day period in May they determined that vapor pressure, net radiation, and wind were sufficient to describe over 78% of the variation in daily melt at a high altitude site in Idaho. The best solitary predictor was mean temperature, which accounted for 49% of the variation in snowmelt. This is in marked contrast with the result of 8% reported by the USACOE (1956) in Table 4 for similar high altitude locations in California and Oregon, utilizing several full snow seasons of data.

Olyphant and Isard (1988) used vertical profiles of temperature, relative humidity, and wind to study the advection of sensible and latent heat and its role in alpine (Colorado) snowmelt, and found advected heat to be very important in late-lying (into summer) snowpacks. The amount of advected heat fell off 5-fold 1 km from the edge of a snowfield. The authors concluded that this heat source may actually exceed solar radiation late in the snow season in windy alpine environments.

Most recently MacLean (1991) showed that ground heat transfer in the winter was not sufficient to cause melt on a day to day basis at a site in

Quebec, but said nothing about this component in autumn or spring.

Male and Granger (1981) summarized the evaporation measurements in a semi-desert open area of the Soviet Union, and for an open area, presumably in the Western U. S. Both showed daily evaporation from the snowpack in January of less than 0.2 mm. This increased as the months progressed to an April value of 0.6 to 1.0 mm per day. Reference is also made to a reported 1.6 mm/day evaporation loss in Sweden under cold, dry Arctic air, and as much as 0.95 mm/d condensation onto the snowpack under warm, moist maritime air.

Finally, Bertle (1966), in the Sierra Nevada of California, among others described in detail the effect of rain on snow, which required knowledge of snowpack densities before the onset of rain. This was necessary to determine how close the pack was to its free water holding capacity.

Efforts toward spatially widespread methods of snowmelt prediction have been made throughout the research history. Most of the early work emphasized point calculations, which gradually were incorporated into basin-wide systems (e.g.; Anderson, 1973, Fleming, 1975). This first involved weighting point measurements according to their location within different areas of snowcover. Later, empirical information concerning the relative rates of snowcover depletion was also included. Recently satellite based remote sensing of entire regions has begun to come into favor, in determining areal snowcover (Dozier, 1987), as has airplane based SWE detection through the measurement of terrestrial gamma radiation attenuation. This latter technique measures terrestrial gamma radiation emitted from snow-free terrain, and the reduction from the same area when covered by snow. The difference is due to attenuation by the SWE within the snowpack (Carroll & Carroll, 1989).

Judging by the limited number and type of meteorological variables available from Co-Op stations for statistical regression model development, this thesis appears to return to a simpler era in snowmelt research. Since fiscal limitations make it impossible for detailed measurements, common at research sites, to be instituted at Co-Op stations, the trade-off of physical sophistication for wider spatial coverage is probably worthwhile. This could be checked empirically by using data from highly instrumented sites as input to both physically rigorous models and to those developed in this thesis, and comparing results.

By examining more recent ground-based efforts this project has been assisted by the understanding obtained since degree-day models were first applied to the problem. With this background model development could begin by drawing on these investigations to build a list of potential predictors.

4. Model Development

Developing models using NWSO data which could then predict SWE at Co-Op stations was a three step process. First, NWSO datasets were error-checked and manipulated to create potential predictors. Second, rigorous exploratory model development techniques were employed on the data set from one NWSO. Finally, the results of exploratory model building were extended to the remaining NWSOs, and further methods for simplifying the final station models into more general-use forms were utilized. The following sections detail the entire developmental process, examine the products as they compare with more traditional degree-day methods, and present a set of models designed for widespread applicability in SWE prediction.

4.1 Data Preparation

National Weather Service Offices have included SWE in their daily climate data summaries since the early 1950s. Maximum and minimum air temperatures, snowfall, and precipitation are reported for the midnight to midnight period. The depth of the snowpack is measured every morning at 7:00 a. m. E.S.T. (12:00 UTC), and reported as an integer if greater than two inches. SWE is measured at 1:00 p. m. E.S.T. (18:00 UTC). Temperatures are reported in degrees Fahrenheit, snowfall to the tenth of an inch, while precipitation and SWE are measured to the hundredth of an inch.

The National Climatic Data Center in Asheville, NC, makes available data tapes consisting of National Weather Service Office daily climatological

summaries. The data used for this investigation were subsets of the records for the 15 NWSOs in New York and New England (see Figure 1), created and supplied by the Northeast Regional Climate Center at Cornell University in Ithaca, NY. Table 5 describes the length of record used in this study for each NWSO. For each station the period of record ran from the beginning of SWE measurements in the 1950's through 1986. With the exception of Worcester, MA, all records were for at least 30 years.

Table 5. National Weather Service Offices, their station identifiers, and length of record used for this work.

<u>NWSO</u>	Identifier	<u>Length of Dataset</u>
Albany, NY	ALB	1952-1986
Binghamton, NY	BGM	1952-1986
Boston, MA	BOS	1953-1986
Bridgeport, CT	BDR	1952-1986
Buffalo, NY	BUF	1952-1986
Burlington, VT	BTV	1952-1986
Caribou, ME	CAR	1952-1986
Concord, NH	CON	1952-1986
Hartford, CT	BDL	1954-1986
LaGuardia - NYC, NY	LGA	1952-1986
Portland, ME	PWM	1953-1986
Providence, RI	PVD	1953-1986
Rochester, NY	ROC	1953-1986
Syracuse, NY	SYR	1952-1986
Worcester, MA	WOR	1959-1986

The purpose of the developmental portion of this work was to predict the amount of SWE at NWSOs using only predictor variables available at Co-Op stations. Since the prediction of SWE was to coincide with the actual time of SWE measurement, it was important not to consider any predictors

whose daily values could be affected by events occurring after the afternoon SWE measurement. For example, the maximum temperature for a given day probably occurs after the SWE measurement. The preceding day's maximum temperature was, therefore, included with the initial predictors, but not the maximum for the current day. Figure 3 shows the timing of observations at NWSOs of the variables also measured at Co-Op stations.

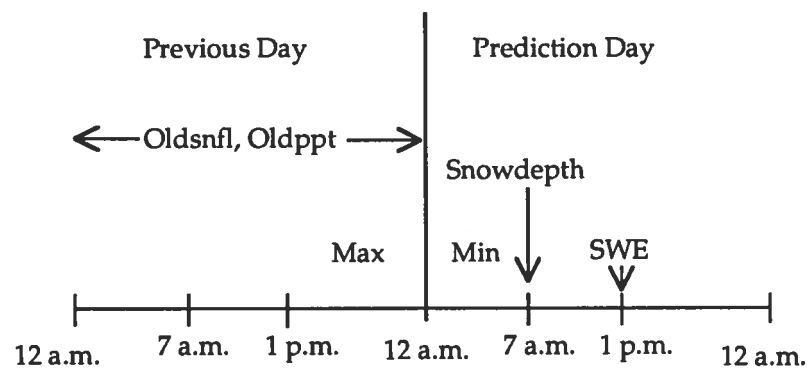


Figure 3. NWSO timing of variables. Refer to Table 6 for explanation of variable abbreviations.

A potential source of error exists in the relationship between daily snowdepth and SWE because of the 6-hour period between their respective measurements. Neither snowmelt nor additional snowfall or rainfall during this period would be a measured quantity with respect to these datasets. For example, a mid-morning snowfall could create a large SWE, but the already observed snow depth for the same day could be much smaller than expected. However, the snow depth on the following day would reflect the event. Therefore, days with mid-morning snowfall, depending on the magnitude of the event, might not have easily predicted values of SWE. The measured snow depth, however, still precedes the

SWE measurement and may be used as a predictor. Since snowfall and precipitation can also occur in the eleven hours between the SWE measurement and midnight they could not be used to predict SWE on the same date. To ensure the purely predictive nature of a model, it was decided to use the preceding 24 hour precipitation (Oldppt) and snowfall (Oldsnfl) amounts, and the morning snowdepth as possible predictors of the afternoon SWE. Table 6 gives the complete list of potential predictors used in model development, including derived variables yet to be described, along with their physical relationship to snowmelt.

As discussed earlier, other investigators have used such variables as atmospheric moisture content and wind in their regression analyses. Since these variables are not measured at Co-Op stations, an attempt was made to create variables which could furnish some extra information to a prospective model. For example, as shown in table 2, many researchers have reported daily snowmelt as a function of cumulative degrees greater than a base temperature, to represent heat applied to the snowpack. Conversely, some indication of conditions being less than a ceiling temperature could provide a measure of the cold content of the snowpack, indicating the heat required to raise the snowpack to the freezing point and then to ripen, or satisfy the free water holding capacity of the snow.

For this work cumulative melting degree days (Cummdd) were calculated for days when the maximum temperature exceeded 32° F. The cold indicator was named Maxinrow, or the number of consecutive days when the maximum temperature was less than 32° F. Similar variables for

Table 6. Potential predictors used in model building. The prediction day is "today", the previous day is "yesterday", and "previous" means the observation before the most recent. See Figure 3 for a graphical explanation.

Predictor	Abbreviation	Physical role
Measured		
Maximum temperature (yesterday)	Max	shortwave, sensible
Minimum temperature (today)	Min	longwave,sensible,latent
Mean temperature $\{(Max + Min)/2\}$	Mean	allwave
Yesterday's precipitation	Oldppt	water balance
Yesterday's snowfall	Oldsnfl	water balance
7:00 a.m. snow depth (today)	Snowdepth	water balance
Derived		
Square root of snow depth (today)	Sqrtsndp	water balance
Cumulative melting degree days (the running total of $(Max - 32^{\circ}F.)$,for successive days with $Max > 32^{\circ}F.$)	Cummd	allwave, latent
Consecutive days with $Max < 32^{\circ}F.$	Maxinrow	water balance
Consecutive days with $Max > 32^{\circ}F.$	Hotmax	allwave, sensible
Consecutive days with $Min < 32^{\circ}F.$	Mininrow	water balance
Consecutive days with $Min > 32^{\circ}F.$	Hotmin	allwave, latent,sensible
Consecutive days with $Mean < 32^{\circ}F.$	Meaninrow	water balance
Consecutive days with $Mean > 32^{\circ}F.$	Hotmean	allwave, latent,sensible
Previous maximum temperature	Oldmax	shortwave,sensible
Previous minimum temperature	Oldmin	longwave,sensible,latent
Previous mean temperature	Oldmean	allwave,sensible
Previous snow depth	Olddepth	water balance
Max - Min	Range	allwave, shortwave

minimum and mean temperature were developed, for consecutive cold days and also for warm days. For example, Hotmax was the number of consecutive days with a maximum temperature greater than 32° F.

Snowdepth and temperature information for the day before the day of the prediction were also included in the predictor list to investigate if previous information about the snowpack and temperature conditions would be useful.

To prepare the data for variable selection a quality control procedure was performed. Since depth of the snow is reported either as zero, as a trace if less than 2 inches, or as an integer if greater than or equal to 2 inches (5 cm), all observations reporting either zero or trace were removed from the data set. This also applied to zero or trace SWE values, other than those associated with less than 2-inch snow depths. Precipitation less than 0.01 inch and snowfall less than 0.1 inch, both defined as traces, were set to zero, and the variables in Table 6 not already in the data set were created for each SWE observation. In the exceedingly rare situation where a missing value for any variable was reported, the entire observation was removed from further consideration.

Schmidlin (1990), investigating several NWSOs in Indiana and Ohio, described some problems with daily summary datasets ranging from typographical errors to physically impossible values. For this work obvious keypunch errors were corrected, while lapses in continuity or logic were grounds for the omission of the entire observation. Such lapses typically involved dramatic changes in SWE not justified by additional snowfall or rainfall, or by temperature extremes. Removed observations amounted to a very small percentage of the 28- to 35-year datasets. In the worst case, 3 of

138 days with greater than two inches of snow on the ground at LaGuardia Airport in New York City were omitted from 33 years of January observations.

4.2 Exploratory Model Building

Binghamton, NY was arbitrarily selected to be the station used for initial model development. After the Binghamton data set had been assembled, it was divided by month. January days not following a day when rain had fallen were used. Rain-on-snow days were determined by separating all days when "yesterday's" precipitation was non-zero, snowfall was zero, and both maximum and minimum temperatures were above freezing. Rain on snow days defined in this manner amounted to approximately 5% of all observations and, due to rain's ability to dramatically affect SWE (see section 2.3), were set aside for later analysis. The small number of these days suggested they should be reserved until development had reached the point where all of the occurrences at the 15 NWSOs could be pooled, at least by month.

Half of the remaining January data were reserved for use in verification, by placing alternate observations into subsets. This method was used to produce 2 essentially independent data sets. It avoided the potential problem associated with separating a 34 year record into two 17-year periods. Selecting alternate observations reduced the possibility of missing a trend over the entire length of the data record, by developing a model with a subset dominated by a period of above- or below- normal snow seasons.

The developmental half of the data set for January was subjected to several analytical procedures involving least-squares regression. The best

possible R^2 value was obtained by regressing daily SWE against the entire potential predictor list (Table 6). This predictor list was then reduced with a stepwise selection procedure (Neter, et al., 1985; and Appendix A) using SWE as the dependent variable. It is worth noting that days following no precipitation events (solid or liquid) were used first to control against the influence of fresh snow on SWE values. This yielded snow depth (Snowdepth) and Maxinrow as predictors. When days following snow events were included, the variable selection procedure again yielded Snowdepth and Maxinrow, but also included yesterday's snowfall (Oldsnfl), and yesterday's precipitation (Oldppt) as predictors for today's SWE in Binghamton for January.

Standardized residual analysis of the multiple regression results, described in Appendix B, was used to determine if errors were normally distributed or whether transformations of the variables would be necessary (Neter, et al., 1985). Residual plots indicated increasing variance of predicted SWE as snowdepth increased. This suggested the need for a transformation of SWE. A test after Box and Cox (Draper & Smith, 1981; and Appendix C) indicated a square root transformation of SWE would make the residual variance nearly constant over the entire range of snow depth. This would also make the root mean squared error (RMSE) representative of the entire range of data (see Appendix C). Rerunning the selection procedure using the square root of SWE (sqrtSWE) as predictand produced the same predictors, but yielded curvature in the residuals when plotted against snow depth. This directly indicated the need for a transformation of snow depth, and the square root of snow depth (sqrtSndp) was substituted (see Appendix B for details). The resulting regression yielded normally distributed

residuals with essentially constant variance.

The calibrated model was verified by cross validating with the reserved half of the dataset. Root mean squared error and the coefficients of multiple correlation (R^2) were compared for the two dataset halves. The developmental half-set showed a R^2 of 64.9% and a RMSE of 0.2385, while the reserved half-set showed a slightly lower R^2 of 64.1% and a RMSE of 0.2393. Since both were quite similar, one more test remained before combining the data set halves and producing the final January Binghamton model. A bootstrap analysis was performed, whereby 20 samples equivalent in size to the half-data set were selected with replacement from the validation set. This served to create 20 new, essentially independent data sets. Step-wise regression utilizing the full potential predictor list (Table 6) was repeated for each of the new sets and the selected predictors were recorded and tallied. In all 20 runs sqrtSndp and Oldsnfl were both selected, while Maxinrow appeared 19 times and Oldppt 17 times. Meaninrow, selected 14 times, was the only other variable chosen in more than 8 runs out of 20. Since the 4 predictors were selected in most of the 20 runs, the variables were considered stable. The final parameter estimates were determined by combining both halves of the data set and again regressing sqrtSWE against the 4 predictors. For completeness a 5-variable model including Meaninrow was run, and the improvement in R^2 of 0.5% was deemed not sufficient to complicate the final 4-variable model with an extra predictor.

4.3 Results of Model Development

The final model for Binghamton in January used `sqrtSndp`, `Maxinrow`, `Oldsnfl`, and `Oldppt` to predict `sqrtSWE` for all January days with snow on the ground, except those preceded by a day with rain. These predictors were then used on the remaining New York and New England NWSOs, after the data set for each station had been checked, corrected, additional variables had been created, and rain on snow days had been reserved. For each station the full data set was analyzed, first with all of the possible predictors, then with stepwise selection, and finally with the variables selected for Binghamton.

In most cases the stepwise procedure selected the same variables for the other 14 stations as had been selected for Binghamton. At this point 15 models for January existed, but the ultimate goal was to develop the simplest, yet most widely applicable model. Such a model would utilize the same variables, if possible, at all locations. Since this step of the procedure had shown that `sqrtSndp`, `Maxinrow`, `Oldsnfl`, and `Oldppt` were significant predictors at most of the 15 offices, it was decided to force the same predictors on all of the stations for the rest of the winter months.

Models using the same predictors were produced for December and February with virtually the same range for R^2 and RMSEs as January. Tables 7, 8, and 9 show the parameter estimates, the RMSE, and the R^2 for each station, for December, January, and February, respectively. The R^2 indicates that between 43.3% and 87.5% of the variation in `sqrtSWE` was described by the models for the winter months, with a median value of 66.0%. RMSEs ranged from 0.054 at LaGuardia-NYC in December to 0.434 at

Concord in February. With the exception of Oldppt, parameter estimates were very similar from station to station within months. All were of the same order of magnitude for each variable, and Oldppt coefficients exhibited more variability than the others.

Tables 7, 8, and 9 also show the R^2 and RMSE when all potential predictors in Table 6 are regressed against sqrtSWE. During the entire winter period, several stations showed a loss of R^2 in excess of 5% and a corresponding increase in RMSE when the 4-variable model was compared with the model using all of the potential predictors. While reducing the number of predictors in a model will also reduce the R^2 , some of the observed losses may have been larger than this would explain. This indicates that at these stations, predictors other than those developed for Binghamton may have been slightly more appropriate.

Table 7. Final four variable December models for 15 NWSOs in New York and New England. Rain on snow days not included. The dependent variable is sqrtSWE, and the variables were those selected for Binghamton in January and forced on December data. "Best r-squared" and "lowest RMSE" refer to the statistics for models when all potential predictors are forced (see Table 6). Units are inches for oldsnfl and oldppt, and square root of inches for sqrtSndp.

dataset	n	best		4 variable model				oldsnfl	oldppt
		r-squared	RMSE	r-squared	RMSE	constant	sqrtSndp		
Albany	333	0.752	0.168	0.725	0.174	0.029	0.374	-0.014	0.350
Binghamton	438	0.603	0.201	0.555	0.211	-0.058	0.395	-0.010	0.554
Boston	134	0.699	0.163	0.660	0.167	0.043	0.395	-0.020	0.168
Bridgeport	75	0.698	0.121	0.590	0.132	0.089	0.310	-0.023	0.428
Buffalo	394	0.820	0.148	0.788	0.159	-0.060	0.386	0.000	0.217
Burlington	486	0.786	0.143	0.770	0.147	0.003	0.336	-0.013	0.252
Caribou	799	0.773	0.218	0.755	0.225	0.012	0.384	-0.008	0.203
Concord	450	0.623	0.232	0.522	0.258	0.065	0.378	-0.038	0.371
Hartford	222	0.739	0.172	0.656	0.194	-0.045	0.424	-0.025	0.262
LaGuardia NYC	49	0.933	0.045	0.875	0.054	0.063	0.286	-0.025	0.047
Portland	404	0.760	0.195	0.719	0.209	-0.035	0.405	-0.022	0.375
Providence	131	0.508	0.196	0.433	0.203	0.097	0.333	-0.022	0.228
Rochester	381	0.700	0.163	0.655	0.173	-0.067	0.403	-0.003	0.445
Syracuse	318	0.681	0.149	0.647	0.154	-0.080	0.338	-0.004	0.367
Worcester	275	0.540	0.258	0.481	0.269	0.168	0.329	-0.022	0.437

Table 8. Final four variable January models for 15 NWSOs in New York and New England. Rain on snow days not included. The dependent variable is sqrtSWE, and the variables were selected by stepwise regression. "Best r-squared" and "lowest RMSE" refer to the statistics for models when all potential predictors are forced (see Table 6). Units are inches for oldsnfl and oldppt, and square root of inches for sqrtSndp.

dataset	n	best		lowest		4 variable model				oldsnfl	oldppt
		r-squared	RMSE	r-squared	RMSE	constant	sqrtSndp	maxinrow			
Albany	586	0.773	0.197	0.747	0.205	-0.038	0.436	-0.004		-0.077	0.519
Binghamton	688	0.668	0.232	0.639	0.240	-0.103	0.493	-0.013		-0.069	0.378
Boston	307	0.771	0.171	0.748	0.176	-0.005	0.413	-0.021		-0.055	0.420
Bridgeport	242	0.658	0.152	0.614	0.158	0.046	0.354	-0.016		-0.045	0.263
Buffalo	620	0.724	0.271	0.710	0.275	-0.070	0.434	-0.006		-0.052	0.317
Burlington	770	0.716	0.211	0.678	0.223	-0.004	0.380	-0.007		-0.049	0.295
Caribou	960	0.680	0.328	0.642	0.344	0.140	0.386	-0.007		-0.043	0.405
Concord	760	0.544	0.312	0.442	0.342	0.161	0.375	-0.004		-0.060	0.441
Hartford	456	0.655	0.224	0.570	0.247	0.129	0.378	-0.012		-0.051	0.270
LaGuardia NYC	135	0.890	0.074	0.857	0.080	-0.018	0.326	-0.004		-0.051	0.545
Portland	718	0.703	0.292	0.667	0.306	-0.038	0.476	-0.030		-0.060	0.286
Providence	289	0.560	0.163	0.433	0.181	0.260	0.261	0.010		-0.039	0.236
Rochester	651	0.675	0.220	0.589	0.245	0.011	0.422	-0.011		-0.065	0.540
Syracuse	748	0.610	0.247	0.552	0.263	-0.011	0.390	0.002		-0.077	0.670
Worcester	490	0.667	0.213	0.625	0.223	0.332	0.277	-0.009		-0.047	0.350

Table 9. Final four variable February models for 15 NWSOs in New York and New England. Rain on snow days not included. The dependent variable is sqrtSWE, and the variables were those selected for Binghamton in January and forced on February data. "Best r-squared" and "lowest RMSE" refer to the statistics for models when all potential predictors are forced (see Table 6). Units are inches for oldsnfl and oldppt, and square root of inches for sqrtSndp.

dataset	n	best		4 variable model				maxinrow	oldsnfl	oldppt
		r-squared	RMSE	r-squared	RMSE	constant	sqrtSndp			
Albany	518	0.519	0.289	0.497	0.293	0.133	0.394	-0.007	-0.087	0.660
Binghamton	589	0.639	0.284	0.583	0.302	0.068	0.458	-0.010	-0.071	0.328
Boston	252	0.782	0.183	0.682	0.217	0.135	0.372	-0.018	-0.059	0.363
Bridgeport	191	0.641	0.210	0.554	0.228	0.077	0.372	-0.022	-0.034	0.112
Buffalo	526	0.819	0.273	0.794	0.288	-0.317	0.576	-0.011	-0.085	0.442
Burlington	701	0.717	0.257	0.691	0.267	-0.077	0.459	-0.012	-0.068	0.486
Caribou	913	0.734	0.319	0.683	0.347	0.266	0.411	-0.008	-0.058	0.331
Concord	697	0.504	0.410	0.439	0.434	0.244	0.393	0.014	-0.088	0.594
Hartford	350	0.700	0.225	0.617	0.251	0.071	0.400	-0.018	-0.059	0.296
LaGuardia NYC	143	0.835	0.155	0.761	0.180	-0.122	0.390	-0.004	-0.033	0.189
Portland	651	0.687	0.352	0.677	0.355	-0.070	0.529	-0.008	-0.094	0.477
Providence	232	0.863	0.167	0.807	0.195	0.042	0.403	-0.025	-0.067	0.396
Rochester	605	0.714	0.253	0.677	0.266	0.019	0.474	-0.016	-0.064	0.316
Syracuse	464	0.770	0.257	0.707	0.287	-0.047	0.451	-0.022	-0.078	0.634
Worcester	457	0.702	0.249	0.663	0.262	0.213	0.286	-0.003	-0.042	0.359

A parameter estimate divided by its standard error yields its t-ratio. When sample sizes greater than 30 are used, as was the case with all winter month data, the t- distribution resembles the normal distribution. Calculated t-ratios greater than 1.96 indicate a significant predictor at the 95% confidence level, when the variable in question is in a model with other variables. In other words, in multiple regression the t-ratio for a variable's parameter estimate also depends on the presence of other predictors.

Tables 10, 11, and 12 give the t-ratios for the constant and 4 predictors at all 15 stations, for December, January and February. In 34 of the 44 remaining data sets from the three winter months, the variables chosen for Binghamton in January were also all significant predictors. It is clear from t-ratios that removing sqrtSndp would result in a greater loss in the model's ability to describe sqrtSWE variability than would the removal of any of the other three predictors. Oldsnfl and Oldppt are fairly consistent in their importance, while the significance of Maxinrow varies between months and stations. In December, Maxinrow was not a significant predictor at Buffalo, Rochester, or Syracuse, while Oldsnfl and Oldppt were not significant at LaGuardia-NYC. In January, Concord, LaGuardia-NYC, and Syracuse did not show Maxinrow to be a significant predictor. In February, Maxinrow was not significant at LaGuardia-NYC, Portland, or Worcester, nor was Oldsnfl significant at Hartford or LaGuardia-NYC.

Maxinrow's lack of significance as a predictor for Great Lakes and coastal stations at various times during the winter months may simply be a factor of the warming influence of adjacent bodies of water. Sustained sub-freezing maximum temperatures may only be of short duration at these

Table 10. T-ratios for December parameter estimates. With sample sizes greater than 30, the t-distribution resembles the Normal distribution. T-ratio absolute values greater than 1.96 indicate significance at the 95% confidence level.

dataset	constant	sqrtsndp	maxinrow	oldsnfl	oldppt
Albany	0.96	25.64	-3.67	-6.37	5.01
Binghamton	-1.61	20.45	-3.31	-6.40	5.55
Boston	0.77	14.47	-2.66	-3.76	3.27
Bridgeport	1.24	8.16	-2.56	-2.84	3.35
Buffalo	-2.39	35.29	-0.10	-7.12	3.85
Burlington	0.16	37.32	-7.04	-6.35	5.03
Caribou	0.50	48.94	-5.27	-6.34	3.69
Concord	1.57	21.43	-7.24	-5.80	5.05
Hartford	-0.91	18.89	-3.94	-5.22	4.62
LaGuardia-NYC	2.01	16.18	-2.99	-0.76	0.68
Portland	-1.12	30.06	-4.66	-8.72	7.87
Providence	1.18	8.10	-2.72	-3.18	4.58
Rochester	-2.06	25.00	-0.65	-8.41	6.06
Syracuse	-2.33	20.12	-0.84	-6.20	5.16
Worcester	3.24	14.51	-3.29	-5.08	5.69

Table 11. T-ratios for January parameter estimates. With sample sizes greater than 30, the t distribution resembles the Normal distribution. Usually t-ratio absolute values greater than 1.96 indicate significance at the 95% confidence level, but since these variables were selected by a stepwise procedure, the t-ratios correspond to an inflated significance level.

dataset	constant	sqrtsndp	maxinrow	oldsnfl	oldppt
Albany	-1.38	37.97	-2.44	-10.46	7.09
Binghamton	-3.12	33.57	-8.99	-8.54	4.77
Boston	-0.16	28.24	-5.43	-6.91	7.25
Bridgeport	1.13	18.72	-3.34	-4.11	3.00
Buffalo	-2.02	30.62	-2.68	-5.25	2.80
Burlington	-0.14	36.89	-5.70	-6.61	3.57
Caribou	3.59	40.83	-4.99	-4.12	3.39
Concord	3.36	23.26	-1.25	-5.89	4.69
Hartford	3.39	22.37	-3.16	-5.28	3.37
LaGuardia-NYC	-0.74	24.71	-1.45	-6.30	6.97
Portland	-1.08	36.50	-8.18	-7.52	5.31
Providence	6.45	12.96	2.83	-4.23	3.71
Rochester	0.33	28.13	-4.28	-6.80	4.50
Syracuse	-0.32	28.55	1.09	-9.96	6.53
Worcester	11.41	27.75	-3.66	-6.03	5.95

Table 12. T-ratios for February parameter estimates. With sample sizes greater than 30, the t distribution resembles the Normal distribution. T-ratio absolute values greater than 1.96 indicate significance at the 95% confidence level.

dataset	constant	sqrtsndp	maxinrow	oldsnfl	oldppt
Albany	2.99	22.00	-2.04	-6.84	4.85
Binghamton	1.68	28.24	-5.63	-7.20	3.54
Boston	3.24	21.49	-2.97	-5.52	5.26
Bridgeport	1.32	14.62	-3.10	-2.00	0.88
Buffalo	-8.85	39.65	-5.85	-5.86	2.91
Burlington	-2.33	39.16	-8.75	-6.64	4.66
Caribou	6.59	43.70	-5.95	-4.81	2.51
Concord	4.39	22.71	3.00	-5.95	4.19
Hartford	1.69	23.35	-4.13	-5.74	3.58
LaGuardia-NYC	-2.86	19.57	-0.97	-3.06	1.93
Portland	-1.60	36.26	-1.85	-8.03	5.18
Providence	1.22	30.36	-4.37	-5.61	4.05
Rochester	0.59	34.16	-6.18	-6.59	2.98
Syracuse	-1.22	31.82	-6.09	-8.41	5.56
Worcester	6.70	29.18	-0.94	-5.82	5.39

sites and a Maxinrow value of 1 or 2 would not appreciably affect the sqrtSWE. Non-significant Oldsnfl or Oldppt may indicate infrequent snow events followed by several days of snowcover. In these cases Oldsnfl and Oldppt are set to zero most of the time.

The limited usefulness of Maxinrow during short duration cold periods becomes more evident when using the same predictors in November, March, and April. Tables 13, 14, and 15 show parameter estimates and statistics for these months. Tables 16, 17, and 18 contain the corresponding t-ratios for the parameter estimates. In March R^2 ranges from 41.1% for Providence to 90.3% for LaGuardia-NYC and RMSE ranges from 0.066 for LaGuardia-NYC to 0.388 for Concord. This month also has 8 of 15 stations where Maxinrow is not a significant predictor, half of which are Atlantic coastal locations. Some of these also exhibited a large decrease in R^2 and increase in RMSE from the model including all potential predictors. November and April are only included for completeness, since sample sizes show that for most stations an average of only one day with a significant snowpack occurs per year in these months. Note from the R^2 values that only Caribou and Portland, ME have meaningful models for April, although their RMSEs are both in excess of 0.4.

Table 13. Final four-variable November models for 15 NWSOs in New York and New England. Rain on snow days not included. The dependent variable is sqrtSWE. "Best r-squared" and "lowest RMSE" refer to the statistics for the models using all potential predictors (Table 6). Only those stations with at least 32 observations for the entire period of record included.

dataset	best		lowest	4 variable model						
	n	r-squared	RMSE	r-squared	RMSE	constant	sqrtsndp	maxinrow	oldsnfl	oldppt
Albany	42	0.867	0.124	0.578	0.192	0.181	0.316	-0.023	-0.043	0.342
Binghamton	87	0.671	0.164	0.545	0.182	-0.031	0.406	-0.043	-0.044	0.178
Boston	3	-	-	-	-	-	-	-	-	-
Bridgeport	0	-	-	-	-	-	-	-	-	-
Buffalo	73	0.770	0.107	0.753	0.103	-0.044	0.331	-0.002	-0.026	0.278
Burlington	84	0.608	0.121	0.543	0.123	0.034	0.286	-0.011	-0.026	0.284
Caribou	227	0.825	0.135	0.809	0.139	-0.033	0.379	-0.016	-0.023	0.125
Concord	62	0.440	0.168	0.324	0.169	0.280	0.215	0.017	-0.028	0.250
Hartford	15	-	-	-	-	-	-	-	-	-
LaGuardia-NYC	1	-	-	-	-	-	-	-	-	-
Portland	31	-	-	-	-	-	-	-	-	-
Providence	5	-	-	-	-	-	-	-	-	-
Rochester	62	0.774	0.127	0.720	0.130	-0.201	0.463	0.009	-0.059	0.457
Syracuse	57	0.662	0.170	0.587	0.171	-0.129	0.408	0.004	-0.039	0.320
Worcester	39	0.762	0.158	0.612	0.172	0.147	0.294	-0.023	-0.035	0.294

Table 14. Final four-variable March models for 15 NWSOs in New York and New England. Rain on snow days not included. The dependent variable is sqrtSWE. "Best r-squared" and "lowest RMSE" refer to the statistics for the models using all potential predictors (Table 6).

dataset	n	best		lowest	4 variable model						
		n	r-squared	RMSE	r-squared	RMSE	constant	sqrtsndp	maxinrow	oldsnfl	oldppt
Albany	257		0.646	0.204	0.572	0.220	0.138	0.391	-0.011	-0.084	0.523
Binghamton	340		0.647	0.268	0.597	0.282	0.073	0.506	-0.002	-0.077	0.195
Boston	141		0.737	0.227	0.673	0.244	0.042	0.451	-0.022	-0.085	0.401
Bridgeport	55		0.546	0.154	0.422	0.157	0.241	0.226	0.006	-0.058	0.575
Buffalo	219		0.762	0.233	0.625	0.287	-0.062	0.506	-0.019	-0.090	0.396
Burlington	434		0.752	0.271	0.717	0.286	-0.071	0.522	-0.019	-0.097	0.509
Caribou	877		0.782	0.320	0.683	0.384	0.417	0.404	-0.015	-0.028	-0.078
Concord	458		0.625	0.375	0.589	0.388	0.202	0.427	0.036	-0.072	0.247
Hartford	192		0.557	0.278	0.450	0.303	0.083	0.467	-0.054	-0.071	0.192
LaGuardia-NYC	46		0.917	0.069	0.903	0.066	0.033	0.296	0.000	-0.015	0.138
Portland	432		0.714	0.348	0.689	0.359	0.192	0.503	-0.080	-0.095	0.318
Providence	114		0.563	0.239	0.411	0.265	0.237	0.321	0.037	-0.064	0.212
Rochester	284		0.763	0.262	0.725	0.278	-0.089	0.532	-0.013	-0.076	0.281
Syracuse	274		0.666	0.293	0.649	0.295	-0.140	0.551	-0.046	-0.085	0.267
Worcester	300		0.651	0.276	0.565	0.304	0.290	0.293	-0.011	-0.044	0.330

Table 16. T-ratios for November parameter estimates. With sample sizes greater than 30, the t-distribution resembles the Normal distribution. T-ratio absolute values greater than 1.96 indicate significance at the 95% confidence level. Only stations with more than 32 observations in the entire data record included.

dataset	constant	sqrtsndp	maxinrow	oldsnfl	oldppt
Albany	1.82	6.41	-0.47	-2.13	1.67
Binghamton	-0.39	9.46	-2.57	-3.29	1.98
Boston	-	-	-	-	-
Bridgeport	-	-	-	-	-
Buffalo	-0.83	11.92	-0.08	-2.95	3.77
Burlington	0.55	8.39	-0.83	-2.49	2.93
Caribou	-1.18	29.26	-3.34	-3.78	2.39
Concord	3.00	4.46	0.57	-2.02	2.38
Hartford	-	-	-	-	-
LaGuardia-NYC	-	-	-	-	-
Portland	-	-	-	-	-
Providence	-	-	-	-	-
Rochester	-2.48	10.37	0.31	-4.61	4.47
Syracuse	-1.29	7.16	0.12	-2.50	2.90
Worcester	1.39	6.46	-0.60	-2.95	3.12

Table 17. T-ratios for March parameter estimates. With sample sizes greater than 30, the t-distribution resembles the Normal distribution. T-ratio absolute values greater than 1.96 indicate significance at the 95% confidence level.

dataset	constant	sqrtsndp	maxinrow	oldsnfl	oldppt
Albany	2.76	17.77	-1.33	-6.47	4.57
Binghamton	1.34	21.11	-0.67	-5.27	1.54
Boston	0.65	16.68	-0.66	-5.00	3.61
Bridgeport	2.51	4.30	0.42	-3.12	3.86
Buffalo	-0.99	17.45	-2.66	-5.35	3.11
Burlington	-1.62	32.74	-4.10	-6.73	3.52
Caribou	10.36	42.97	-5.54	-2.10	-0.49
Concord	3.70	25.20	2.15	-4.43	1.59
Hartford	0.98	12.32	-2.22	-3.66	1.29
LaGuardia-NYC	0.97	17.34	-0.03	-1.88	2.06
Portland	3.58	30.22	-4.82	-7.44	3.33
Providence	2.54	7.65	1.45	-4.58	2.04
Rochester	-1.77	22.70	-1.83	-6.59	2.19
Syracuse	-2.47	21.87	-5.55	-5.18	1.65
Worcester	6.18	18.70	-0.92	-3.87	4.09

Table 18. T-ratios for April parameter estimates. With sample sizes greater than 30, the t-distribution resembles the Normal distribution. T-ratio absolute values greater than 1.96 indicate significance at the 95% confidence level. Only stations with more than 32 observations in the entire data record included.

dataset	constant	sqrtsndp	maxinrow	oldsnfl	oldppt
Albany	-	-	-	-	-
Binghamton	0.59	3.24	-1.23	-1.96	0.43
Boston	-	-	-	-	-
Bridgeport	-	-	-	-	-
Buffalo	-	-	-	-	-
Burlington	1.38	4.21	-1.53	-0.33	-1.16
Caribou	3.58	25.84	-1.84	-2.55	-0.13
Concord	-	-	-	-	-
Hartford	-	-	-	-	-
LaGuardia-NYC	-	-	-	-	-
Portland	0.83	4.7	-0.52	-1.57	0.54
Providence	-	-	-	-	-
Rochester	-	-	-	-	-
Syracuse	-	-	-	-	-
Worcester	-	-	-	-	-

To give an indication of the accuracy of the models, Table 19 shows 67% prediction intervals, representing values of SWE plus or minus one RMSE for selected levels of untransformed SWE and a range of RMSEs. The wide range at higher actual SWE values is at first disturbing, but quite reasonable when a scatterplot of SWE against snow depth is viewed (see Figure 4). With increasing snow depth, SWE also increases, but becomes more variable. Figure 5 graphically displays the widening prediction interval for an RMSE of 0.25. The slight asymmetry is attributable to the squaring of the untransformed upper and lower limits. Worthy of note is that even at higher values of SWE, 67% of the predictions fall within about $\pm 15\%$ of the observed values.

Table 19. Prediction intervals for values of SWE. Models using sqrtSWE as the dependent variable each have an associated RMSE. The 67% prediction intervals shown below are calculated as follows. SqrtSWE plus or minus one RMSE gives untransformed upper and lower limits. Both are then squared to give 67% prediction limits around actual SWE values.

SWE (inches)	RMSE for sqrtSWE as the dependent variable			
	0.05	0.15	0.2	0.25
0.1	0.073, 0.137	0.030, 0.221	0.014, 0.270	0.004, 0.325
0.25	0.203, 0.303	0.123, 0.423	0.090, 0.490	0.063, 0.563
0.5	0.436, 0.578	0.314, 0.740	0.260, 0.828	0.212, 0.922
1	0.903, 1.110	0.723, 1.323	0.640, 1.440	0.563, 1.563
1.5	1.369, 1.613	1.145, 1.877	1.040, 2.016	0.941, 2.161
2	1.850, 2.132	1.588, 2.434	1.464, 2.592	1.346, 2.756
3	2.822, 3.168	2.496, 3.534	2.341, 3.725	2.190, 3.920
4	3.803, 4.203	3.423, 4.623	3.240, 4.840	3.063, 5.063
5	4.796, 5.244	4.368, 5.712	4.162, 5.954	3.960, 6.200
6	5.760, 6.250	5.290, 6.760	5.063, 7.023	4.840, 7.290
7	6.760, 7.290	6.250, 7.840	6.003, 8.123	5.760, 8.410
8	7.728, 8.294	7.182, 8.880	6.917, 9.181	6.656, 9.487
9	8.703, 9.303	8.123, 9.923	7.840, 10.24	7.563, 10.56
10	9.672, 10.30	9.060, 10.96	8.762, 11.29	8.468, 11.63

Table 19 (continued)

SWE (inches)	RMSE for sqrtSWE as the dependent variable		
	0.3	0.35	0.4
0.1	0.000, 0.384	0.001, 0.449	0.006, 0.518
0.25	0.040, 0.640	0.023, 0.723	0.010, 0.810
0.5	0.168, 1.020	0.130, 1.124	0.096, 1.232
1	0.490, 1.690	0.423, 1.823	0.360, 1.960
1.5	0.846, 2.310	0.757, 2.465	0.672, 2.624
2	1.232, 2.924	1.124, 3.098	1.020, 3.276
3	2.045, 4.121	1.904, 4.326	1.769, 4.537
4	2.890, 5.290	2.723, 5.523	2.560, 5.760
5	3.764, 6.452	3.572, 6.708	3.386, 6.967
6	4.623, 7.563	4.410, 7.840	4.203, 8.123
7	5.523, 8.703	5.290, 9.000	5.063, 9.303
8	6.401, 9.797	6.150, 10.11	5.905, 10.43
9	7.290, 10.89	7.023, 11.22	6.760, 11.56
10	8.180, 11.97	7.896, 12.32	7.618, 12.67

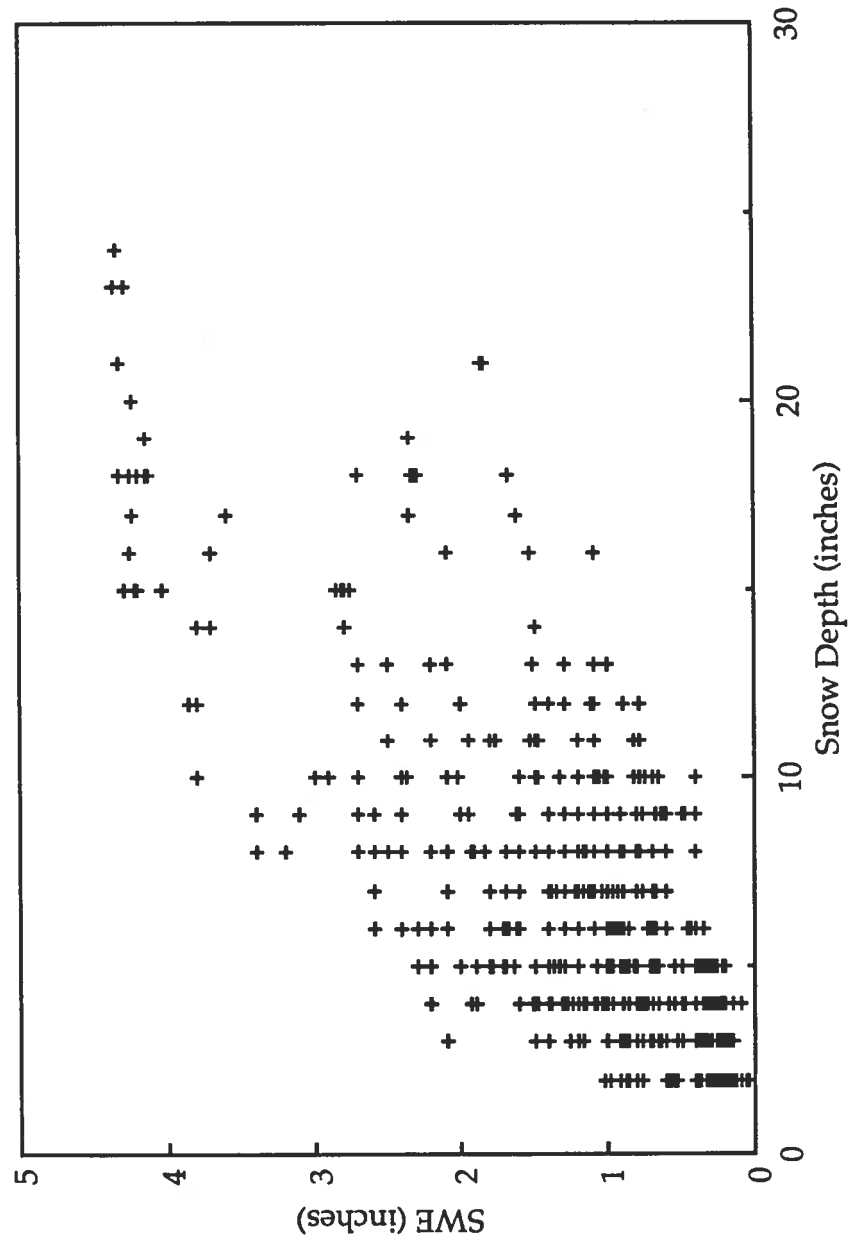


Figure 4. Snowpack water equivalent plotted against snow depth for Binghamton data in January

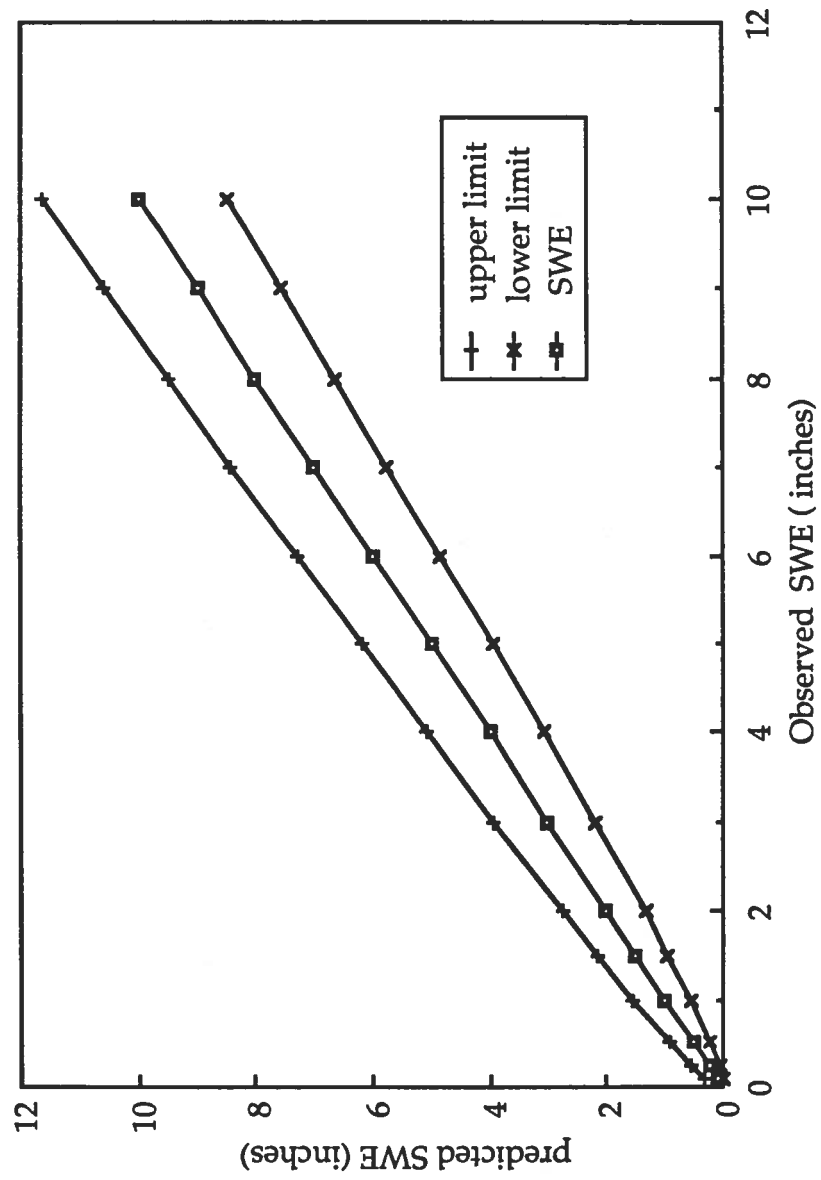


Figure 5. Example 67% prediction limits for $RMSE = 0.25$.

4.4 Comparison of New Models with Degree-Day Models

What must be considered at this point is whether these new models are an improvement over the traditional degree-day models (e.g.; Table 2). Such a comparison may also determine if degree-day models, or at least the inclusion of a degree-day term, would be more appropriate in the autumn and spring months. In other words, would the large decrease in R^2 between the full prediction model and the 4-variable model be less extreme if Cummdd, the cumulative number of degrees with the maximum temperature greater than freezing, were substituted for Maxinrow? It should be noted that for this test no variable selection trials were performed; Cummdd was included as the fourth variable with sqrtSndp, Oldsnfl, and Oldppt. The results of both four variable models for the winter months are presented in tables 20, 21, and 22 in terms of R^2 and RMSE. It is clear that although most stations and months showed very little difference in R^2 and RMSE between the models, the models incorporating Maxinrow are almost always slightly better than the Cummdd models. The same comparisons were performed for November, March, and April, and the results are shown in Tables 23, 24, and 25. Although the Cummdd models show slightly improved performance in these months, the Maxinrow models are still usually better. In general, substituting Cummdd for Maxinrow does not regain any of the precision lost when the full models are reduced to the four-variable models. Substituting Cummdd for Maxinrow would just increase the prediction interval range by approximately 0.15 inches (3.5 mm) in the most extreme case of a 10 inch (25 cm) SWE value for Concord in December.

Table 20. December comparisons between Cummdd and Maxinrow models. 4-variable models incorporating sqrtSndp, Oldsnfl, and Oldppt, with Maxinrow or Cummdd as the fourth variable.

Station	December Cummdd		December Maxinrow	
	RMSE	r-squared	RMSE	r-squared
Albany	0.177	0.715	0.174	0.725
Binghamton	0.213	0.546	0.211	0.555
Boston	0.172	0.641	0.167	0.660
Bridgeport	0.137	0.553	0.132	0.590
Buffalo	0.159	0.789	0.159	0.788
Burlington	0.154	0.748	0.147	0.770
Caribou	0.229	0.746	0.225	0.755
Concord	0.270	0.477	0.258	0.522
Hartford	0.199	0.633	0.194	0.656
LaGuardia-NYC	0.049	0.897	0.054	0.875
Portland	0.213	0.706	0.209	0.719
Providence	0.208	0.400	0.203	0.433
Rochester	0.173	0.654	0.173	0.655
Syracuse	0.155	0.647	0.154	0.647
Worcester	0.274	0.461	0.269	0.481

Table 21. January comparisons between Cummdd and Maxinrow models. 4-variable models incorporating sqrtSndp, Oldsnfl, and Oldppt, with Maxinrow or Cummdd as the fourth variable.

Station	January Cummdd		January Maxinrow	
	RMSE	r-squared	RMSE	r-squared
Albany	0.206	0.744	0.205	0.747
Binghamton	0.252	0.601	0.240	0.639
Boston	0.185	0.723	0.176	0.748
Bridgeport	0.161	0.597	0.158	0.614
Buffalo	0.276	0.708	0.275	0.710
Burlington	0.224	0.674	0.223	0.678
Caribou	0.345	0.639	0.344	0.642
Concord	0.333	0.471	0.342	0.442
Hartford	0.248	0.564	0.247	0.570
LaGuardia-NYC	0.080	0.857	0.080	0.857
Portland	0.315	0.649	0.306	0.667
Providence	0.184	0.417	0.181	0.433
Rochester	0.248	0.581	0.245	0.589
Syracuse	0.261	0.556	0.263	0.552
Worcester	0.225	0.618	0.223	0.625

Table 22. February comparisons between Cummdd and Maxinrow models. 4-variable models incorporating sqrtSndp, Oldsnfl, and Oldppt, with Maxinrow or Cummdd as the fourth variable.

Station	February Cummdd		February Maxinrow	
	RMSE	r-squared	RMSE	r-squared
Albany	0.293	0.496	0.293	0.497
Binghamton	0.306	0.572	0.302	0.583
Boston	0.218	0.677	0.217	0.682
Bridgeport	0.230	0.550	0.228	0.554
Buffalo	0.294	0.786	0.288	0.794
Burlington	0.277	0.668	0.267	0.691
Caribou	0.344	0.689	0.347	0.683
Concord	0.436	0.432	0.434	0.439
Hartford	0.256	0.602	0.251	0.617
LaGuardia-NYC	0.163	0.805	0.180	0.763
Portland	0.355	0.677	0.355	0.677
Providence	0.195	0.807	0.195	0.807
Rochester	0.270	0.669	0.266	0.677
Syracuse	0.287	0.708	0.287	0.707
Worcester	0.257	0.676	0.262	0.663

Table 23. November comparisons between Cummdd and Maxinrow models. 4-variable models incorporating sqrtSndp, Oldsnfl, and Oldppt, with Maxinrow or Cummdd as the fourth variable. Only stations with more than 32 observations during the data record included.

Station	November Cummdd		November Maxinrow	
	RMSE	r-squared	RMSE	r-squared
Albany	0.179	0.632	0.192	0.578
Binghamton	0.186	0.523	0.182	0.545
Boston				
Bridgeport				
Buffalo	0.103	0.754	0.103	0.753
Burlington	0.123	0.542	0.123	0.543
Caribou	0.142	0.800	0.139	0.809
Concord	0.170	0.322	0.169	0.324
Hartford				
LaGuardia-NYC				
Portland				
Providence				
Rochester	0.127	0.732	0.130	0.720
Syracuse	0.171	0.588	0.171	0.587
Worcester	0.173	0.610	0.172	0.612

Table 24. March comparisons between Cummdd and Maxinrow models. 4-variable models incorporating sqrtSndp, Oldsnfl, and Oldppt, with Maxinrow or Cummdd as the fourth variable.

Station	March Cummdd		March Maxinrow	
	RMSE	r-squared	RMSE	r-squared
Albany	0.221	0.569	0.220	0.572
Binghamton	0.282	0.596	0.282	0.597
Boston	0.244	0.673	0.244	0.673
Bridgeport	0.156	0.426	0.157	0.422
Buffalo	0.291	0.613	0.287	0.625
Burlington	0.280	0.729	0.286	0.717
Caribou	0.375	0.698	0.384	0.683
Concord	0.387	0.591	0.388	0.589
Hartford	0.306	0.436	0.303	0.450
LaGuardia-NYC	0.065	0.905	0.066	0.903
Portland	0.359	0.688	0.359	0.689
Providence	0.267	0.405	0.265	0.411
Rochester	0.277	0.726	0.278	0.725
Syracuse	0.308	0.618	0.295	0.649
Worcester	0.299	0.580	0.304	0.565

Table 25. April comparisons between Cummdd and Maxinrow models. 4-variable models incorporating sqrtSndp, Oldsnfl, and Oldppt, with Maxinrow or Cummdd as the fourth variable. Only stations with more than 32 observations during the data record included.

Station	April Cummdd		April Maxinrow	
	RMSE	r-squared	RMSE	r-squared
Albany				
Binghamton	0.326	0.230	0.320	0.255
Boston				
Bridgeport				
Buffalo				
Burlington	0.304	0.301	0.301	0.318
Caribou	0.416	0.662	0.425	0.647
Concord				
Hartford				
LaGuardia-NYC				
Portland	0.389	0.515	0.406	0.472
Providence				
Rochester				
Syracuse				
Worcester				

A more precise test of the predictive ability of Cummdd was also performed. Since most degree-day models (Table 2) utilize only degree-days as a predictor for snowmelt, Cummdd alone was used to predict the daily change in untransformed SWE. The R^2 and RMSE obtained from January data, shown in Table 26, reveal that essentially no variation in the change in daily SWE is described by a model using Cummdd as sole predictor.

Table 26. Statistics for predicting the change in the daily SWE using only Cummdd as the predictor. January results only.

Station	RMSE	r-squared
Albany	0.250	0.001
Binghamton	0.254	0.000
Boston	0.393	0.010
Bridgeport	0.311	0.010
Buffalo	0.422	0.000
Burlington	0.364	0.000
Caribou	0.555	0.010
Concord	0.241	0.010
Hartford	0.271	0.026
LaGuardia-NYC	0.228	0.000
Portland	0.303	0.010
Providence	0.294	0.031
Rochester	0.269	0.000
Syracuse	0.236	0.000
Worcester	0.294	0.070

4.5 Discussion of Monthly Station Models

The wide range of R^2 values for stations in any given month may be attributed to a combination of different climatologies and measurement error. The type or types of snow which characterize a particular area are determined by the climatology of each location. For example, coastal stations usually receive snowfall from weather systems moving up the

Atlantic coastline. These tend to be very moist and warm, providing uniformly wet or high-density snow to the observing sites. This may explain the generally high R^2 values found at coastal stations.

The other extreme appears to be Concord, NH, with uniformly low R^2 values. This station is located far enough inland to be influenced not only by warm, moist coastal storms, but also colder systems moving up the Ohio Valley and across the Great Lakes, and cold Canadian outbreaks. These three scenarios probably result in a wide variation in snow characteristics, possibly accounting for low values of R^2 .

Other stations tend to be influenced by either Great Lakes systems alone, or only systems coming from Canada, resulting in less variability of snowpack characteristics and higher R^2 values.

The other influence on R^2 is measurement error, since three possible methods of determining SWE are in use. Schmidlin and Edgell (1989) investigated NWSOs in Indiana and Ohio and learned that a snowpack core may either be melted or weighed to determine SWE, or if neither method is feasible, SWE may be estimated. Since variability was found to exist between the techniques, the predictive ability among the models developed in this investigation may be affected. Further examination of this problem could lead to model improvements and is recommended.

The physical role of the 4 predictors is clear for all except Maxinrow. While *sqrtsndp*, *Oldsnfl*, and *Oldppt* are either components or related to components of the water balance of the snowpack, *Maxinrow* is unusual. It is highly correlated with cumulative freezing degree days (the running total of 32° F. - maximum temperature, for consecutive days with the maximum temperature less than freezing). Table 27 illustrates a consistent negative correlation between *Maxinrow* and the mean density of the snowpack for

Table 27. Correlation between Maxinrow and mean snowpack density by month.

Station	December	January	February
Albany	-0.438	-0.434	-0.257
Binghamton	-0.269	-0.465	-0.408
Boston	-0.475	-0.545	-0.316
Bridgeport	-0.574	-0.494	-0.402
Buffalo	-0.501	-0.393	-0.222
Burlington	-0.494	-0.401	-0.418
Caribou	-0.422	-0.461	-0.479
Concord	-0.496	-0.304	-0.024
Hartford	-0.554	-0.406	-0.495
LaGuardia-NYC	-0.448	-0.524	-0.238
Portland	-0.384	-0.456	-0.311
Providence	-0.403	-0.167	-0.396
Rochester	-0.322	-0.403	-0.402
Syracuse	-0.354	-0.318	-0.247
Worcester	-0.437	-0.465	-0.295

the 15 NWSOs in the three winter months. High mean snowpack density never occurs with larger values of Maxinrow , as is shown in Figure 6 for January Binghamton data. This points to Maxinrow as a weak guide to snowpack ripeness, or how close the snowpack is to being isothermal and at its free-water holding capacity. For most of the stations and months Maxinrow consistently serves to reduce the SWE. If Maxinrow equals zero then the square root of SWE may be that of a ripe or nearly ripe snowpack. If Maxinrow is non-zero the resulting water content is possibly being corrected for non-ripeness. Therefore, Maxinrow may also be describing a component of the snowpack water balance.

Perhaps a more intuitive approach would be to consider snowfall and snowpack characteristics under various temperature scenarios. A large Maxinrow indicates an extended period of below-freezing maximum temperatures. Snow falling under these conditions would probably be of low density, as would the resulting snowpack. Smaller values of Maxinrow could either indicate warmer conditions and a snowpack of higher density, or recent warming of a low-density pack. It would be more likely accompanied by snowfall of high density. Whichever the case, the result would be a snowpack of higher density with higher SWE than the snowpack under prolonged cold. Whereas the degree-day approach reduces daily melt to a constant value if the appropriate temperature falls below the base temperature and a constant term is present, Maxinrow as an indicator of thermal conditions does not fail below freezing, supporting the observation from data records that SWE decreases do occur with sub-freezing temperatures.

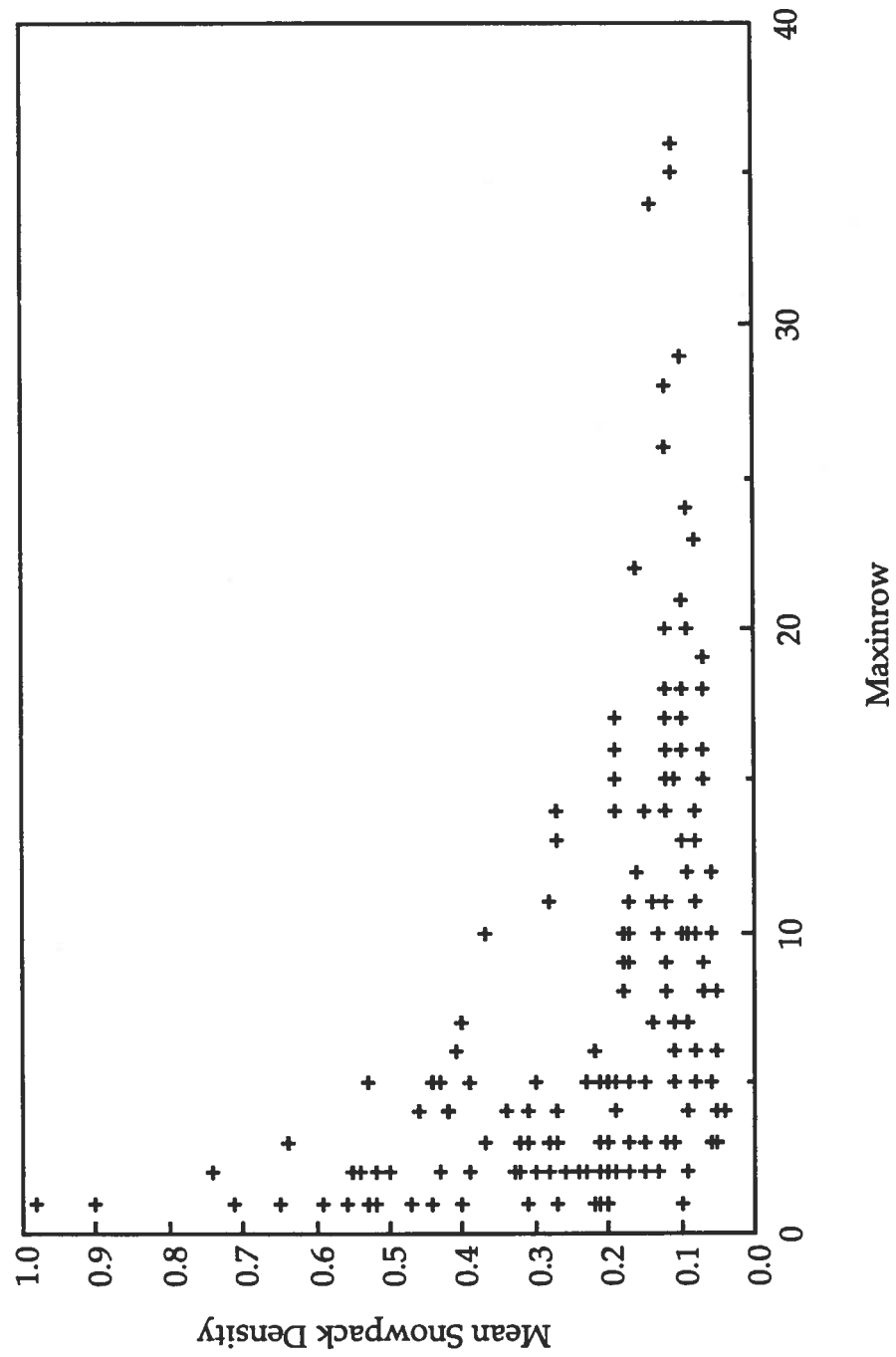


Figure 6. Mean snowpack density vs. Maxinrow for Binghamton in January

4.6 Development of Grouped Models

Since the same predictors were significant and their coefficients were similar for most of the stations in the winter months, the possibility of grouping suggested they be forced on all of the stations in December and February. The goal of producing a prediction model for Co-Op stations located between NWSOs could be greatly simplified by combining NWSO-derived equations, rather than having 3 monthly models for each of 15 stations during the winter. An approach not previously described in the snow literature was used to create models with wider applicability than provided by monthly station formulas.

Slope and intercept models with dummy variables is a method which can be used to group many stations and test whether one parameter estimate per variable is suitable for all stations within the group, or whether parameter estimates are site-specific (Neter, et al., 1985 and Appendix D). If the parameter estimate for each variable is suitable for all of the stations, and only the intercept terms are specific for each location, this analysis creates a family of parallel lines with separate intercepts for each station. The result is one model with more general application possibilities than the original 15 monthly station models.

Groups were subjectively formed which encompassed stations sharing geographic and topographic similarities, and are outlined in Figure 7. The groups checked included Coastal (Portland, Boston, Providence, Bridgeport, LaGuardia-New York City), Mountain (Caribou, Concord, Burlington, Albany, Worcester, Hartford), and Western New York (Buffalo, Rochester, Binghamton, Syracuse). The 15 stations were also combined into a single "Total" group. Tables 28, 29, and 30 (a-d) shows R^2 , RMSE, station

intercepts, and the parameter estimates for the various December, January, and February grouped models. Rain on snow days, previously reserved because of their infrequent occurrences, are included as a dummy variable functioning as a correction factor added to the intercept calculation.

Grouping across the three winter months of December, January and February resulted in an additional set of models. Table 31 (a-d) shows the three-month winter models for the geographic groups and the winter "Total" model involving all 15 stations. This grouping procedure not only created separate intercepts for each station, but also dummy variables which served to provide correction factors for month, and for those 5% of all observations which followed a day where rain fell on snow, as before. Although the R^2 for all of the grouped models varies, 72% of the variation in sqrtSWE is still being described by the "Total" winter model, with a RMSE of 0.28.

The correction factors for month show that for identical conditions less water is contained in the snowpack in January than February, and in December than in either of the other winter months. It is difficult to determine the reason for this situation. Perhaps it is more likely for later snowpacks to have undergone melting and refreezing. Percolation of liquid water through the snowpack followed by freezing may result in an increase in snowpack density due to the presence of ice. December snowpacks may have lower SWE values on average simply because they have not experienced as many freeze-thaw cycles. The rain-on-snow correction factor reflects the additional SWE present in a snowpack after receiving rain, compared to one which has not received liquid precipitation.

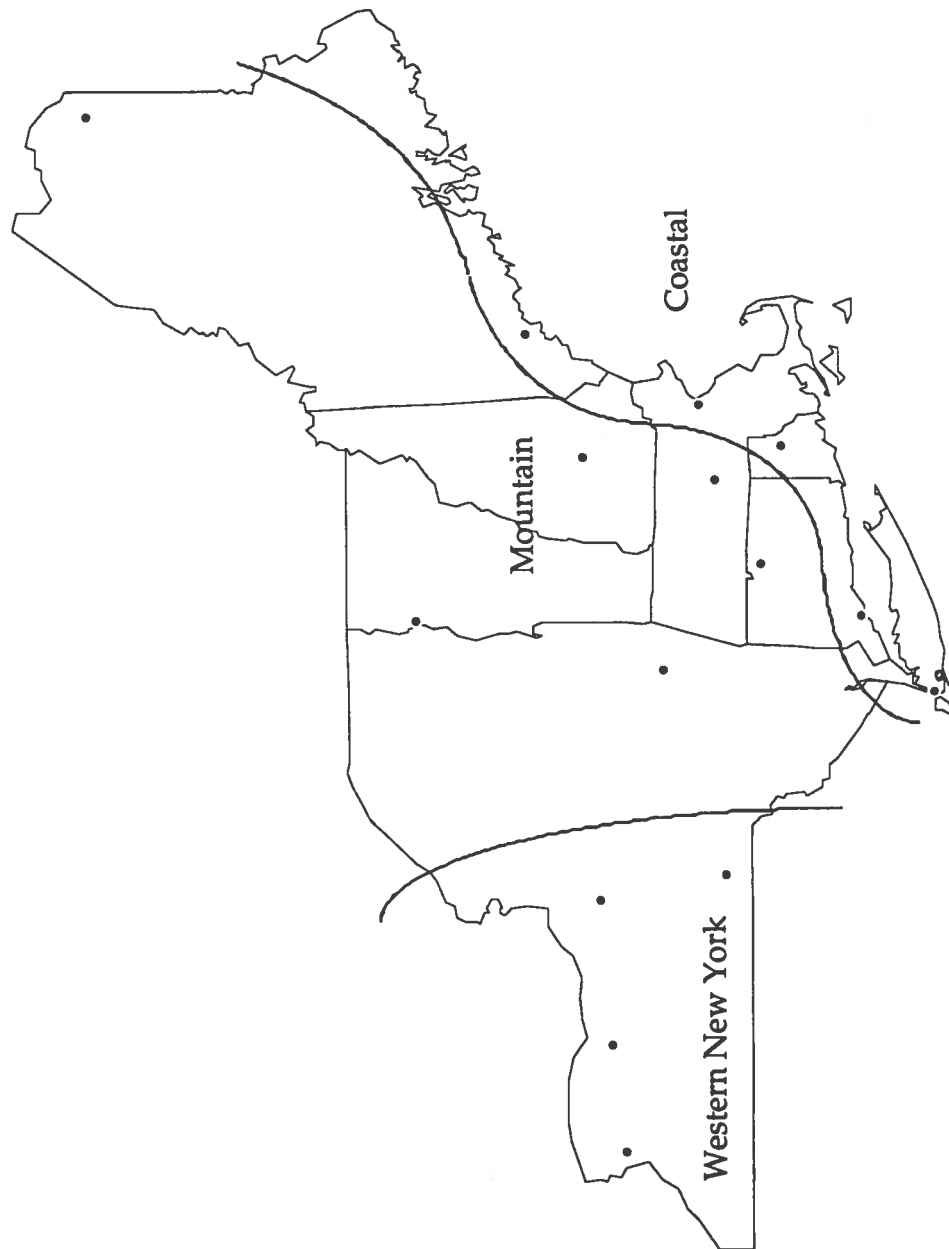


Figure 7. Coastal, Mountain, and Western New York grouped regions.

Table 28a. December coastal grouping, showing station intercepts, pooled parameter estimates, rain-on-snow correction factor, and statistics. A t-ratio value less than 0.05 indicates a significant predictor at the 95% confidence level.

Intercept	Estimates	std.err.	t-ratio	pr of > t
Boston	0.041	0.025	1.63	0.102
Bridgeport	-0.059	0.028	-2.08	0.037
LaGuardia-NYC	-0.123	0.032	-3.81	0.000
Portland	0.005	0.025	0.20	0.844
Providence	-0.018	0.025	-0.72	0.472
Slope				
sqrtsndp	0.390	0.010	38.09	0.000
maxinrow	-0.021	0.003	-6.45	0.000
oldsnfl	-0.043	0.004	-10.40	0.000
oldppt	0.266	0.026	10.29	0.000
Correction to intercept				
rain on snow	0.065	0.030	2.14	0.033

R-squared = 0.693

RMSE = 0.192

n=839

Table 28b. December mountain grouping, showing station intercepts, pooled parameter estimates, rain-on-snow correction factor, and statistics. A t-ratio value less than 0.05 indicates a significant predictor at the 95% confidence level.

Intercept	Estimates	std.err.	t-ratio	pr of > t
Albany	0.043	0.017	2.56	0.000
Burlington	-0.060	0.016	-3.75	0.016
Caribou	0.077	0.017	4.47	0.001
Concord	0.053	0.016	3.33	0.000
Hartford	0.044	0.018	2.40	0.000
Worcester	0.063	0.018	3.56	0.010
Slope				
sqrtsndp	0.366	0.005	68.57	0.000
maxinrow	-0.012	0.001	-10.54	0.000
oldsnfl	-0.043	0.003	-13.82	0.000
oldppt	0.289	0.025	11.66	0.000
Correction to intercept				
rain on snow	0.128	0.022	5.88	0.000

r-squared = 0.686

RMSE = 0.225

n=2687

Table 28c. December western New York grouping, showing station intercepts, pooled parameter estimates, rain-on-snow correction factor, and statistics. A t-ratio value less than 0.05 indicates a significant predictor at the 95% confidence level.

Intercept	Estimates	std.err.	t-ratio	pr of > t
Buffalo	-0.043	0.019	-2.33	0.020
Rochester	-0.020	0.017	-1.14	0.256
Binghamton	-0.042	0.017	-2.48	0.013
Syracuse	-0.157	0.019	-8.48	0.000
Slope				
sqrtsndp	0.382	0.008	49.52	0.000
maxinrow	-0.007	0.002	-4.11	0.000
oldsnfl	-0.042	0.003	-12.68	0.000
oldppt	0.281	0.033	8.55	0.000
Correction to intercept				
rain on snow	0.083	0.027	3.12	0.002

r-squared =0.660

RMSE = 0.181

n=1586

Table 28d. December total grouping, showing station intercepts, pooled parameter estimates, rain-on-snow correction factor, and statistics. A t-ratio value less than 0.05 indicates a significant predictor at the 95% confidence level.

Intercept	Estimates	std.err.	t-ratio	pr of > t
Albany	0.028	0.014	1.98	0.048
Binghamton	-0.009	0.013	-0.74	0.461
Boston	0.055	0.019	2.91	0.004
Bridgeport	-0.045	0.024	-1.86	0.064
Buffalo	-0.015	0.014	-1.13	0.259
Burlington	-0.079	0.013	-6.01	0.000
Caribou	0.055	0.013	4.12	0.000
Concord	0.037	0.013	2.89	0.004
Hartford	0.031	0.016	1.95	0.051
LaGuardia-NYC	-0.104	0.030	-3.46	0.001
Portland	0.023	0.013	1.70	0.090
Providence	-0.007	0.019	-0.38	0.704
Rochester	0.006	0.013	0.44	0.663
Syracuse	-0.130	0.014	-9.18	0.000
Worcester	0.048	0.015	3.20	0.001
Slope				
sqrtsndp	0.374	0.004	93.52	0.000
maxinrow	-0.011	0.001	-12.96	0.000
olds nfl	-0.042	0.002	-21.19	0.000
oldppt	0.279	0.016	17.68	0.000
Correction to intercept				
rain on snow	0.105	0.015	7.10	0.000

r-squared = 0.696

RMSE = 0.207

n=5112

Table 29a. January coastal grouping, showing station intercepts, pooled parameter estimates, rain-on-snow correction factor, and statistics. A t-ratio value less than 0.05 indicates a significant predictor at the 95% confidence level.

Intercept	Estimates	std. err.	t-ratio	pr of > t
Boston	-0.028	0.022	-1.30	0.194
Bridgeport	-0.106	0.022	-4.76	0.000
LaGuardia-NYC	-0.160	0.025	-6.29	0.000
Portland	0.063	0.023	2.78	0.005
Providence	-0.020	0.021	-0.96	0.335
Slope				
sqrtsndp	0.427	0.008	53.62	0.000
maxinrow	-0.019	0.002	-8.86	0.000
oldsnfl	-0.055	0.004	-12.49	0.000
oldppt	0.303	0.030	10.22	0.000
Correction to intercept				
rain on snow	0.130	0.031	4.26	0.000

r-squared = 0.715

RMSE = 0.245

n=1772

Table 29b. January mountain grouping, showing station intercepts, pooled parameter estimates, rain-on-snow correction factor, and statistics. A t-ratio value less than 0.05 indicates a significant predictor at the 95% confidence level.

Intercept	Estimates	std.err.	t-ratio	pr of > t
Albany	0.128	0.016	7.84	0.000
Burlington	0.015	0.016	0.93	0.351
Caribou	0.199	0.020	9.78	0.000
Concord	0.179	0.017	10.38	0.000
Hartford	0.124	0.017	7.22	0.000
Worcester	0.056	0.018	3.05	0.002
Slope				
sqrtsndp	0.372	0.005	76.53	0.000
maxinrow	-0.007	0.001	-8.51	0.000
oldsnfl	-0.047	0.003	-13.63	0.000
oldppt	0.308	0.030	10.29	0.000
Correction to intercept				
rain on snow	0.069	0.021	3.25	0.001

r-squared = 0.687

RMSE = 0.287

n=4260

Table 29c. January western New York grouping, showing station intercepts, pooled parameter estimates, rain-on-snow correction factor, and statistics. A t-ratio value less than 0.05 indicates a significant predictor at the 95% confidence level.

Intercept	Estimates	std. err.	t-ratio	pr of > t
Binghamton	0.007	0.018	0.38	0.704
Buffalo	-0.057	0.020	-2.87	0.004
Rochester	-0.017	0.018	-0.92	0.357
Syracuse	-0.079	0.019	-4.20	0.000
Slope				
sqrtsndp	0.430	0.007	61.96	0.000
maxinrow	-0.007	0.001	-7.19	0.000
oldsnfl	-0.062	0.004	-15.25	0.000
oldppt	0.405	0.045	9.08	0.000
Correction to intercept				
rain on snow	0.108	0.026	4.15	0.000

r-squared = 0.621

RMSE = 0.260

n=2830

Table 29d. January total grouping, showing station intercepts, pooled parameter estimates, rain-on-snow correction factor, and statistics. A t-ratio value less than 0.05 indicates a significant predictor at the 95% confidence level.

Intercept	Estimates	std.err.	t-ratio	pr of > t
Albany	0.072	0.014	5.29	0.000
Binghamton	0.096	0.013	7.45	0.000
Boston	0.019	0.017	1.10	0.270
Bridgeport	-0.057	0.019	-3.05	0.002
Buffalo	0.043	0.014	3.05	0.002
Burlington	-0.044	0.013	-3.33	0.001
Caribou	0.113	0.016	7.24	0.001
Concord	0.111	0.014	8.01	0.000
Hartford	0.070	0.015	4.74	0.000
LaGuardia-NYC	-0.126	0.024	-5.26	0.000
Portland	0.122	0.014	8.99	0.001
Providence	0.019	0.017	1.13	0.258
Rochester	0.067	0.013	5.07	0.000
Syracuse	0.003	0.013	0.27	0.790
Worcester	-0.009	0.015	-0.56	0.574
Slope				
sqrtsndp	0.395	0.004	111.34	0.000
maxinrow	-0.007	0.001	-12.61	0.000
oldsnfl	-0.052	0.002	-23.13	0.000
oldppt	0.328	0.019	17.14	0.000
Correction to intercept				
rain on snow	0.090	0.014	6.24	0.000

r-squared = 0.689

RMSE = 0.272

n=8862

Table 30a. February coastal grouping, showing station intercepts, pooled parameter estimates, rain-on-snow correction factor, and statistics. A t-ratio value less than 0.05 indicates a significant predictor at the 95% confidence level.

Intercept	Estimates	std.err.	t-ratio	pr of > t
Boston	-0.073	0.027	-2.74	0.006
Bridgeport	-0.137	0.028	-4.90	0.000
LaGuardia-NYC	-0.245	0.030	-8.05	0.000
Portland	0.115	0.027	4.21	0.000
Providence	-0.115	0.028	-4.16	0.000
Slope				
sqrtsndp	0.464	0.009	54.00	0.000
maxinrow	-0.011	0.003	-3.99	0.000
oldsnfl	-0.064	0.006	-11.65	0.000
oldppt	0.320	0.040	8.03	0.000
Correction to intercept				
rain on snow	0.166	0.037	4.52	0.000

r-squared = 0.743

RMSE = 0.295

n = 1548

Table 30b. February mountain grouping, showing station intercepts, pooled parameter estimates, rain-on-snow correction factor, and statistics. A t-ratio value less than 0.05 indicates a significant predictor at the 95% confidence level.

Intercept	Estimates	std.err.	t-ratio	pr of > t
Albany	0.151	0.019	7.81	0.000
Burlington	0.099	0.019	5.10	0.000
Caribou	0.350	0.025	14.11	0.000
Concord	0.299	0.020	14.78	0.000
Hartford	0.069	0.021	3.23	0.001
Worcester	-0.068	0.022	-3.11	0.002
Slope				
sqrtsndp	0.389	0.005	72.57	0.000
maxinrow	-0.007	0.001	-7.87	0.000
oldsnfl	-0.054	0.004	-13.23	0.000
oldppt	0.309	0.037	8.39	0.000
Correction to intercept				
rain on snow	0.139	0.027	5.15	0.000

r-squared = 0.719

RMSE = 0.333

n = 3824

Table 30c. February western New York grouping, showing station intercepts, pooled parameter estimates, rain-on-snow correction factor, and statistics. A t-ratio value less than 0.05 indicates a significant predictor at the 95% confidence level.

Intercept	Estimates	std.err.	t-ratio	pr of > t
Binghamton	-0.014	0.020	-0.69	0.490
Buffalo	-0.096	0.021	-4.49	0.000
Rochester	-0.036	0.020	-1.77	0.076
Syracuse	-0.171	0.023	-7.44	0.000
Slope				
sqrtsndp	0.490	0.007	67.79	0.000
maxinrow	-0.010	0.001	-9.74	0.000
oldsnfl	-0.073	0.005	-14.96	0.000
oldppt	0.391	0.051	7.69	0.000
Correction to intercept				
rain on snow	0.163	0.029	5.72	0.000

r-squared = 0.688

RMSE = 0.291

n = 2308

Table 30d. February total grouping, showing station intercepts, pooled parameter estimates, rain-on-snow correction factor, and statistics. A t-ratio value less than 0.05 indicates a significant predictor at the 95% confidence level.

Intercept	Estimates	std.err.	t-ratio	pr of > t
Albany	0.059	0.016	3.61	0.000
Binghamton	0.129	0.016	8.13	0.000
Boston	0.006	0.021	0.29	0.772
Bridgeport	-0.061	0.024	-2.58	0.010
Buffalo	0.052	0.017	3.14	0.002
Burlington	-0.005	0.016	-0.30	0.762
Caribou	0.193	0.019	10.28	0.000
Concord	0.184	0.016	11.25	0.000
Hartford	-0.020	0.019	-1.09	0.274
LaGuardia-NYC	-0.176	0.027	-6.43	0.000
Portland	0.216	0.016	13.27	0.000
Providence	-0.032	0.022	-1.44	0.150
Rochester	0.105	0.016	6.79	0.000
Syracuse	-0.009	0.018	-0.49	623.000
Worcester	-0.180	0.018	-9.90	0.000
Slope				
sqrtsndp	0.427	0.004	110.67	0.000
maxinrow	-0.008	0.001	-11.77	0.000
olds nfl	-0.061	0.003	-21.99	0.000
oldp pt	0.327	0.024	13.82	0.000
Correction to intercept				
rain on snow	0.153	0.018	8.73	0.000

r-squared = 0.721

RMSE = 0.316

n = 7680

Table 31a. Winter coastal grouping, showing station intercepts, pooled parameter estimates, rain-on-snow correction factor, and statistics. A t-ratio value less than 0.05 indicates a significant predictor at the 95% confidence level. The model is for February data, with corrections for December and January.

Intercept	Estimates	std. err.	t-ratio	pr of > t
Boston	0.032	0.017	1.95	0.051
Bridgeport	-0.047	0.017	-2.76	0.006
LaGuardia-NYC	-0.127	0.019	-6.86	0.000
Portland	0.132	0.017	7.91	0.000
Providence	0.012	0.016	0.72	0.473
Slope				
sqrtsndp	0.440	0.005	84.28	0.000
maxinrow	-0.016	0.002	-10.75	0.000
olds nfl	-0.058	0.003	-20.35	0.000
oldppt	0.306	0.019	15.73	0.000
Correction to intercept				
December	-0.178	0.012	-15.39	0.000
January	-0.090	0.009	-9.77	0.000
rain on snow	0.129	0.020	6.46	0.000

r-squared = 0.732

RMSE = 0.262

n=4159

Table 31b. Winter mountain grouping, showing station intercepts, pooled parameter estimates, rain-on-snow correction factor, and statistics. A t-ratio value less than 0.05 indicates a significant predictor at the 95% confidence level. The model is for February data, with corrections for December and January.

Intercept	Estimates	std. err.	t-ratio	pr of > t
Albany	0.207	0.011	17.82	0.000
Burlington	0.118	0.012	10.19	0.000
Caribou	0.307	0.014	22.27	0.000
Concord	0.283	0.012	23.66	0.000
Hartford	0.217	0.013	16.24	0.000
Worcester	0.099	0.013	7.80	0.000
Slope				
sqrtsndp	0.382	0.003	124.71	0.000
maxinrow	-0.008	0.001	-14.04	0.000
oldsnfl	-0.050	0.002	-23.06	0.000
oldppt	0.310	0.018	16.78	0.000
Correction to intercept				
December	-0.231	0.008	-28.97	0.000
January	-0.119	0.007	-17.32	0.000
rain on snow	0.099	0.014	7.10	0.000

r-squared = 0.720

RMSE = 0.296

n=10771

Table 31c. Winter western New York grouping, showing station intercepts, pooled parameter estimates, rain-on-snow correction factor, and statistics. A t-ratio value less than 0.05 indicates a significant predictor at the 95% confidence level. The model is for February data, with corrections for December and January.

Intercept	Estimates	std. err.	t-ratio	pr of > t
Binghamton	0.062	0.012	5.13	0.000
Buffalo	0.002	0.013	0.19	0.852
Rochester	0.048	0.012	3.89	0.000
Syracuse	-0.058	0.013	-4.35	0.000
Slope				
sqrtsndp	0.450	0.004	105.01	0.000
maxinrow	-0.009	0.001	-13.37	0.000
oldsnfl	-0.061	0.002	-24.77	0.000
oldppt	0.360	0.026	13.84	0.000
Correction to intercept				
December	-0.210	0.009	-24.44	0.000
January	-0.090	0.007	-12.48	0.000
rain on snow	0.121	0.016	7.49	0.000

r-squared = 0.688

RMSE = 0.257

n=6724

Table 31d. Winter total grouping, showing station intercepts, pooled parameter estimates, rain-on-snow correction factor, and statistics. A t-ratio value less than 0.05 indicates a significant predictor at the 95% confidence level. The model is for February data, with corrections for December and January. As an example, the model for Binghamton in January would be $\text{SqrtSWE} = 0.155 - 0.096 + 0.408 * \text{Sqrtsndp} - 0.008 * \text{Maxinrow} - 0.054 * \text{Oldsnfl} + 0.318 * \text{Oldppt}$. If rain had fallen on the day before the prediction, add 0.118 to the intercept.

Intercept	Estimates	std. err.	t-ratio	pr of > t
Albany	0.128	0.009	13.58	0.000
Binghamton	0.155	0.009	17.36	0.000
Boston	0.092	0.012	7.73	0.000
Bridgeport	0.011	0.013	0.84	0.400
Buffalo	0.106	0.010	11.17	0.000
Burlington	0.033	0.009	3.60	0.000
Caribou	0.192	0.100	18.76	0.000
Concord	0.191	0.009	20.47	0.000
Hartford	0.101	0.010	9.79	0.000
LaGuardia-NYC	-0.079	0.016	-4.86	0.000
Portland	0.205	0.009	22.06	0.000
Providence	0.068	0.012	5.67	0.000
Rochester	0.180	0.009	19.18	0.000
Syracuse	0.044	0.010	4.64	0.000
Worcester	0.011	0.010	1.03	0.304
Slope				
sqrtsndp	0.408	0.002	182.60	0.000
maxinrow	-0.008	0.000	-20.16	0.000
oldsnfl	-0.054	0.001	-38.15	0.000
oldppt	0.318	0.012	26.77	0.000
Correction to intercept				
December	-0.200	0.005	-39.35	0.000
January	-0.096	0.005	-21.20	0.000
rain on snow	0.118	0.009	12.45	0.000

r-squared = 0.720

RMSE = 0.280

n=21654

Grouped models, whether for individual months or the entire winter season, show consistently high R^2 and low RMSE. Individual groups by month range from an R^2 of 62.1% and RMSE of 0.245 for Western New York in January to 74.3% and 0.295 for the Coastal region in February. When the groups are combined into a "Total" monthly group, the R^2 and RMSE values range only from 68.9% and 0.272 in January to 72.1% and 0.316 in February. Despite the variability of monthly station models and the different density types of snow which fall, underlying SWE characteristics are not overwhelmingly site-specific, at least among the locations investigated. Differences are easily accounted for within the intercept term for each station.

At this point a remaining question is which, if any, of the models is most appropriate to use with data from a given Co-Op station. The small difference in R^2 among groups may indicate all models perform equally well. Independent verification on Co-Op snow survey data, discussed in the next section, addresses this issue.

5. Model Verification on Independent Data

As mentioned in the introduction to this thesis, the National Cooperative Observer (Co-Op) Program consists of over 11,000 stations, primarily staffed by volunteers, under the supervision of state cooperative program managers based in National Weather Service Forecast Offices. These observers report daily values of maximum and minimum temperatures, precipitation, snowfall, and snow depth.

The New York observers also participate in a periodic snow survey under the auspices of the Northeast Regional Climate Center. Beginning the first Monday in January, and at 28 day intervals through February, followed by 14 day intervals into May, the observers determine the SWE in addition to recording the regular variables. All observations at these stations are taken at the same time of day, usually in the morning. Oldsnfl and Oldppt are for the 24 hours immediately preceding the SWE and Snowdepth measurement. Therefore, there is no time lag as is the case with the NWSO observations, and errors due to this lost information are eliminated for the present purpose. Figure 8 illustrates the timing of data collection at Co-Op sites, including SWE determination during snow surveys. It should be compared with the timing of data collection at NWSO sites in Figure 3.

5.1 Data Preparation

Twenty-two stations (see Figure 9 and Table 32) with at least 20 years of data were chosen for verification to ensure a length of record long enough for statistical analysis. Two of the stations reported afternoon

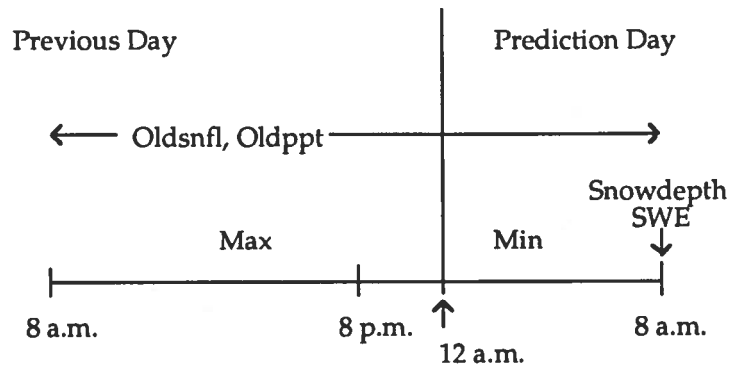


Figure 8. Timing of variable observations at Co-Op stations.

measurements of all variables, which only meant that the maximum temperature used in calculating *Maxinrow* occurred just before the observation rather than the previous afternoon. The remaining stations favored 8:00 a.m., as in Figure 8. It was decided to use only January and February Co-Op data to verify the models because the frequency of observations in later months decreases sharply. Only those snow survey dates with at least 2 inches (5 cm) of snow depth were used. For these observations *Maxinrow* and *sqrtSndp* were determined.

The snow survey data for each Co-Op station was used to verify all of the models developed for a particular NWSO. For example, January snow survey data from a Co-Op station near Binghamton would have its *sqrtSWE* predicted by the January Binghamton model, the Western New York and "Total" January models using Binghamton's intercept, and the Western New York and "Total" Winter models, also using Binghamton's intercept. Initially, the set of models from geographically proximate NWSOs (e.g.; Buffalo for Colden, Albany for Grafton) were used for predictions at the Co-Op stations. Since the Co-Op stations were between NWSOs, verification was attempted with the models for both nearby stations, or, in the case of Old Forge, those for Syracuse, Albany, and Burlington. Generally, when the

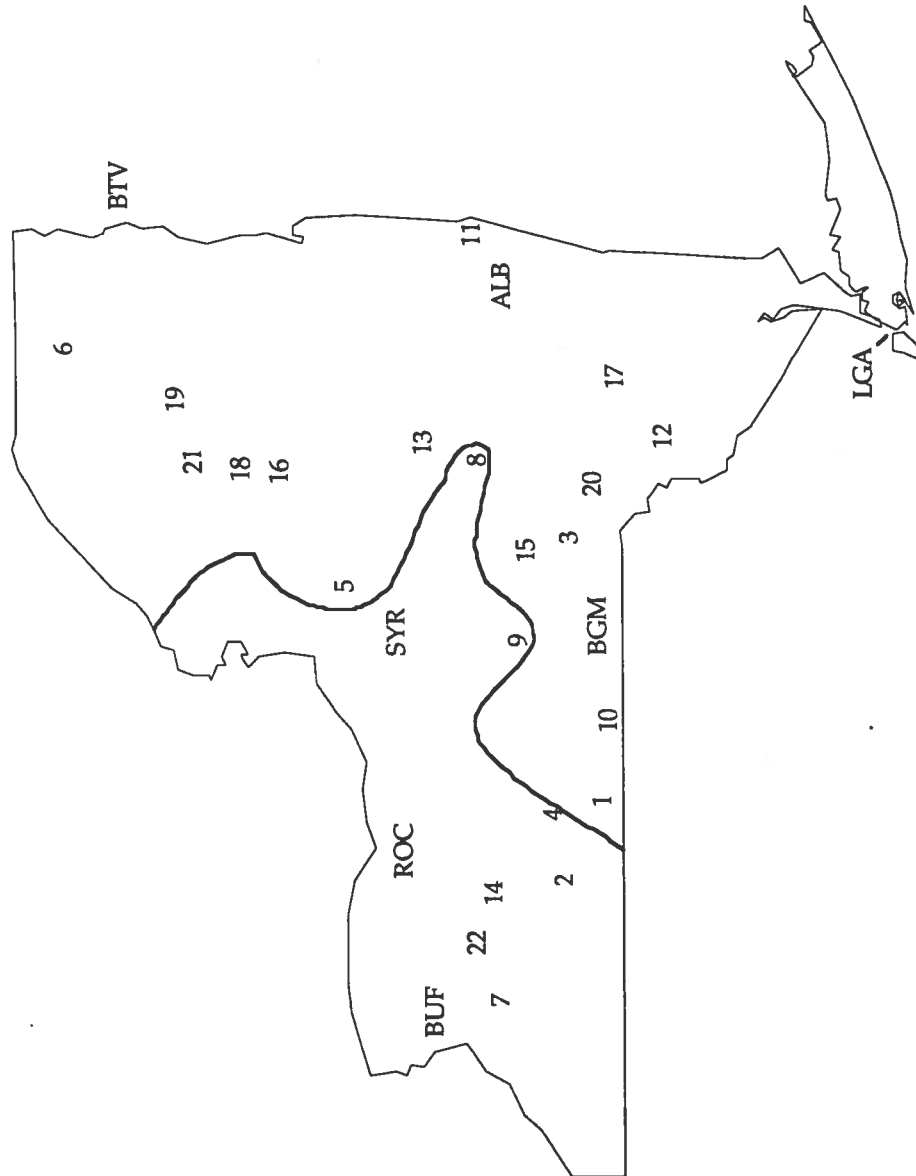


Figure 9. Co-Op stations used in verification studies. Refer to numbers in Table 32 for station names. For reference NWSO identifiers are listed in Table 5. Lake Effect snow areas are found roughly to the west of the curved line through the central part of New York.

Table 32. New York National Cooperative Observer stations used in verification studies with their years of snow survey data. The identification numbers correspond to those in figure 8. "Jan. obs." and "Feb. obs" refer to the number of snow survey observations at each Co-Op station in January and February.

<u>Station</u>	<u>Years of Record</u>	<u>Jan. obs.</u>	<u>Feb. obs.</u>
1. Addison	1948 - 1986	15	11
2. Alfred	1938 - 1990	35	24
3. Bainbridge	1938 - 1990	24	12
4. Bath	1954 - 1990	10	10
5. Camden	1942 - 1986	27	23
6. Chasm Falls	1939 - 1980	30	30
7. Colden	1965 - 1990	21	19
8. Cooperstown	1941 - 1990	28	21
9. Cortland	1948 - 1990	28	22
10. Elmira	1947 - 1990	19	11
11. Grafton	1952 - 1984	30	23
12. Liberty	1942 - 1990	38	37
13. Little Falls	1937 - 1985	37	39
14. Mount Morris	1955 - 1986	15	13
15. Norwich	1938 - 1990	23	27
16. Old Forge	1937 - 1990	40	32
17. Slide Mountain	1941 - 1990	16	13
18. Stillwater Reservoir	1937 - 1990	43	35
19. Tupper Lake - Sunmount	1937 - 1990	43	42
20. Walton	1941 - 1980	28	22
21. Wanakena	1937 - 1990	51	48
22. Warsaw	1955 - 1990	11	9

grouped models were tested, the intercept for the nearest NWSO was used.

The fraction of model-described variation (see Appendix E) of observed values was calculated for each model. RMSEs were also determined, and standardized residuals were plotted against snow depth and other predictors for each location in an effort to detect biases or weaknesses in the models.

5.2 Verification Results and Discussion

With few exceptions at least one set of models described at least 60% of the observed variability of sqrtSWE at each Co-Op station in New York for both January and February. Usually all of the models within a NWSO derived set performed equally well. In the cases where sets of models from several NSWOs were tested against the same Co-Op station, those from one NWSO usually outperformed the others. When standardized residuals were plotted against snowdepth all stations in Western and Central New York exhibited no problems, indicating very good response to the models. RMSEs were very similar to those for developmental NWSO data sets themselves (compare with statistics listed in Tables 8 and 9). This may be partially due to the manner in which RMSE is calculated for a non-developmental station (see Appendix E). For Adirondack stations, however, sqrtSWE was uniformly underpredicted by Burlington and Albany models. Investigation of January and February minimum temperatures revealed more similarity between Adirondack stations and Caribou than with Albany or Burlington. Applying the Caribou models corrected most of this problem; the beginnings of a trend toward underprediction was then only visible from residual plots when the actual

SWE exceeded about 4 inches (10 cm) in January and about 6 inches (15 cm) in February, both of which are near the upper range of observed values.

Table 33 shows the NWSO whose models best predicted the sqrtSWE at each Co-Op station for both January and February. Figure 10 is a graphic for January where arrows extend from each Co-Op station to the corresponding NWSO listed in Table 33. Figure 11 is the same presentation for February. For both figures numbers are length-of-record average monthly minimum temperatures (°F). Figure 12 shows station elevation in feet above mean sea level, with arrows from Co-Op stations to preferred NWSOs.

Tables 34 and 35 show more detailed results of verification tests for January and February, respectively. Each Co-Op station is shown with model-described variation and RMSE for each of the 5 models derived at the NWSO listed in Table 33. Note that in some cases the winter "Total" model had the best performance, while in others the regional models were better. In a few instances the January or February single station model was better than any of the grouped models. In many cases there tends to be little difference between any of the models in a set. These results are included for the benefit of a prospective user in determining whether one of the models within a set is more suited for prediction at a particular location.

Table 33. Co-Op stations and preferred NWSO models, with average model described variation and RMSE.

Station	preferred models	January		RMSE	preferred models	February	
		described variation				described variation	RMSE
Addison	Buffalo	0.65		0.22	Binghamton	0.54	0.27
Alfred	Buffalo	0.60		0.21	Buffalo	0.55	0.29
Bainbridge	Binghamton	0.80		0.18	Binghamton	0.80	0.21
Bath	Buffalo	0.81		0.17	Buffalo	0.39	0.23
Camden	Caribou	0.72		0.27	Caribou	0.72	0.38
Chasm Falls	Caribou	0.75		0.20	Caribou	0.82	0.22
Colden	Rochester	0.80		0.19	Rochester	0.77	0.31
Cooperstown	Syracuse	0.67		0.22	Syracuse	0.66	0.27
Cortland	Syracuse	0.71		0.23	Syracuse	0.77	0.25
Elmira	Binghamton	0.75		0.17	Binghamton	0.68	0.23
Grafton	Caribou	0.78		0.19	Caribou	0.90	0.13
Liberty	Caribou	0.69		0.22	Caribou	0.76	0.19
Little Falls	Caribou	0.69		0.17	Caribou	0.75	0.22
Mt. Morris	(bad data; no variation described by any model)				Rochester	0.56	0.27
Norwich	Albany	0.32		0.28	Albany	0.78	0.22
Old Forge	Caribou	0.63		0.30	Caribou	0.53	0.33
Slide Mountain	Caribou	0.73		0.31	Caribou	0.74	0.40
Stillwater	Caribou	0.73		0.26	Caribou	0.64	0.28
Tupper Lake	Caribou	0.73		0.20	Caribou	0.63	0.31
Walton	Binghamton	0.70		0.23	Caribou	0.78	0.21
Wanakena	Caribou	0.69		0.23	Caribou	0.68	0.26
Warsaw	Buffalo	0.77		0.24	Rochester	0.78	0.18

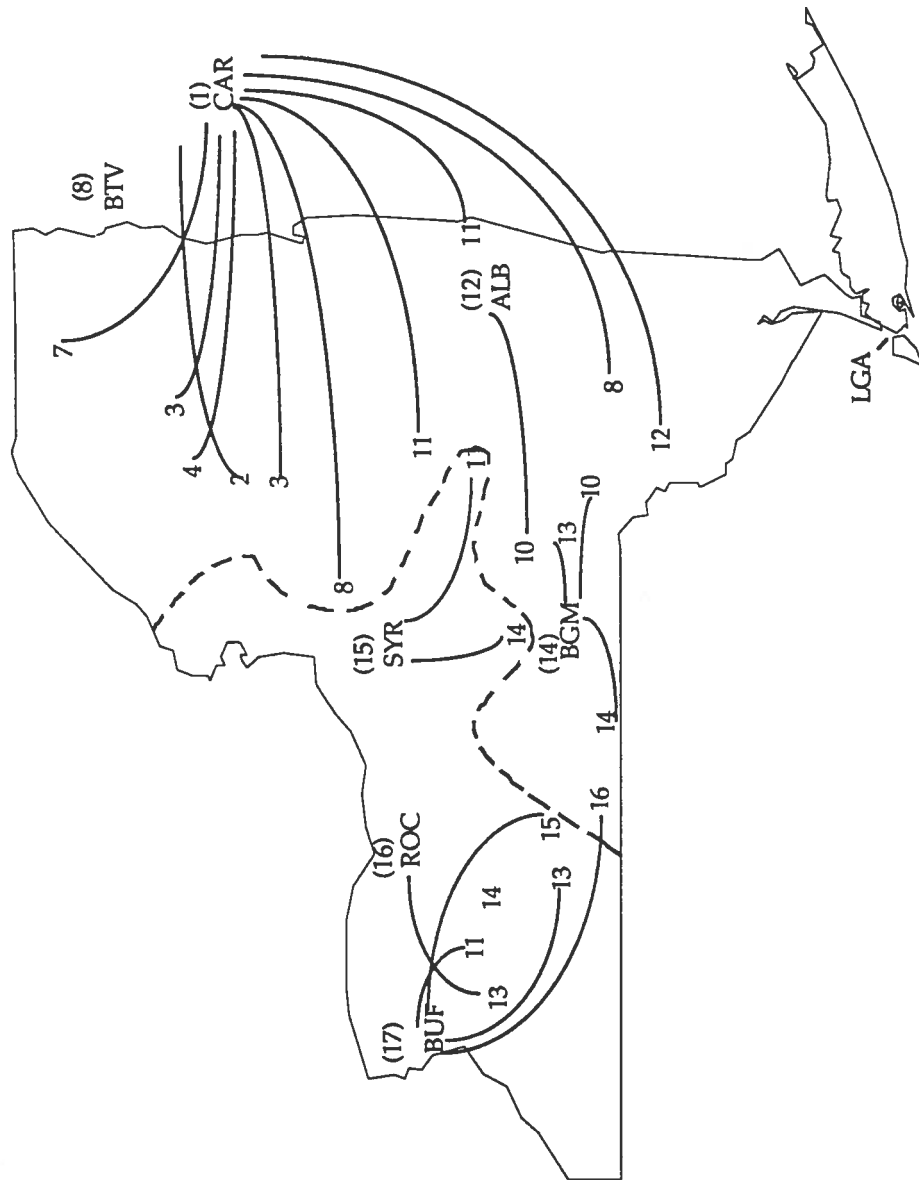


Figure 10. Average January minimum temperatures at Co-Op stations used in verification studies. Lines connect Co-Op stations with NWSO whose models are best predictors for the station. Lake Effect area is west of dashed line through state. NWSO minimums in parentheses.

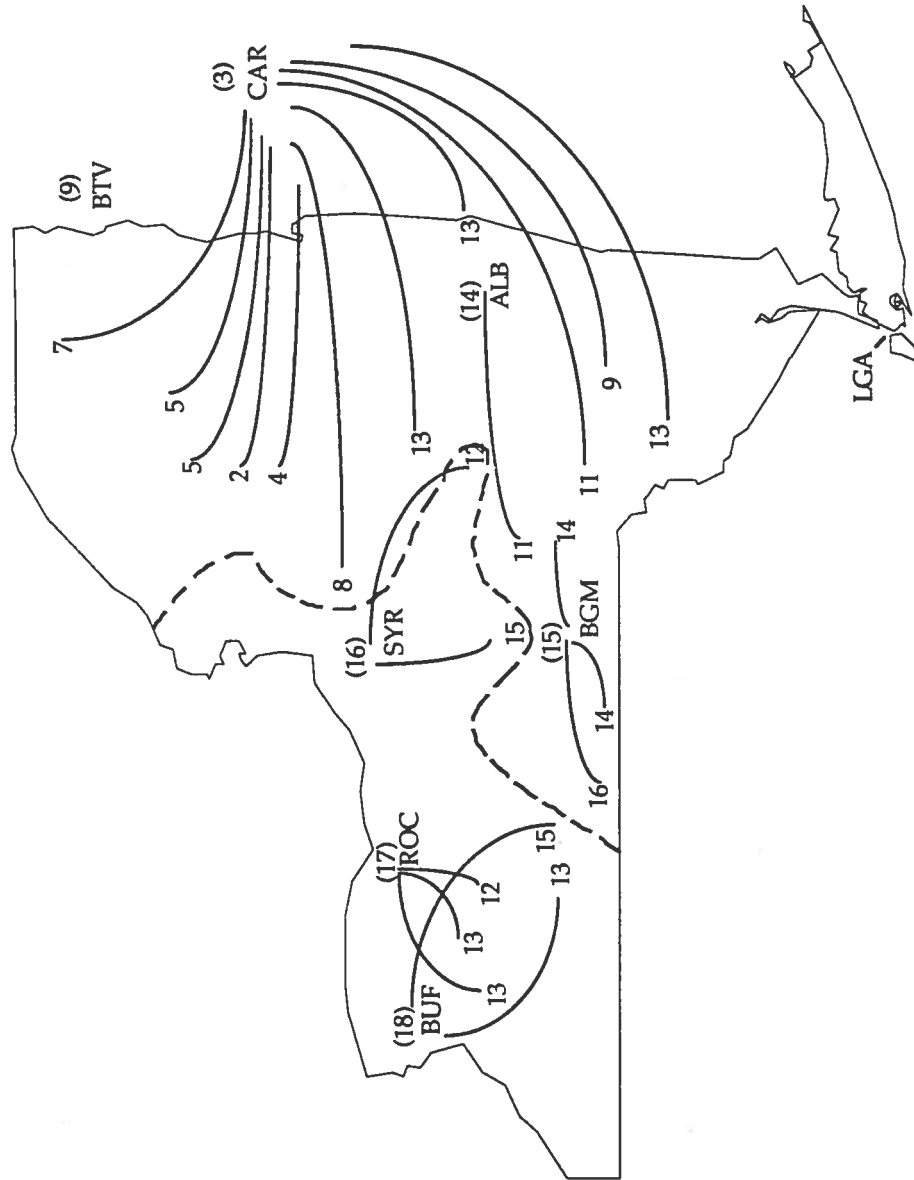


Figure 11. Average February minimum temperatures at Co-Op stations used in verification studies. Lines connect Co-Op stations with the NWSO whose models are best predictors for the station. Lake Effect area is west of dashed line through state. NWSO minimums in parentheses.

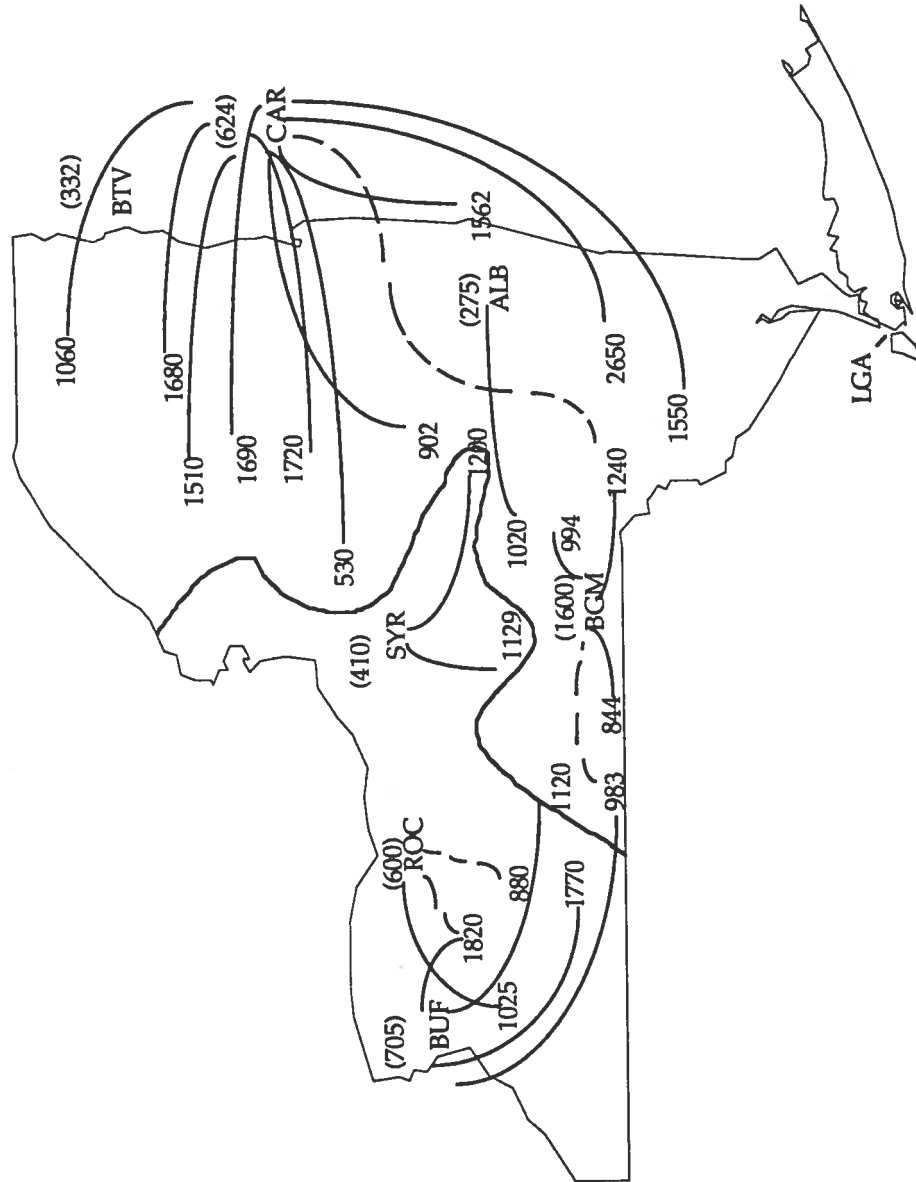


Figure 12. Co-Op station elevations in feet above mean sea level. NWSO elevations in parentheses. Solid lines connect Co-Op stations with NWSO whose models are the best predictors for that station. Broken lines connect to an NWSO if different for February.

Table 34. Results of using the most appropriate NWSO-derived models at each Co-Op station in January. For each Co-Op station the model described variation and RMSE for each of the 5 models tested are listed. J refers to the NWSO January model, Jwny or Jmtn refers to the Western New York or Mountain grouped model, and Jtotal refers to the January "Total" model. JDF refers to the Winter model, either Western New York, Mountain, or "Total". MDV denotes fraction of model described variation, RMSE denotes root mean squared error.

Western New York	J			Jwny			Jtotal			JDFwny			JDFwinter		
	MDV	RMSE		MDV	RMSE		MDV	RMSE		MDV	RMSE		MDV	RMSE	
Addison using Buffalo	0.65	0.23		0.65	0.22		0.65	0.23		0.66	0.22		0.66	0.22	
Alfred using Buffalo	0.60	0.21		0.61	0.21		0.60	0.21		0.58	0.22		0.60	0.21	
Bath using Buffalo	0.82	0.16		0.81	0.17		0.80	0.18		0.81	0.17		0.80	0.17	
Colden using Buffalo	0.78	0.20		0.79	0.20		0.77	0.21		0.81	0.19		0.78	0.20	
Warsaw using Buffalo	0.78	0.23		0.78	0.23		0.75	0.25		0.80	0.23		0.76	0.24	
Warsaw using Rochester	0.77	0.24		0.78	0.24		0.75	0.25		0.79	0.23		0.74	0.26	
Colden using Rochester	0.80	0.19		0.81	0.19		0.78	0.20		0.81	0.18		0.79	0.19	

Table 34 . (continued)

Western New York (continued)

	J		Jwny		Jtotal		JDFwny		JDFwinter	
	MDV	RMSE	MDV	RMSE	MDV	RMSE	MDV	RMSE	MDV	RMSE
Bainbridge using Binghamton	0.82	0.17	0.80	0.18	0.78	0.19	0.80	0.18	0.79	0.18
Elmira using Binghamton	0.71	0.19	0.76	0.17	0.75	0.17	0.75	0.17	0.77	0.17
Walton using Binghamton	0.80	0.19	0.70	0.23	0.62	0.26	0.74	0.21	0.63	0.25
Cooperstown using Syracuse	0.64	0.23	0.65	0.23	0.70	0.21	0.65	0.23	0.70	0.21
Cortland using Syracuse	0.70	0.23	0.70	0.23	0.73	0.22	0.69	0.23	0.72	0.22

Table 34 (continued)

Mountain	J			Jmtn			Jtotal			JDFmtn			JDFwinter		
	MDV	RMSE		MDV	RMSE		MDV	RMSE		MDV	RMSE		MDV	RMSE	
Norwich using Albany	0.27	0.29		0.35	0.28		0.33	0.28		0.35	0.28		0.32	0.28	
Camden using Caribou	0.74	0.26		0.70	0.27		0.70	0.26		0.70	0.27		0.72	0.27	
Chasm Falls using Caribou	0.76	0.19		0.74	0.20		0.75	0.20		0.75	0.20		0.76	0.19	
Grafton using Caribou	0.77	0.20		0.78	0.19		0.78	0.19		0.79	0.19		0.79	0.19	
Liberty using Caribou	0.68	0.22		0.69	0.22		0.69	0.22		0.69	0.22		0.69	0.21	
Little Falls using Caribou	0.67	0.18		0.70	0.17		0.67	0.18		0.72	0.17		0.70	0.17	
Old Forge using Caribou	0.64	0.30		0.60	0.31		0.62	0.30		0.64	0.30		0.67	0.28	
Slide Mountain using Caribou	0.72	0.32		0.72	0.31		0.73	0.31		0.73	0.31		0.74	0.30	

Table 34 (continued)

Mountain (continued)

Stillwater Reservoir using Caribou			Tupper Lake - Sunmount using Caribou			Wanakena using Caribou		
Model	MDV	RMSE	Model	MDV	RMSE	Model	MDV	RMSE
J	0.73	0.26	J	0.73	0.20	J	0.69	0.23
Jmntn	0.70	0.28	Jmntn	0.71	0.21	Jmntn	0.67	0.24
Jtotal	0.72	0.27	Jtotal	0.72	0.20	Jtotal	0.68	0.24
JDFmntn	0.73	0.26	Jdfmntn	0.73	0.20	Jdfmntn	0.69	0.23
JDFtotal	0.75	0.25	Jdftotal	0.74	0.19	Jdftotal	0.70	0.23

Table 35. Results of using the most appropriate NWSO-derived models at each Co-Op station in February. For each Co-Op station the model described variation and RMSE for each of the 5 models tested are listed. F refers to the NWSO February model, Fwny or Fmtn refers to the Western New York or Mountain grouped model, and Ftotal refers to the February "Total" model. FDJ refers to the Winter model, either Western New York, Mountain, or "Total". MDV denotes fraction of model described variation, RMSE denotes root mean squared error.

Western New York											
	F		Fwny		Ftotal		FDJwny		FDJtotal		
	MDV	RMSE	MDV	RMSE	MDV	RMSE	MDV	RMSE	MDV	RMSE	
Alfred using Buffalo	0.49	0.31	0.52	0.3	0.58	0.28	0.57	0.28	0.59	0.28	
Bath using Buffalo	0.08	0.30	0.36	0.25	0.52	0.21	0.46	0.23	0.54	0.21	
(small sample size)											
Colden using Buffalo	0.82	0.28	0.77	0.31	0.69	0.37	0.74	0.34	0.68	0.38	
Warsaw using Buffalo	0.83	0.17	0.79	0.18	0.72	0.21	0.75	0.20	0.71	0.21	
Warsaw using Rochester	0.82	0.17	0.81	0.17	0.76	0.19	0.77	0.19	0.75	0.20	
Colden using Rochester	0.80	0.29	0.81	0.29	0.74	0.34	0.77	0.32	0.74	0.34	

Table 35. (continued)

Western New York (continued)

	F			Fwny			Ftotal			FDJwny			FDJtotal		
	MDV	RMSE		MDV	RMSE		MDV	RMSE		MDV	RMSE		MDV	RMSE	
Mt. Morris using Rochester	0.56	0.27		0.52	0.28		0.58	0.26		0.56	0.27		0.57	0.26	
Cooperstown using Syracuse	0.65	0.27		0.65	0.27		0.68	0.26		0.66	0.27		0.67	0.26	
Cortland using Syracuse	0.72	0.28		0.77	0.25		0.79	0.25		0.79	0.24		0.79	0.24	
Addison using Binghamton	0.54	0.27		0.52	0.28		0.54	0.27		0.54	0.27		0.55	0.27	
Bainbridge using Binghamton	0.81	0.20		0.81	0.20		0.80	0.21		0.81	0.21		0.78	0.22	
Elmira using Binghamton	0.71	0.22		0.66	0.23		0.66	0.23		0.68	0.23		0.68	0.23	

Table 35. (continued)

Mountain	F		Fmntn		Ftotal		FDjmntn		FDjtotal	
	MDV	RMSE	MDV	RMSE	MDV	RMSE	MDV	RMSE	MDV	RMSE
Norwich using Albany	0.78	0.22	0.78	0.22	0.78	0.22	0.78	0.22	0.78	0.22
Camden using Caribou	0.72	0.37	0.72	0.38	0.74	0.36	0.70	0.39	0.71	0.38
Chasm Falls using Caribou	0.83	0.21	0.82	0.22	0.84	0.21	0.79	0.24	0.80	0.23
Grafton using Caribou	0.91	0.12	0.90	0.13	0.92	0.12	0.89	0.14	0.88	0.14
Liberty using Caribou	0.81	0.17	0.77	0.19	0.77	0.19	0.70	0.20	0.71	0.21
Little Falls using Caribou	0.78	0.20	0.75	0.22	0.76	0.21	0.73	0.23	0.72	0.23
Old Forge using Caribou	0.61	0.31	0.58	0.32	0.61	0.31	0.46	0.36	0.48	0.36

Table 35. (continued)

Mountain (continued)		F			F _{mtn}			F _{total}			FDJ _{mtn}			FDJ _{total}		
		MDV	RMSE		MDV	RMSE		MDV	RMSE		MDV	RMSE		MDV	RMSE	
Slide Mountain using Caribou		0.76	0.38		0.72	0.42		0.74	0.40		0.72	0.42		0.74	0.40	
Stillwater Reservoir using Caribou	0.71	0.26			0.67	0.27		0.70	0.26		0.56	0.32		0.58	0.31	
Tupper Lake- Sunmount using Caribou	0.66	0.30			0.64	0.31		0.65	0.30		0.60	0.32		0.62	0.31	
Walton using Caribou	0.82	0.19			0.80	0.20		0.82	0.19		0.73	0.24		0.72	0.23	
Wanakena using Caribou	0.73	0.24			0.71	0.25		0.70	0.25		0.64	0.28		0.63	0.28	

The high percentage of described variation of sqrtSWE and low RMSE of Co-Op stations using NWSO models when compared with those values obtained from the developmental data is surprising until one examines the timing of variable observation (refer to Figure 8). The lack of lost snowfall and precipitation information affecting NWSO models may explain why described variation at Co-Op stations tend to be better than at the developmental sites. These results suggest that the models have wide applicability in the region.

While most Co-Op stations tended to have sqrtSWE predicted by models from the same NWSO in both months, several stations preferred different sets of models for the two months. This concept of "best models" was actually only a matter of an additional 1 or 2 percent model-described variation. In the cases of Colden and Warsaw, Buffalo and Rochester models were virtually equal in their ability to predict sqrtSWE in a given month.

Proximity to a NWSO and similar minimum monthly temperatures are not as important in Western and Central New York as is the presence or absence of Lake Effect snow at a site. This phenomenon may be briefly described as large amounts of low density snow caused by extremely cold air traversing a warm body of water such as a Great Lake. The air entrains large quantities of moisture before being forcibly lifted by frictional convergence at the lakeshore, by the orographic influence of terrain rapidly increasing in elevation, or a combination of the two mechanisms. This triggers precipitation, resulting in large accumulations of snowfall.

Those stations in Western New York which receive Lake Effect snow may have their sqrtSWE equally well predicted by Buffalo and Rochester

models. In Central New York, Lake Effect stations are well predicted by Syracuse models. The remaining Central New York stations are best predicted by Binghamton models.

In the Adirondack and Catskill Mountains a two-step process must be followed to determine if Caribou supplies the models of choice. First, single-digit (°F) average monthly minimum temperatures are indicative of a station where sqrtSWE is best predicted by Caribou models. Second, double-digit (°F) minimum temperatures for stations with elevations greater than 1200 feet also are best predicted by Caribou models. Of the stations tested only Little Falls does not match these criteria, but is also severely underpredicted by models from any station except Caribou. Norwich did not meet the criteria for Caribou models, and sqrtSWE there is best represented by Albany models.

For operational purposes, after checking temperature and elevation criteria and snow origin, if a Co-Op station has a record of snow survey observations, it should be used in making the final determination of which NWSO-derived models are appropriate for the site in question. In the absence of snow surveys the "Total" Winter model should be applied, while implementing a periodic snow survey program to develop a dataset for determining the optimal model. It should also be noted that caution must be exercised when working with SWEs greater than 4 inches (10 cm) in January, and 6 inches (15 cm) in February since the tendency for underprediction begins at these values. Further work with SWE values in this range is recommended.

It would be interesting to expand the Co-Op verifications to stations outside of New York and determine if the models are truly regional. It

seems quite probable that the number of stations supplying daily SWE data can be reliably increased from 6 to over 250 in New York State, and with further calibration, from 15 (see Figure 1) to over 500 (see Figure 2) in the entire Northeastern United States, with further applications in adjacent Canadian provinces.

Since these models only require knowledge of a few variables, it is reasonable to suggest a further use. Output from meteorological forecast models or subjective forecasts from operational meteorologists may be used as input into SWE prediction models. Maximum temperature forecasts could be used to estimate the future value of *Maxinrow*. Precipitation and snowfall predictions could provide values of *Oldsnfl* and *Oldppt*, and could be used to determine incremental increases in *Snowdepth*, or decreases if fair weather was forecast. These prognostic values could be used to forecast various SWE scenarios, taking the models described in this thesis beyond the role of merely specifying SWE for the current day to the level of actually predicting SWE amounts in the future.

6. Summary

Complete SWE and corresponding daily climatological summary records at 15 NWSOs in the Northeastern United States were used to develop daily SWE station prediction models for each of the winter months, as well as November, March, and April. R^2 values ranging between approximately 43% and 88% were achieved. The monthly station models were then grouped regionally by month and then by season to produce more generalized models. R^2 values for the grouped models ranged between approximately 62% and 72%. Even when the models are used for the extreme case of 10-inch (25 cm) values of SWE, 67% of all predictions still fall within about $\pm 15\%$ of the observed amount.

Validation tests using independent Co-Op station snow survey data yielded similar or better percentages of model-described variation, regardless of whether an individual station or grouped model was applied. A possible upper limit of 4 inches of actual SWE in January and 6 inches in February before underprediction begins was noted when using the models for areas of deep snowcover.

Since no knowledge of previous SWE is required for this approach, it appears that this work successfully fills a gap in the data network by allowing daily cooperative observer data to be used in providing useful estimates of SWE. The accessibility of this data on a real-time basis and ease of calculation should allow this technique to be readily incorporated into systems requiring knowledge of SWE and snowmelt.

7. Appendix A - Stepwise Selection

Stepwise selection was employed to find the statistically best predictors from the list of 19 potential predictors (see Table 6). In order to understand the procedure some background statistics are required, after Neter, et al. (1985).

The t-ratio, or t-statistic, is simply the ratio of a parameter estimate to its standard error. When this ratio is greater than approximately 2.0, the parameter estimate is significantly different from zero at roughly the 95% confidence level, and implies the associated variable is a statistically significant predictor. In the case of multiple regression, the corresponding variable is a statistically significant component of a model, when considered with the other predictors in the model. In other words, variable X is a significant predictor when variables Y and Z are already in the model. The square of the t-statistic is the F-statistic, and this is used in stepwise selection to dictate the addition or removal of a variable from the model. Since the order in which variables are selected by stepwise is not determined *a priori*, the p-value corresponding to a given variable is an overstatement of statistical significance. However, a t-ratio of 2, or F-ratio of 4, is still a reasonable criterion for variable selection.

The mechanics of the procedure are presented as follows. In the first step the dependent variable, which initially was SWE, was regressed against each of the potential predictors. (In later stages, the transformed square root of SWE was also subjected to this procedure.) The F-statistic for the predictor in each of the 19 single predictor equations was calculated. Statistical packages used for this procedure allow user selection of criteria for entering and removing variables from the model. The criterion used was an F-value

larger than 4 for a variable to enter the model, and an F-value less than 4 to be removed. Although a technique involving matrix manipulation (Neter, et al., 1985), known as the sweep algorithm, is more elegant and efficient, an intuitive interpretation of the procedure follows.

The variable in the first step with the largest F-statistic greater than 4 was added to the model. In the next step the initially selected variable was regressed against SWE with each of the remaining potential predictors, in 18 separate 2-variable models. The F-statistic for each of the 18 variables being checked was calculated. The additional variable which, when in a model containing the first variable, had the largest F-statistic greater than 4, was the second variable selected for addition to the model. At this point the F-statistic of the first variable was tested to see if it had become less than 4, causing removal.

The procedure continued in this manner. After a variable had been added to the model, those already included were each checked to determine if their F-statistic had fallen sufficiently for the variable to be removed. The procedure stopped when no further additions or removals could be performed. As the text explains, this was not the final model. Standardized residual analysis, variable transformation, cross validation, and bootstrap techniques, described in Appendix B and Model Development, had to be performed before the model was finalized.

8. Appendix B - Standardized Residual Analysis

Before embarking on a description of standardized residual analysis a brief review of some statistics is necessary. The following discussion draws heavily on Neter, et al. (1985).

In multiple regression the difference between the observed and predicted values is the residual or error:

$$(e) = \text{observed} - \text{predicted} \quad (\text{B1})$$

Therefore, a positive residual indicates underprediction, while a negative residual is a result of overprediction. If one squares each residual, the result is the squared residual or error:

$$(\text{SE}) = (\text{observed} - \text{predicted})^2 \quad (\text{B2})$$

and then the sum of squared residuals or errors is:

$$(\text{SSE}) = \sum (\text{observed} - \text{predicted})^2 \quad (\text{B3})$$

Equation (B4) then shows the mean squared error.

$$(\text{MSE}) = \frac{\sum (\text{observed} - \text{predicted})^2}{\text{sample size} - (\# \text{ of predictors}) - 1} \quad (\text{B4})$$

In this work the original model for Binghamton in January had 4 predictors and was written:

$$y = b_0 + b_1(X_1) + b_2(X_2) + b_3(X_3) + b_4(X_4) \quad (B5)$$

If n = sample size, then the denominator in (B4) was $n-5$. The reduction of the denominator may be considered as the penalty for estimating the population parameters from a sample. Each estimated parameter causes the loss of one degree of freedom.

Finally, the root mean squared error, also known as the standard deviation, or standard error of the predicted values, is found by:

$$(RMSE) = \left(\frac{\sum(\text{observed} - \text{predicted})^2}{\text{sample size} - (\# \text{ of predictors}) - 1} \right)^{1/2} \quad (B6)$$

The standardized residual is then obtained by:

$$\text{Standardized residual} = \frac{\text{observed} - \text{predicted}}{RMSE} \quad (B7)$$

and indicates how many standard deviations a prediction is from being a perfect fit.

If the standardized residuals calculated for a particular regression model are plotted against one of the predictors and are normally distributed, with constant variance throughout the range of data, about 95% of the standardized residuals will fall between the values of -2 and +2. In other words, within two standard deviations of a perfect fit. This is illustrated schematically in Figure B1.

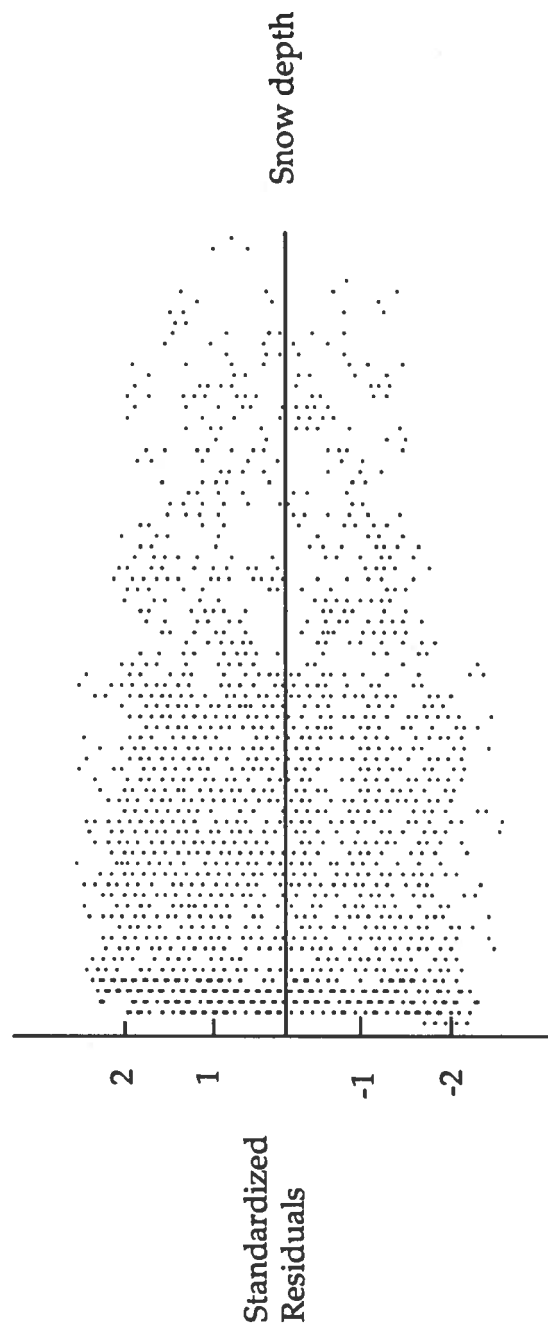


Figure B1. Idealized standardized residual plot showing no need for any variable transformation.

However, a standardized residual plot of the 4-variable model, incorporating snow depth, Maxinrow, and the previous 24 hour snowfall and precipitation as predictors for SWE is depicted in Figure B2, using January data for Caribou. The variance of the plot becomes larger with increasing snow depth. This violates the assumption of constant variance throughout the range of data, required to obtain a RMSE representative of the entire data set. The RMSE for this figure would probably be accurate for the midrange of predictor values; in other words, a 95% confidence interval would contain about the appropriate number of data points in that area, but would contain 100% of the points at the low end, and perhaps only 70% at the high end. The perceived accuracy of the model would be poorer than reality at the low end and too great at the high, because intervals calculated with the nonrepresentative RMSE would be said to contain 95% of all points everywhere in the data. A transformation of the dependent variable was indicated.

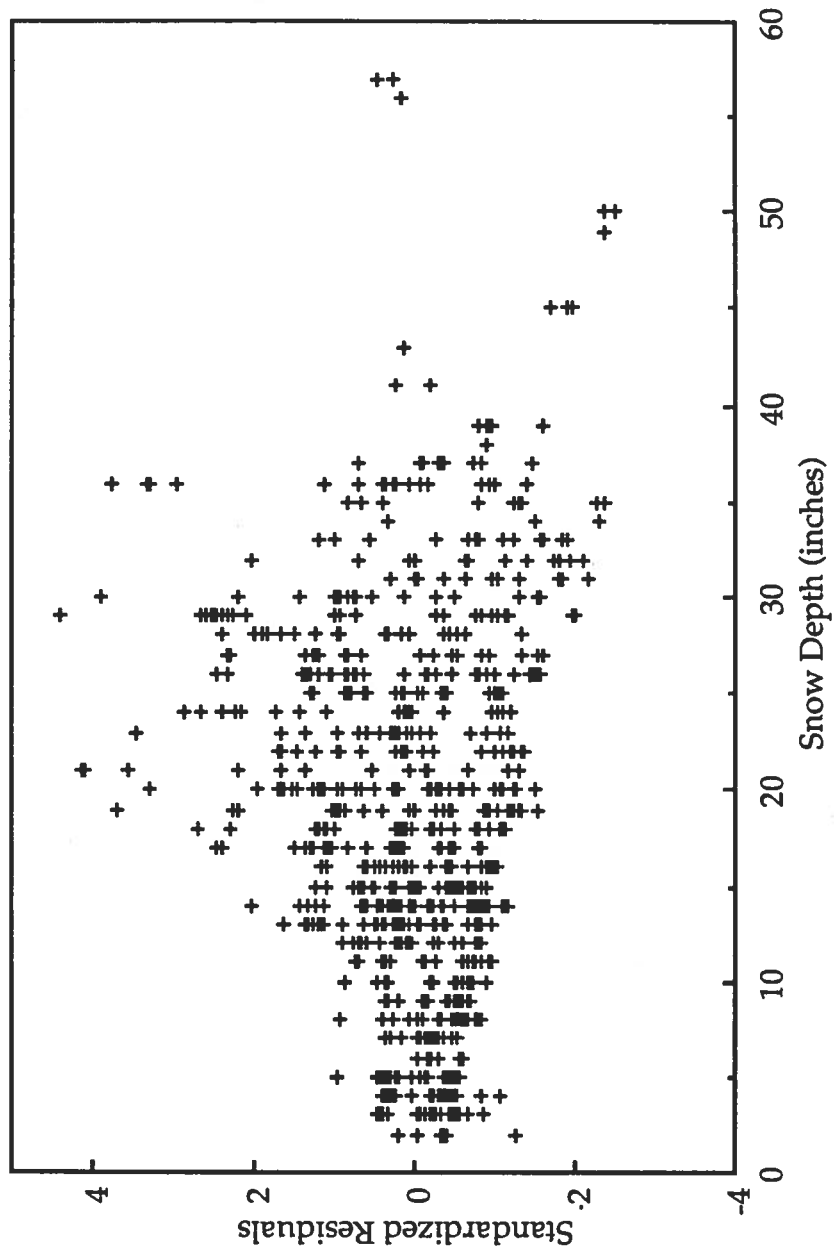


Figure B2. Standardized residual plot showing increasing variance. January Caribou data.

The technique after Box and Cox (Draper & Smith, 1981), described in detail in Appendix C, was used to determine the best power for the transformation. Here the appropriate power was 0.5, giving the square root of SWE as the dependent variable. The standardized residual plot for that 4-variable model is shown in Figure B3, still using January data from Caribou. Although the variance had been made more constant, the curvature indicated a problem among the predictors. Note how underprediction is occurring in the mid-range of the predictor values, while overprediction is occurring at both extremes. The correction was determined by examining the scatterplot of SWE against snow depth, seen earlier as Figure 4. The curvature of this plot resembles the function $y = \sqrt{x}$. If a best fit straight line were connected to the origin and extended through the data, it would overpredict the extremes and underpredict the mid-range. Transforming Snowdepth to its square root in the model should correct for this tendency. The standardized residual plot for the new 4-variable model predicting for $\sqrt{\text{SWE}}$ yielded Figure B4, using the same January data from Caribou.

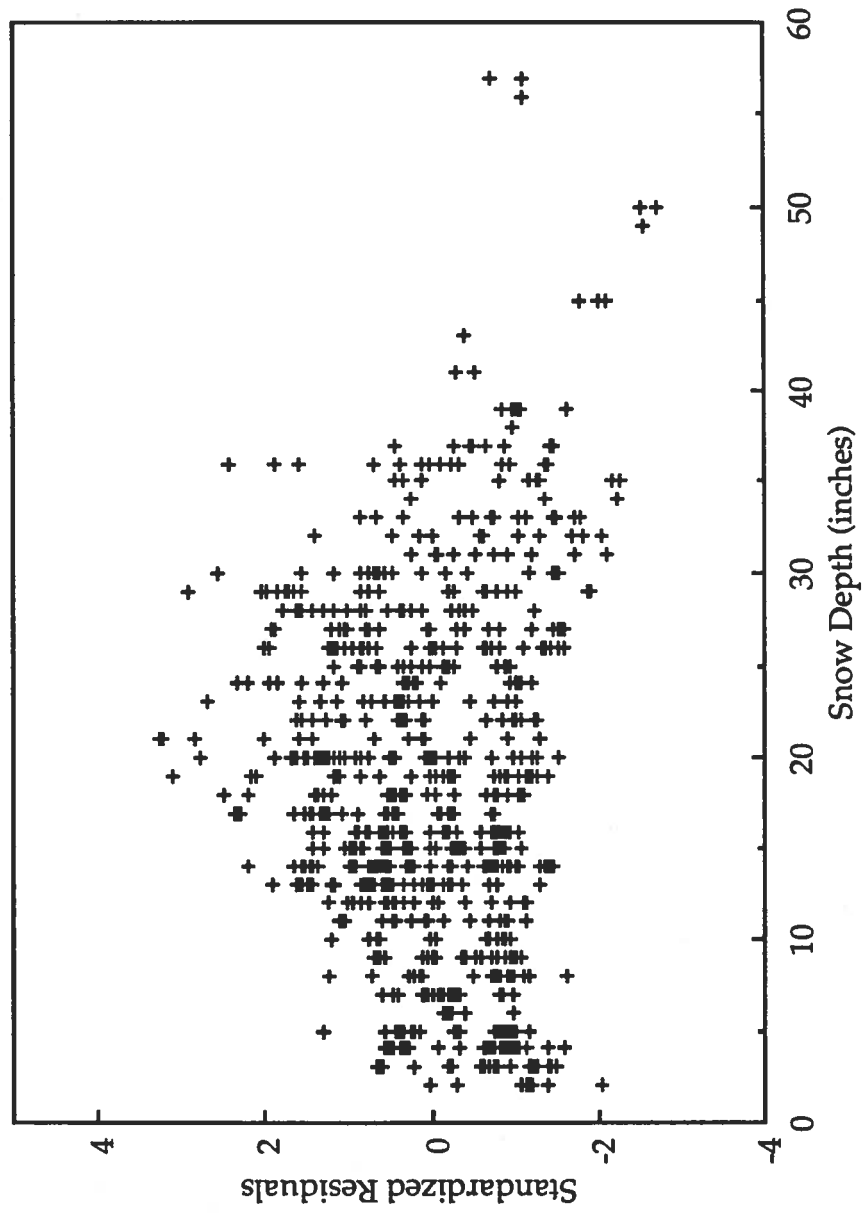


Figure B3. Standardized residual plot showing curvature. January Caribou data.

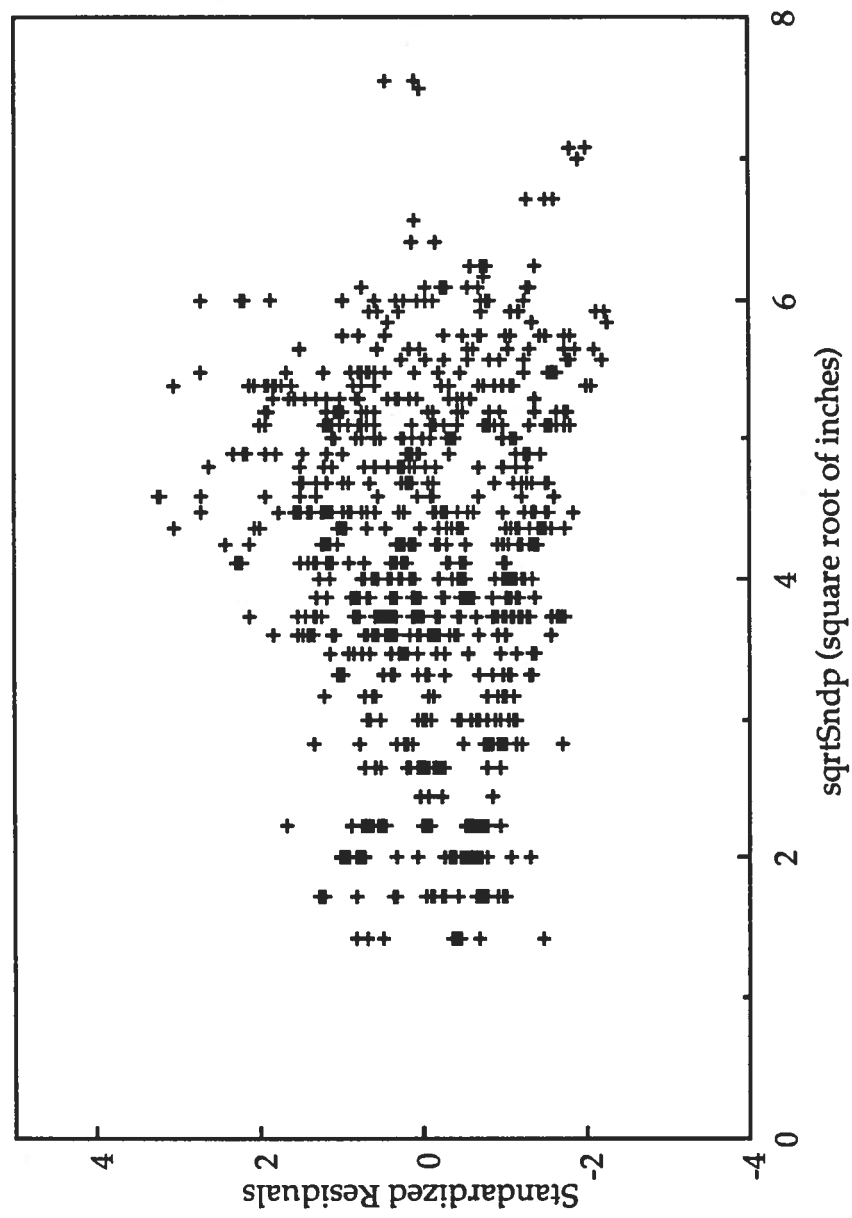


Figure B4. Standardized residual plot for transformed model. January Caribou data.

9. Appendix C - Method of Box and Cox

When standardized residual analysis reveals non-constant variance among the residuals from a multiple regression model, a transformation of the dependent variable is often in order. Power transformations are part of a flexible family which includes all of the most commonly used transformations. An objective method for determining the proper power of transformation, assuming such a transformation to be appropriate, was developed by Box and Cox as summarized in Draper and Smith (1981). If the power is denoted λ , and the errors are assumed to be normally distributed, a maximum likelihood method may be employed.

A range of λ is selected, and increments of λ are used. In this case λ between -1 and 1 at 0.1 increments were selected. The dependent variables were then transformed to sets of W , where

$$\begin{aligned} W &= (Y^\lambda - 1)/\lambda \text{ for } \lambda \neq 0 \\ \ln Y &\quad \text{for } \lambda = 0 \end{aligned} \tag{C1}$$

For the range of λ examined, this yielded 21 sets of transformed data. For each set the transformed dependent variable was regressed against the predictors, and then the following equation was calculated for every λ level:

$$L(\lambda) = -0.5 n (SSE/n) + (\lambda - 1) \sum \ln Y_i \quad (C2)$$

where

$L(\lambda)$ = likelihood function of the regression parameters for the given value of λ

n = sample size

$SSE = \sum (\text{observed} - \text{predicted})^2$

Y_i = observed values of the dependent variable

This produced 21 values of $L(\lambda)$, which were then plotted against λ . The resulting curve was used in determining the best λ for transformation, by merely taking the power associated with the maximum $L(\lambda)$ value. Table C1 shows actual $L(\lambda)$ values for January data from Binghamton. Although 0.4 was the best power, some subjectivity in choosing the transformation power is permissible. Therefore 0.5 was selected for ease of interpretation. The final result from this procedure gave sqrtSWE as the dependent variable.

Table C1. Method of Box and Cox. The maximum $L(\lambda)$ value is associated with the λ which is the appropriate power for transformation of the dependent variable.

λ	$L(\lambda)$
-0.4	47.9
-0.3	61.1
-0.2	72.7
-0.1	82.3
0	90.4
0.1	96.7
0.2	101.3
0.3	104.4
0.4	105.6
0.5	105.3
0.6	103.5
0.7	100.0
0.8	94.8
0.9	88.6
1	81.3

10. Appendix D - Slope and Intercept Models with Dummy Variables

The method of slope and intercept models with dummy, or binary variables was used to group station models. The goal was to determine if one parameter estimate per variable was appropriate for all of the stations within a group, or whether the variable requires site-specific parameter estimates. The reason for determining this should be clear. One parameter estimate suitable for the developmental stations within a geographic grouping means that all other locations within that group should also be served by that single parameter estimate. The contribution of that variable in a prediction model would then be a straightforward arithmetic calculation.

While the matrix mechanics are described in Neter, et al. (1985), a brief summary using the extreme case of grouping 15 stations and 3 winter months is provided here. The SAS® Proc GLM system (SAS, 1985) considers 3 classes of variables besides the 4 main effect (i.e.; *sqrtSndp*, *Maxinrow*, *Oldsnfl*, and *Oldppt*) predictors. These classes are viewed as sets, or levels, of binary or dummy variables. Statistical considerations require one fewer binary variables than the number of levels in a class to avoid linear dependency (see Neter, et al., p.329-330, 1985). Thus, for 14 of the 15 stations, if prediction is occurring for data from one particular station, its binary variable has a value of 1, while the others are set to zero. For the 15th station all 14 binaries are set to zero. The other classes are the 3 months, requiring 2 binaries, and rain on snow versus no rain on snow, which utilizes a single binary variable.

A more intuitive interpretation of the procedure would be to assume that the system is actually developing a model for one station in February with no rain-on-snow. The intercept term would be b_0 and would already include information about the month and lack of rain-on-snow. The intercept term for the second station would be $b_0 + b_1$, the third station, $b_0 + b_2$, and so on until the 15th station intercept was calculated from $b_0 + b_{14}$. If a different month were involved, the dummy variable associated with that month would allow a correction factor to be added to the intercept. For the second station in December this would be represented as $b_0 + b_1 + b_{19}$, if the coefficients for the 4 variables in the model used b_{15} through b_{18} . Yet another dummy variable would allow an additional correction factor to be added to the intercept if rain had fallen on snow. In a three month model where the correction factor for December is b_{19} , and for January is b_{20} , the intercept for a rain-on-snow event in December would be represented as $b_0 + b_1 + b_{19} + b_{21}$ for the second station. For all of these cases the full prediction model would also include b_{15} - b_{18} multiplied by sqrtSndp , Maxinrow , Oldsnfl , and Oldppt respectively.

Before these final models were developed, interactions were considered. Since it is possible for each of the four main predictors to vary by city, terms representing this were included. Interaction is also possible for predictors varying by month, and was included as another set of terms. Finally, rain on snow can affect sqrtSndp and Oldppt , so additional interactive terms were included for these.

Table D1 lists the number of terms which would appear if the model with all possible components were written in equation form, and briefly describes that equation.

Table D1. Summary of terms appearing in the 15-station winter grouped model.

Intercept	1
Stations - 1	14
Variables	4
Months - 1	2
Rain on Snow	1
4 variables * 14 stations	56
4 variables * 2 months	8
<u>2 variables * rain on snow</u>	<u>2</u>
Total	88

the predicted value of sqrtSWE would equal

$$b_0 + b_1X_1 + b_2X_2 + \dots + b_{87}X_{87}$$

Initially the total winter model began with the 87 terms summarized in Table D1. T-ratios were calculated for each group of interactive terms in the model, as well as main effect predictors, as the ratio of parameter estimates to standard errors, in order to determine if the parameter estimates were significantly different from zero. If the corresponding p-value was greater than 0.05, the term was non-significant at the 95% confidence level. When this was true of the last term entered in the model it could be safely removed. The model with remaining terms was then rerun. This sequential removal, known as backward elimination (Neter, et al., 1985), was performed until the only remaining terms were the main variables, the station intercepts, which were always among the most important variables, and the binary variables for rain on snow and for month. Table D2 shows the t-ratios for each term, R^2 , and RMSE at each step in the removal process. It is important to note that many interactions were removed which had significant t-ratios, such as Oldppt with rain-on-snow. In each case the

resulting change in R^2 and RMSE was quite small. Although statistically significant, the presence of these terms was operationally meaningless. The small loss in statistical accuracy was more than balanced by the development of a model which was extremely simple to operate.

Table D2. Sequential removal of terms from the grouped winter model, showing r-squared, RMSE, f-values for each term or group of terms, and the probability of a larger f value. * denotes interactions among 15 cities, 3 months, and rain- or no rain-on-snow. Ras denotes rain on snow days.

variables	r-squared	73.6	73.5	73.5	73.5	73.5	73.5
	root MSE=s	0.273	0.273	0.273	0.273	0.273	0.273
	f-value	pr of > f	f-value	pr of > f	f-value	pr of > f	pr of > f
city	990.3	0	987.47	0	987.38	0	987.41
sqrtsndp	40284.79	0	40169.55	0	40165.91	0	40167.03
maxinrow	521.8	0	520.32	0	520.27	0	520.29
oldsnsfl	1200.13	0	1196.7	0	1196.59	0	1196.62
oldppt	1097.65	0	1094.51	0	1094.41	0	1094.44
month	839.07	0	836.67	0	836.59	0	836.62
ras	163.54	0.0001	163.07	0.0001	163.06	0.0001	163.06
sqrtsndp*city	48.8	0	48.66	0	48.66	0	48.66
maxinro*city	6.92	0.0001	6.9	0.0001	6.9	0.0001	6.9
oldsnsfl*city	4.65	0.0001	4.64	0.0001	4.64	0.0001	4.64
oldppt*city	3.12	0.0001	3.11	0.0001	3.11	0.0001	3.11
sqrtsndp*mon	114.04	0	113.71	0	113.7	0	113.71
maxinrow*mo	4.67	0.0094	4.66	0.0095	4.66	0.0095	4.66
oldsnsfl*month	31.67	0.0001	31.58	0.0001	31.57	0.0001	31.57
oldppt*month	0.7	0.4956	0.7	0.4966	0.7	0.4967	0.4967
sqrtsndp*ras	2.96	0.0852	2.95	0.0856			
oldppt*ras	62.87	0.0001					

Table D2. (continued)

r-squared	73.4	73.4	73.1	73.1	73.1
root MSE=s	0.273	0.273	0.275	0.275	0.275
variables	f-value	pr of > f	f-value	pr of > f	f-value
city	984.62	0	984.28	0	972.84
sqrtsndp	40053.49	0	40039.97	0	39574.21
maxinrow	518.82	0	518.64	0	512.61
oldsnsfl	1193.24	0	1192.84	0	1178.96
oldppt	1091.34	0	1090.98	0	1078.29
month	834.25	0	833.97	0	824.27
ras	162.6	0.0001	162.55	0.001	160.66
sqrtsndp*city	48.52	0	48.5	0	47.94
maxinro*city	6.88	0.0001	6.88	0.0001	6.8
oldsnsfl*city	4.63	0.0001	4.62	0.0001	4.57
oldppt*city	3.1	0.0001	3.1	0.0001	
sqrtsndp*mon	113.38	0	113.35	0	
maxinrow*mo	4.64	0.0096			

Table D2. (continued)

r-squared	73.0	72.9		72.0	
root MSE=s	0.275	0.276		0.280	
variables	f-value	pr of > f	f-value	pr of > f	pr of > f
city	970.59	0	966.97	0	938.63
sqrtsndp	39482.85	0	39335.45	0	38182.63
maxinrow	511.42	0	509.52	0	494.58
oldsnsfl	1176.24	0	1171.85	0	1137.5
oldppt	1075.8	0	1071.78	0	1040.37
month	822.37	0	819.3	0	795.29
ras	160.29	0.0001	159.69	0.0001	155.01
sqrtsndp*city	47.83	0	47.65	0	0.0001
maxinro*city	6.79	0.0001			

11. Appendix E - Developmental vs. Independent Data Sets

- Some Considerations

In least squares regression, the percentage of model-described variation in the dependent variable is equal to R^2 only for the data set for which the regression model was developed:

$$R^2 = 1 - \text{SSE}/\text{SSTO} = 1 - \frac{\sum(\text{observed} - \text{predicted})^2}{\sum(\text{observed} - \text{mean of the observed})^2} \quad (\text{E1})$$

The predictions from a least squares regression model are also unbiased, a condition critical to this discussion because it implies the sum of residuals equals zero.

In an independent data set, such as that from a Co-Op station (see Section 5), the same relationships do not hold when a NWSO model is applied. There is no guarantee of unbiased predictions. In fact, for many Co-Op stations the correlations (r) between observed and predicted sqrtSWE values were quite high. However, standardized residual analysis, discussed in more detail in Appendix B, revealed consistent underprediction at Adirondack stations (see Figure E1 for an example), despite these high correlations. If one assumed that the amount of model-described variation in these cases was simply the square of r , the results were unrealistically high. This was due to a concept not often mentioned in textbooks. Only for the developmental set treated with its own model does equation (E1) refer to the described variation. For an independent data set

$$1 - (\text{SSE}/\text{SSTO}) = \text{fraction of model-described variation} \neq R^2 \quad (\text{E2})$$

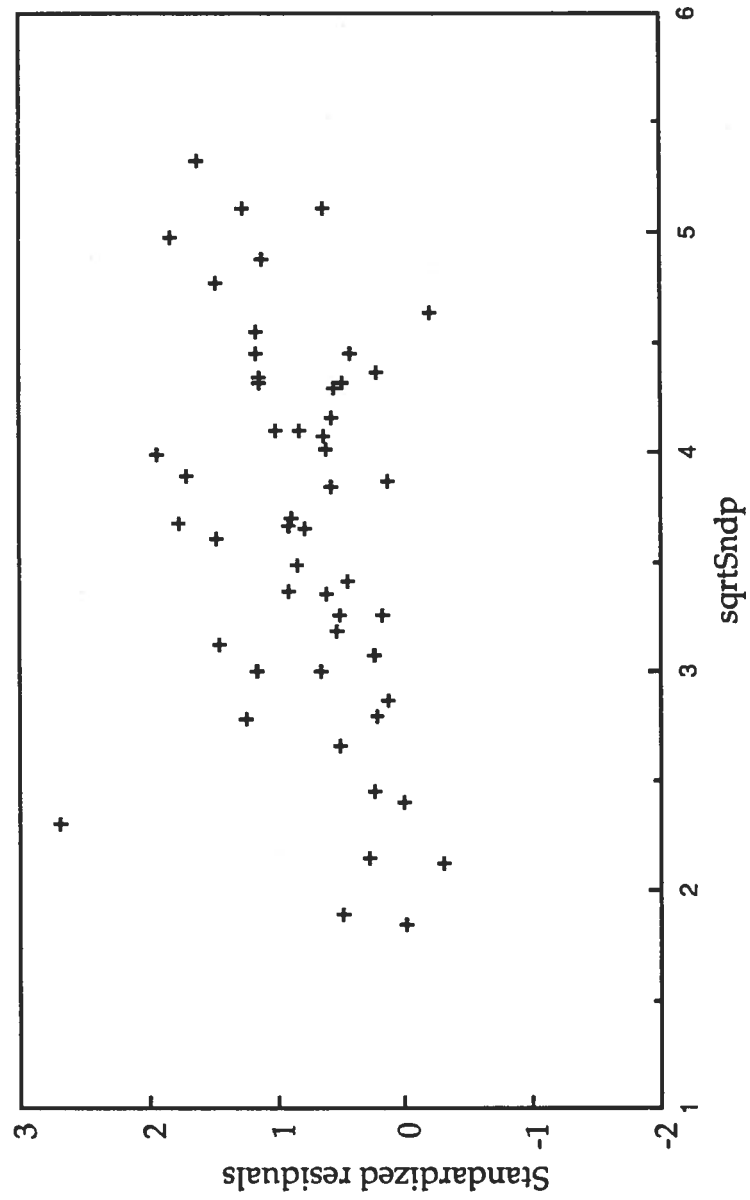


Figure E1. Underprediction for Wanakena using Burlington's January model.

With this understanding it became evident that the high correlation between observed and predicted values indicated that instead of falling on essentially the same line when plotted against sqrtSndp, observed and predicted values described nearly parallel lines. The standardized residual plots, exemplified by Figure E1, showed that the sum of the residuals could not possibly have equalled zero, revealing the bias present in the predictions. The amount of described variation, calculated by equation (E2) yielded the low fraction expected of consistently underpredicted values. As the text mentions, Caribou-derived models did not underpredict for Adirondack stations, and yielded high fractions of model-described variation.

Another difference between developmental and verification data sets is the method for calculating RMSE. For developmental data sets RMSE is calculated as described in Appendix B :

$$(MSE) = \frac{\sum(\text{observed} - \text{predicted})^2}{\text{sample size} - (\# \text{ of predictors}) - 1} \quad (B4)$$

The reduction in the denominator is the penalty for estimating population parameters from a sample. When applied to an independent data set this model is then assumed to be the equation describing the underlying population. There is, then, no penalty for estimation and mean squared error is simply

$$\text{Mean squared error (MSE)} = \frac{\sum(\text{observed} - \text{predicted})^2}{\text{sample size}} \quad (\text{E3})$$

This, along with the much smaller sample sizes for snow survey data, may contribute to why the Co-Op derived RMSEs are often superior to those from developmental sites.

12. Literature Cited

1. Anderson, E. A., *National Weather Service River Forecast System - Snow Accumulation and Ablation Model*, NOAA Technical Memorandum NWS Hydro-17, U. S. Department of Commerce, Washington, D. C., 219 pp. November, 1973.
2. _____, *A Point Energy and Mass Balance Model of a Snow Cover*, NOAA Tech. Rep. NWS-19, U. S. Department of Commerce, Washington, D. C., 150 pp., 1976.
3. Baker, D. G., R. H. Skaggs, & D. L. Ruschy, Snow Depth Required to Mask the Underlying Surface, *J. Appl. Meteorol.* 30: 387-392, 1991.
4. Bertle, F. A., *Effect of Snow Compaction on Runoff from Rain on Snow*, Engineering Monograph No. 35, Bureau of Reclamation, Washington, D.C., 1966.
5. Bruce, J. P., & R. H. Clark, *Introduction to Hydrometeorology*, Pergamon Press, Toronto, 257pp., 1966.
6. Buttle, J. M., Effects of Suburbanization Upon Snowmelt Runoff, *Hydrol. Sci. J.*, 35: 285-302, 1990.
7. _____. & F. Xu, Snowmelt Runoff in Suburban Environments, *Nord. Hydrol.* 19: 19-40, 1988.
8. Carr, D. A., *Snowpack Modeling Using Daily Climatological Data*, Poster Presentation, 45th Annual Meeting, Eastern Snow Conference, Lake Placid, NY, 1988.
9. Carroll, S. S., & T. R. Carroll, Effect of Uneven Snow Cover on Airborne Snow Water Equivalent Estimates Obtained by Measuring Terrestrial Gamma Radiation, *Water Resour. Res.* 25: 1505-1510, 1989.

10. Dozier, Jeff, Recent Research in Snow Hydrology, *Rev. of Geophys.* 25:153-161, 1987.
11. Draper, N. R. & H. Smith, *Applied Regression Analysis*, 2nd ed., John Wiley & Sons, New York, 1981.
12. Ffolliott, P. F., G. J. Gottfried, & M. B. Baker, Jr., Water Yield from Forest Snowpack Management: Research Findings in Arizona and New Mexico, *Water Resour. Res.* 25: 1999-2007, 1989.
13. Fleming, G., *Computer Simulation in Hydrology*, Elsevier Environmental Science Series, New York, 333 pp., 1975.
14. Garstka, W. U., L. D. Love, B. C. Goodell & F. A. Bertle, *Factors Affecting Snowmelt and Streamflow*, U. S. Bureau of Reclamation, 189 pp., 1958.
15. Kuz'min, P. P., *Melting of Snow Cover*, (1961) Israel Program for Scientific Translations, 290 pp., 1972.
16. MacLean, A., A Study of Ground Heat Flux and Associated Changes in Snowpack Water Equivalent and Soil Moisture, *Proceedings of the 48th Eastern Snow Conference*, 1991 (in press).
17. Male, D. H. & R. J. Granger, Snow Surface Energy Exchange, *Water Resour. Res.* 17: 609-627, 1981.
18. Morris, E. M., "Snow and Ice" from *Hydrological Forecasting*, edited by Anderson, M. G. and T. P. Burt, John Wiley & Sons, 604 pp., 1985.
19. *National Cooperative Observer Newsletter*, 1:1-2, 1983.
20. Neter, J., W. Wasserman, & M. H. Kutner, *Applied Linear Statistical Models*, 2nd edition, Irwin, Homewood, IL, 1985.
21. Oke, T. R., *Boundary Layer Climates*, Methuen, New York, 372 pp., 1978.
22. Olyphant, G. A & S. I. Isard, The Role of Advection in the Energy Balance of Late-Lying Snowfields: Niwot Ridge, Front Range, Colorado, *Water Resour. Res.* 24: 1962-1968, 1988.

23. Prévost, M., R. Barry, J. Stein & A. P. Plamondon, Snowmelt Modeling in a Balsam Fir Forest: Comparison between an Energy Balance Model and Other Simplified Models, *Can. J. For. Res.* 21: 1-10, 1991.
24. Pysklywec, D. W., K. S. Davar & D. I. Bray, Snowmelt at an Index Plot, *Water Resour. Res.* 4: 937-946, 1968.
25. Quick, M. C. & A. Pipes, *The UBC Watershed Model*, Proceedings of Symposium in Bratislava, Application of Mathematical Models in Hydrology and Water Resource Systems, International Association of Hydrological Science, Pub. No. 115, 1975.
26. SAS Institute Inc. *SAS[®] User's Guide: Statistics, Version 5 Edition*. Cary, NC: SAS Institute Inc., 956pp., 1985.
27. Schmidlin, T. W., A Critique of the Record of "Water Equivalent of Snow on the Ground" in the United States, *J. Appl. Meteorol.* 29:1136-1141 1990.
28. _____, & D. J. Edgell, Observations on the Measurement of Shallow Snow Covers, *Preprints, 6th Conference on Applied Climatology*, Boston, Amer. Meteor. Soc., 70-71, 1989.
29. U. S. Army Corps of Engineers, *Snow Hydrology, Summary Report on Snow Investigations*, 437pp., 1956.
30. Wiesner, C. J., *Hydrometeorology*, Chapman & Hall, Ltd., London, 232 pp. 1970.
31. Wilson, W. T., An Outline of the Thermodynamics of Snow-Melt, *Trans. Am. Geophys. Union*, Part 1: 182-195, July, 1941.
32. Work, R. A., *Stream-Flow Forecasting from Snow Surveys*, USDA Circular no.. 914, Washington, 16 pp., 1953.
33. Zuzel, J. F. & L. M. Cox , Relative Importance of Meteorological Variables in Snowmelt, *Water Resour. Res.* 11: 174-176, 1975.

NRCC RESEARCH SERIES

Knapp, W.W. and K.L. Eggleston, *Some Impacts of Recent Climate Variability on the Northeast*, NRCC Research Publication RR 91-1.

Wilks, D.S., *Gamma Distribution Probability Tables for Use in Climatology*, NRCC Research Publication RR 91-2.

CORNELL
UNIVERSITY

Department of Soil, Crop and Atmospheric Sciences
Ithaca, New York 14853

Produced by the
Northeast Regional Climate Center
7/93 30 125-8435